Mending broken hearts - Cardiac regeneration in zebrafish

By

Fabian Klaus Kruse

Your work is going to fill a large part of your life, and the only way to be truly satisfied is to do what you believe is great work. And the only way to do great work is to love what you do. If you haven't found it yet, keep looking. Don't settle. As with all matters of the heart, you'll know when you find it.

Steve Jobs

Cover design by Laurence Garric (*EUR*êKA*! Art & Science*)

The research described in this thesis was performed at the Hubrecht Institute of the Royal Dutch Academy of Arts and Sciences (KNAW), within the framework of the Graduate School of Life Sciences "Cancer, Stem Cells and Developmental Biology" (CS&D) program of Utrecht University.

The research described in this thesis was supported by a grant of the Dutch Heart Foundation (CVON2011-12 HUSTCARE).

ISBN: 978-94-6233-659-9
Printed by: Gildeprint - Enschede

Mending broken hearts – Cardiac regeneration in zebrafish

Gebroken hart heling – Hart regeneratie in zebravissen
(met een samenvatting in het Nederlands)

Proefschrift

ter verkrijging van de graad van doctor
aan de Universiteit Utrecht
op gezag van de rector magnificus, prof.dr. G.J. van der Zwaan,
ingevolge het besluit van het college voor promoties
in het openbaar te verdedigen op

donderdag 31 augustus 2017
des middags te 4.15 uur

door

Fabian Klaus Kruse

geboren op 18 januari 1987 te Lüdenscheid, Duitsland

Promotor: Prof. dr. J.P.W.M. Bakkers

Financial support by the Dutch Heart Foundation for the publication of this thesis is gratefully acknowledged.

Table of contents

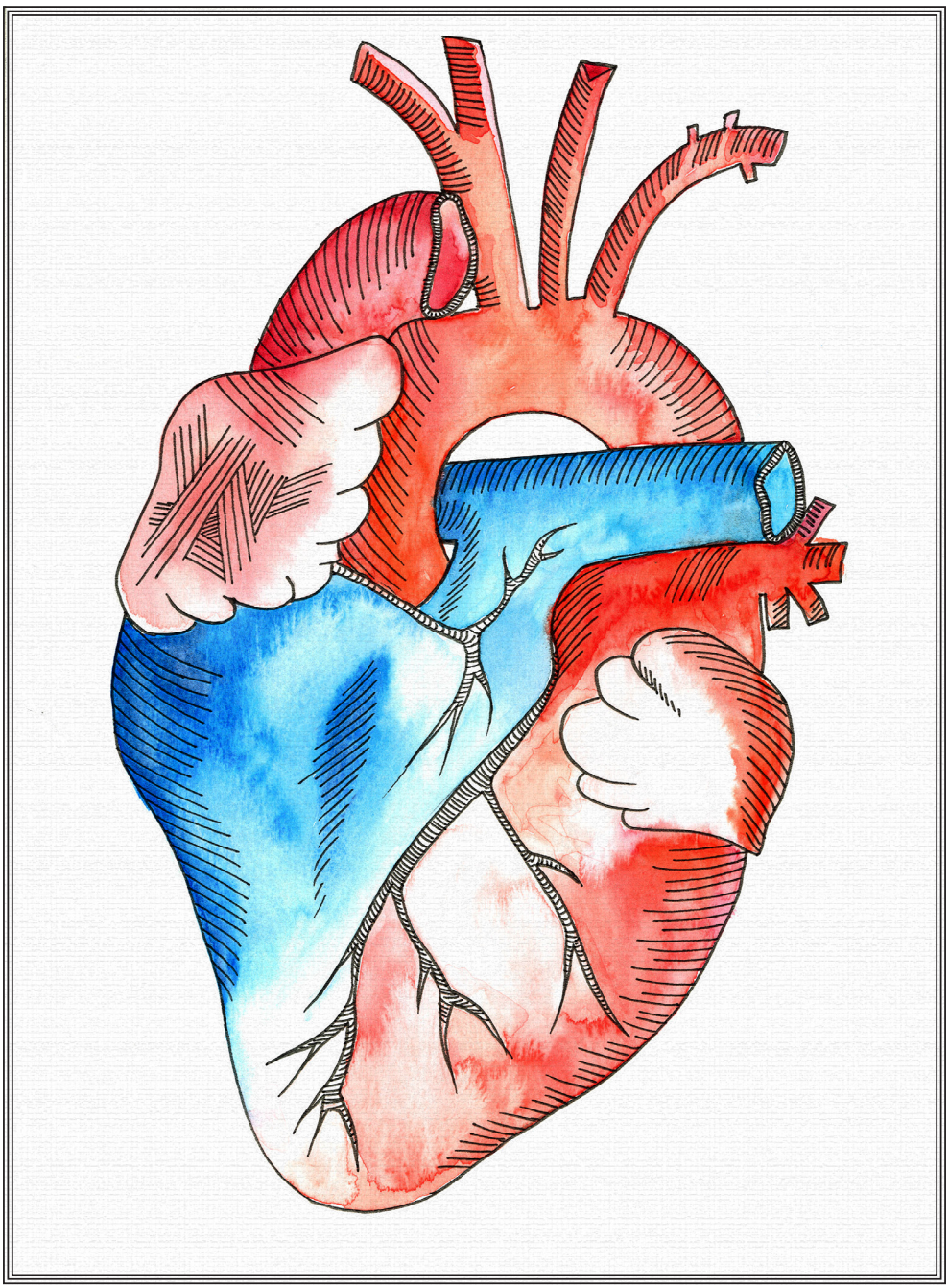

1

General introduction

Fabian Kruse & Jeroen Bakkers

Hubrecht Institute and University Medical Centre Utrecht, Utrecht, The Netherlands

I. Cardiovascular Disease in Humans

Cardiovascular disease is the leading global cause of death, accounting for more than 30% of all deaths. It claims more lives than all forms of cancer combined [1]. Bearing these facts in mind, research in this field is direly needed.

A heart attack, also known as *myocardial infarction* (MI) or *ischemic injury to the heart*, happens when the blood flow through one of the coronary arteries is obstructed (Figure 1). The result of that is insufficient supply of oxygen and nutrients towards the heart muscle cells, causing massive death of over a billion heart cells [2]. However, there is no significant replacement of the lost muscle tissue; instead, scar tissue is formed. Scarring is essential to initially keep the organ intact, but a non-contractile scar cannot restore cardiac output – i.e. pump a sufficient amount of blood through the body – and can cause arrhythmia (irregularities in the heart beat) that can lead to cardiac arrest. Being a non-regenerative organ in humans, the heart could greatly benefit from regenerative therapy. Over the past 15 years, two main therapeutic strategies have been pursued to address this issue: (1) transplantation of exogenous cells and (2) stimulation of a regenerative response in the surviving endogenous heart cells. While the transplantation of cells has been tested in human trials, but shown to be non-beneficial to myocardial repair, the stimulation of the remaining heart muscle cells for regeneration is further away from clinical testing.

In the strategy using exogenous cells, a wide array of cell types has been injected into injured mammalian hearts as part of animal experiments and clinical studies. Major hurdles during this process are the potential of a given cell type to engraft in sufficient numbers in the correct place, i.e. the injury site in the heart, as well as the ability to generate new cardiomyocytes. Moreover, such cells would need to electrically couple to the existing myocardium to ensure proper contraction of the heart. The cell types that have been mainly investigated in preclinical animal models and humans are bone marrow mononuclear cells (BM-MNC), mesenchymal stem/stromal cells (MSC), cardiac stem/progenitor cells (CSC), as well as embryonic stem cells (ESC) and induced pluripotent stem cells (iPSC). Unfortunately, the outcome of several clinical trials has shown that the overall efficacy of injected BM-MNCs, MSCs and CSCs is inconsistent and modest, albeit safe [3, 4]. Contrary to this, recent results using iPSCs for cardiac repair in monkeys offers hope. iPSCs are generated by taking an abundant cell type, usually fibroblasts, from a patient before "reprogramming" these cells through genetic engineering and external factors to a desired cell type. In a study from 2016, Shiba and colleagues generated iPSC-derived cardiomyocytes and transplanted these into monkeys subjected to myocardial infarction, observing improved cardiac function 4 and 12 weeks after transplantation [5]. A negative side-effect was, however, transplantation-induced ventricular tachycardia, i.e. a significantly increased heart rate. To improve homing and grafting of the injected cells, the immune system of the animals was suppressed. The risks associated with long-term immunosuppression, as well as the relatively short follow-up time, highlight the limitations of this study. Moreover, only one iPS cell line has been tested.

Future experiments and clinical trials will show if this approach can be successful in healing the heart in the long run.

The stimulation of an endogenous regenerative response in surviving cardiomyocytes would be less invasive, but faces similar challenges. In the ideal case the heart tissue would be stimulated to regenerate through the supplementation of an exogenous factor, for example proteins that prompt cell division and regeneration of cardiomyocytes. The foundation for such strategies is the fact that mammalian cardiomyocytes are still able to proliferate and divide, as shown by several reports [6, 7]. Taking advantage of the uptake and integration of the carbon-14 isotopes, generated by nuclear bomb tests during the Cold War, the age of human cardiomyocytes could be calculated. Between 0.5-1% of heart muscle cells turn over annually, signifying that new cardiomyocytes continue to be formed throughout life [6]. A to-date unidentified stimulus could potentially boost the number of proliferating cardiomyocytes in the aftermath of a heart attack.

II. Mammalian studies of heart repair

Mice are a widely used model organism to study the response to a heart attack in an experimental setting. In a groundbreaking report from 2011 Porello showed that neonatal mice still retain the potential to regenerate [8]. When a piece of the heart was cut off one day after birth, scar-less regeneration was observed. This regenerative capacity was lost, however, when mice were injured 7 days after birth. Importantly, these results suggest that the mammalian heart has the intrinsic capacity to repair its heart, raising hopes that regeneration in the adult heart should be possible - if induced in the proper manner.

Further supporting this hypothesis is the fact that adult mouse cardiomyocytes still proliferate during ageing, albeit at a very low rate [7]. This study also showed that the source of the newly formed myocardial cells were pre-existing cardiomyocytes. Kindled by these promising results, several groups tried to enhance heart muscle proliferation in the adult mouse heart. Most prominently, the Hippo signaling pathway has been proven to control mammalian heart size. If this growth-regulatory pathway was inhibited, mouse embryos displayed elevated cardiomyocyte proliferation and uncontrolled heart growth, resulting in abnormally large hearts [9]. Hippo over-activation, on the other hand, blocks neonatal heart regeneration and repair [10]. Hippo-deficient adult hearts exhibit increased proliferative activity in cardiomyocytes under “unstressed” circumstances [11]. If the Hippo-deficient heart is stressed by myocardial infarction, however, the heart can regenerate and recover [10, 11]. Moreover, the transcription factor Pitx2, which also plays an important role during heart development, can interact with Hippo signaling. Pitx2, if overexpressed, induces regeneration in adult infarcted mouse hearts through antioxidant functions [12].

Another developmental pathway shown to positively affect heart regeneration in mammals is the Neuregulin-1/ERBB2/ERBB4 pathway. The growth factor Neuregulin-1, which binds

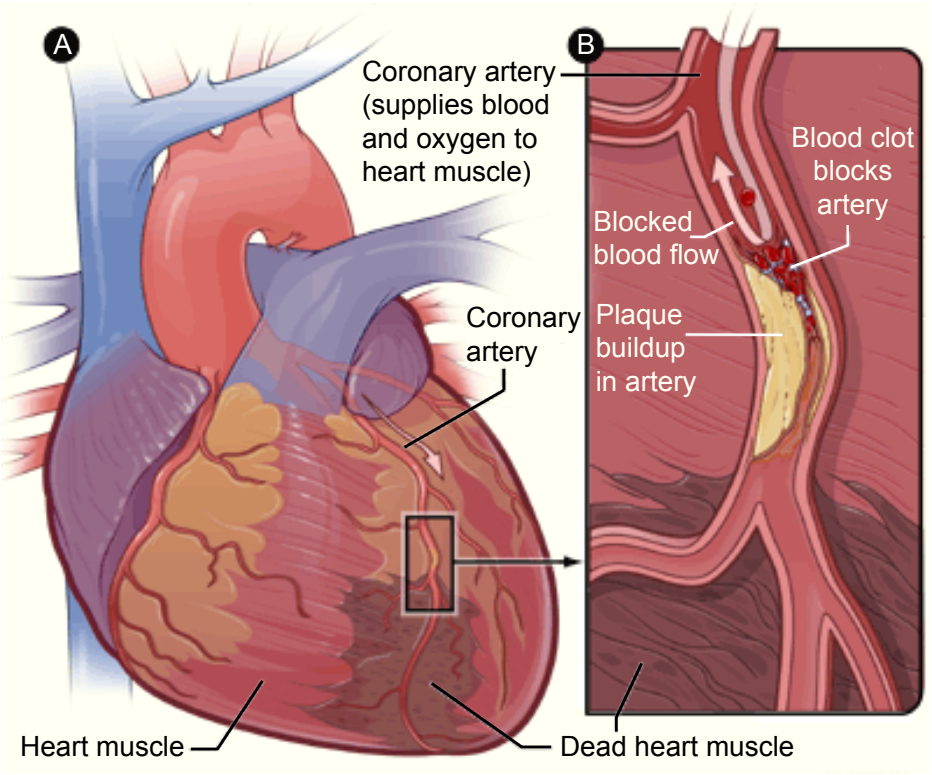

(modified after NIH - National Heart, Lung and Blood Institute)

Figure 1: Myocardial infarction of the human heart. *(A) Occlusion of the coronary artery leads to reduced blood flow in parts of the heart muscle resulting in massive cell death. (B) Plaque buildup in the artery leads to a restriction of the artery, which can be blocked by a blot clot. This effectively prevents blood flow to the heart muscle tissue which is supported by this artery.*

to the receptors ERBB2 and ERBB4, improves cardiac function in injured mice and also in heart failure patients, through diverse roles in angiogenesis, contractility, stress resistance and cardiomyocyte survival [13, 14]. It can also induce cardiomyocyte proliferation; however, this trait is dependent on the rate-limiting receptor ERBB2, which expression declines shortly after birth [15]. If ERBB2 is experimentally induced after birth, the unstressed heart grows uncontrollably, similar to Hippo-deficient hearts. Transient activation of ERBB2 after myocardial infarction leads to anatomical and functional recovery [15]. Remarkably, the authors showed proliferation not only of mono-, but also bi-nucleated cardiomyocytes, which were considered to be incapable of cell division.

Similarly, hypoxia has recently been shown to induce proliferation of cardiomyocytes in mice [16], as can administration of recombinant Follistatin-like 1 protein [17]. Future studies will need to address the feasibility of inducing any of these pathways (at the right level) in the

infarcted human heart, which still remains a major hurdle towards regenerative therapies. While all of these factors hold promise to improve cardiac function of patients in the future, they still represent separate, unconnected events of the regenerative process. Having a more complete understanding of the different processes required for heart regeneration and their interconnection would greatly increase our ability to conceive new therapeutics to treat myocardial infarction through targeting of the endogenous cell population.

III. The Zebrafish – a model to study naturally occurring heart regeneration

Human beings are fascinated with regeneration. We marvel at the ability of salamanders to re-grow their tail, for example, while we are unable to re-grow even a lost fingertip. To regenerate the heart would be an extraordinary feat. In order to boost regenerative therapies of the heart, it is worthwhile to study heart regeneration in animals that naturally possess this ability. Zebrafish, for example, are able to regenerate almost every part of their body including their tail, brain and heart [18].

Danio rerio, the official name of the zebrafish, has been used as a model organism for decades. Zebrafish have been extensively used to study development, the intricate process in which a fertilized egg grows and forms into a living organism. As early as 1934 the zebrafish has been suggested as a suitable model for developmental biology [19]. It was not until the late 1960s when George Streisinger was among the first to actually establish zebrafish as a system for molecular biology at the University of Oregon in Eugene. Some of the reasons that make *danio rerio* such a good model organism are the small size, while still being a vertebrate like humans. They form an excellent model to study embryogenesis because of their fast development and the large numbers of embryos per lay. Moreover, these embryos are transparent, making it easy for researchers to follow the formation of specific tissues and organs. Another strong point is the genetic modifiability, making the zebrafish useful for geneticists reviewed in [20].

III-1. Injury models

More than a decade ago, research in adult zebrafish uncovered a robust capacity for cardiac muscle regeneration. Initial studies employed a resection model, surgically removing approximately 20% of the ventricle [21]. This creates an injury that stimulates a major regenerative response alike to regeneration of an amputated limb. Here, the heart regenerates within 60 days. The second commonly used injury method in the adult zebrafish heart is the genetic ablation technique [22]. This method employs the tamoxifen-inducible CreER recombinase (expressed cardiomyocyte-specifically) to enable expression of cytotoxic diphtheria toxin A chain upon induction. Cell death of heart muscle cells is triggered diffusely over the course of a week, affecting both cardiac chambers. Analysis showed that more than 60% of ventricular myocardium can be ablated before significantly affecting animal survival. Recovery after this

injury takes only 30 days.
Importantly, myocardial infarction is characterized by local death of heart muscle – unlike the physical removal of tissue during resection and the diffuse/mosaic cell death of cardiomyocytes in the genetic ablation model. These considerations prompted the development of a third injury model. The so-called cryoinjury technique induces a large, locally restricted region of damaged/dying heart cells through freezing the ventricular apex with a dry ice or liquid nitrogen-cooled probe [23-25]. This complex injury resembles mammalian myocardial infarction in the best way and leads to consistent regeneration in the course of 90 days.
While each of these injury models has its advantages and disadvantages, together they lead to a better understanding of the molecular factors driving heart regeneration in the zebrafish.

III-2. Cellular source of regenerated myocardium: To Stem-cell or not to stem-cell
The first question biologists ask themselves when facing a regenerating organ is "where does the new tissue come from?". There are several possibilities of how the zebrafish myocardium could potentially regenerate. Firstly, regeneration can occur by proliferation of stem cells that reside in the heart, which differentiate into cardiomyocytes. Secondly, other cell types could trans-differentiate to become cardiomyocytes and form the new tissue. Lastly, pre-existing cardiomyocytes could re-enter the cell cycle in order to generate new heart muscle cells.
Independent of each other, two research groups have genetically labelled and traced cardiomyocytes during regeneration to address this question [26, 27]. Both studies show that the majority of newly formed myocardium originates from pre-existing cardiomyocytes, suggesting only a minor role – if at all – of stem cells during heart regeneration. Instead, it has been assumed, although never proven, that regenerating cardiomyocytes dedifferentiate to a certain extent. Some groups have suggested that dedifferentiation is evidenced by disassembly of the sarcomeric structures, which are needed to generate contractile force in working heart muscle [26]. Interestingly, disassembly of the sarcomeres is also apparent during cardiomyocyte proliferation in the embryonic and neonatal mouse heart [28, 29]. Dedifferentiation to a progenitor-like cell seems logical: cardiomyocytes are highly specialized cells and their extremely organized intracellular structure is potentially one of the reasons hindering re-entry of the cell cycle and proliferation [28]. Our contribution on if, and how far, cardiomyocytes have to dedifferentiate will be addressed in **Chapter 4** of this thesis, clearing up some of the controversy surrounding this topic.

III-3. All in due time: a time course of heart regeneration
Regeneration of the heart is a tightly regulated and timed process. Arguably one of the first events after injury is activation of the endocardium, a cell layer lining the inside of the cardiac chambers [30]. Within 3 hours post amputation, endocardial cells round up and detach from the myocardium, while starting to express *raldh2*. Subsequent retinoic acid signaling has been shown to be required for, but not sufficient to induce, cardiomyocyte proliferation.

During the next stage an inflammatory response is triggered by the innate immune system, which will be introduced in more detail below. Shortly after, many processes are initiated simultaneously: activation of the epicardium (a cellular layer covering the outside of the heart), fibroblast proliferation and cardiomyocyte proliferation.

The epicardium is essential for cardiac regeneration. If epicardial cells are genetically ablated, i.e. killed, cardiomyocyte proliferation is inhibited and regeneration is blocked [31]. One of the epicardial functions is re-expression of embryonic markers like *tbx18* around 2 days after amputation [32]. The injury-induced activation starts globally in the whole ventricle before restricting to the apex. Lineage tracing demonstrated that some epicardial cells undergo epithelial-to-mesenchymal transition (EMT) and give rise to fibroblasts and pericyte-like perivascular mural cells of the coronary vessels [33-35]. Furthermore, the epicardium plays an essential role in inducing cardiomyocyte proliferation [30, 32].

Fibroblasts appearing in the wound region produce scar tissue, especially collagen, starting at 14 days after cryoinjury (dpi). This scar tissue, however, is removed after about 45 days, the mechanism of which has not been identified. Other functions of fibroblasts have not been well characterized. We have found that a fibroblast-like cell type resides in close proximity to the proliferating cardiomyocytes, as shown in **Chapter 3**, suggesting a role in inducing/maintaining cardiomyocyte regeneration.

In summary, it has become clear in the recent years that the intricate process of heart regeneration is well coordinated. Various cell types contribute to their own regeneration and have been shown to influence cardiomyocyte proliferation, as well.

III-4. Molecular factors driving Cardiomyocyte proliferation

The very limited proliferation of adult cardiomyocytes is one of the major hurdles preventing mammalian heart regeneration. As such, it has been the focus for zebrafish cardiac regeneration studies.

Upon injury, several genes are up-regulated in cardiomyocytes. Among these are transcription factors known for their requirement during heart development in the embryo such as *gata4*, *nkx2.5*, *hand2*, *tbx5* and *tbx20* [32]. These cardiac transcription factors are induced during heart regeneration, but their functional requirement has not been addressed. Jak1/Stat3 signaling, on the other hand, was identified to be essential for cardiac regeneration: experimental cardiomyocyte-specific, cre-inducible knockdown restricted cardiomyocyte proliferation and regeneration [36]. Jak/Stat signaling is often induced by the immune injury response [reviewed in 37]. The immune system has been shown to also induce NF-kB signaling in cardiomyocytes. Aberrant NF-kB signaling had a negative effect on the regeneration of the heart [38]. As such, NF-kB has been implicated to be a key node between cardiac injury and tissue regeneration. As introduced above, signaling from other cell types like the epicardium can induce regeneration of the myocardium. Epicardial derived Fibroblast Growth Factor (FGF), Platelet-Derived Growth Factor (PDGF) and Neuregulin 1 (NRG1) have all been shown

to support regeneration of the myocardium [32, 34, 39, 40]. Of these molecules, NRG1 has been demonstrated to also induce cardiomyocyte proliferation in mammalians [13-15], as introduced in part II. Moreover, Transforming Growth Factor (TGFb) signaling, whose source is unknown, is necessary for successful regeneration of the heart [41]. Insulin-like Growth Factor (IGF), probably originating from the endocardium, epicardium or macrophages, is similarly needed for regeneration to progress [42]. Lastly, Notch signaling also plays a role in promoting cardiomyocyte proliferation. Interestingly, both knock-down and over-expression abolished heart regeneration, suggesting a high sensitivity to perturbations in Notch signaling [43].
While all of these signaling pathways (Figure 2) are necessary for achieving cardiomyocyte proliferation, little is known about how these signaling pathways interact to guide cardiomyocyte replacement.

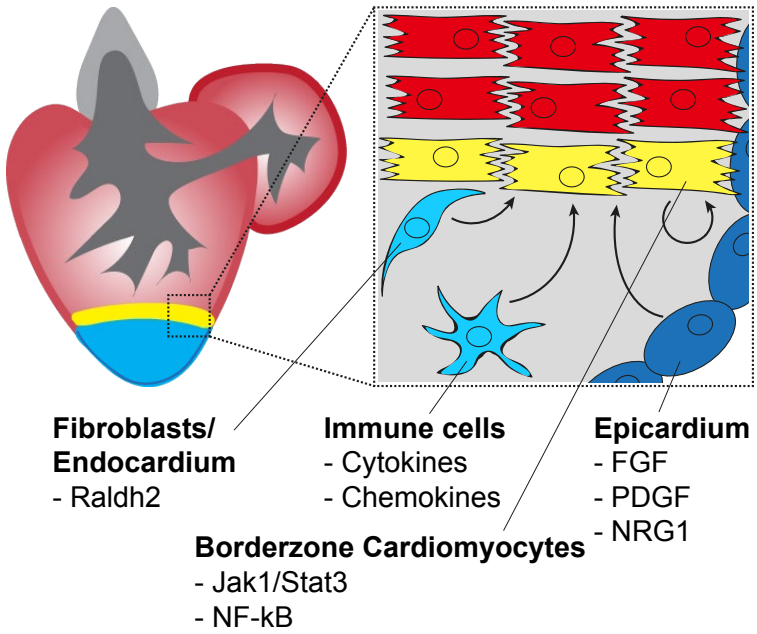

Figure 2: Molecular pathways guiding cardiomyocyte regeneration after injury in zebrafish. *Molecular factors originating from various cell types (Epicardium, Immune cells, Fibroblasts, Endothelium and Cardiomyocytes) have been shown to influence proliferation of borderzone cardiomyocytes during heart regeneration.*

III-5. An underestimated factor: the immune response during cardiac regeneration
The innate immune system is the first line of defense against harmful factors in the body. The innate immune system is represented by the white blood cells, also called leukocytes. A major part of the innate immune response are the phagocytic cells, mainly neutrophils and macrophages. Phagocytes are immune cells that engulf pathogens and particles. As such,

they are also important for the removal of dead tissue, for instance after an insult to the heart, thereby playing an important role in the healing process following injury.

Neutrophils are among the first-responders of inflammatory cells, being a hallmark of acute inflammation [44]. Macrophages are the largest phagocytes. Traditionally, there are two types of macrophages. The proinflammatory subtype of M1 "killer" macrophages is activated by IFNg. M2 "repair" macrophages on the other hand encourage wound healing and repair, counteracting damage by prolonged immune system activation [45]. Thus, the timing of macrophage recruitment during heart regeneration needs to be firmly controlled. Initially, the dead tissue needs to be cleared. But afterwards the pro-repair-function of M2 macrophages is necessary to efficiently repair the heart. This classification has been suggested to be an oversimplification that only characterizes two extreme states [46]. However, for the scope of this thesis the M1-M2 concept suffices, especially because there is still much debate about how to classify macrophages.

The role of macrophages during inflammation or scar formation has been studied in detail. However, it is unclear what part they play during cardiac regeneration. *In vitro* studies have shown that activated macrophages secrete a variety of signaling molecules like interleukin-10, FGF-1, leukemia inhibitory factor and IGF-1, inhibiting apoptosis of hypoxic cardiomyocytes [47]. These results suggest an important, if not crucial, role of the immune response during regeneration. Initial studies in neonatal mice, which still retain the ability to regenerate the heart, indicate that myocardial regeneration is dependent on macrophages [48-50]. Interestingly, macrophage depletion in the regenerating neonatal heart did not impair heart muscle proliferation, but rather re-vascularization [48].

Experiments on zebrafish have confirmed a critical role for the early immune response in regeneration. Inhibition of the inflammatory response with glucocorticoids led to excessive collagen deposition, as a consequence of reduced phagocyte recruitment, diminished angiogenesis and cell proliferation [51]. De Preux and colleagues addressed the dynamics of white blood cells during zebrafish heart regeneration in more detail using a leukocyte-specific antibody. They found that leukocyte numbers peak at 4 dpi. Moreover, inhibition of the innate immune response using clodrosomes or PLX3397 strongly suppressed mitotic activity in cardiomyocytes and heart regeneration in general [52]. While these studies shed light on the importance of the early immune response for cardiac regeneration, more experiments are needed to understand which roles are played by the various parts of the immune system. **Chapter 5** will address this topic in more detail, providing detailed dynamics of macrophages and neutrophils.

IV. Single cell biology: how to detect differences between neighboring cells?

Almost every cell in the body of an organism contains the exact same DNA, which harbors all the genes. So how do cells develop different fates, acquire different properties and have

different functions? If a macrophage and a cardiomyocyte contain the same DNA, how can they be so different? Why does one cardiomyocyte proliferate while its neighbor does not? The answer lies in the fact that only a defined set of genes is "active" within a certain cell type. During the development from a fertilized egg to a mature organism, cells gradually differentiate into diverse fates, with gene expression becoming progressively restricted. The variety and strength of the genes expressed defines the type and function of a cell. Conversely, the cell type can also be inferred by a characteristic gene-signature. One of the fundamental concepts in biology is that DNA is transcribed to RNA, which in turn is translated into protein. Generally, proteins carry out the vast majority of functions in a cell. Proteins can be detected by means of immunohistochemistry, for example. In simplified terms, an antibody specifically binds to a protein-of-interest, which can be visualized by different means, e.g. fluorescent staining. Since there are only a finite number of fluorescent spectra that can be reliably differentiated, this approach is limited to only a handful of proteins-of-interest per sample. However, it allows single-cell specific study of protein localization. Similarly, RNAs encoding these proteins can be detected by (fluorescent) *in-situ* hybridization, providing single-cell resolution for a finite number of RNAs-of-interest (Figure 3).

On the contrary, "omics" studies, such as proteomics, transcriptomics and metabolomics, have become increasingly powerful in the recent decade. Most notably in this context, a technique widely used is RNA-sequencing, also referred to as transcriptomics. Here, all the RNAs from a tissue-of-interest are sequenced in an unbiased manner. Opposed to the targeted staining-approaches introduced above, RNA-sequencing provides information on the expression levels of all genes, allowing the identification of new RNAs/genes that were not known to be expressed in the tissue-of-interest. The drawback of this approach – until recently – was that large amounts of input material were needed: whole organs or tissues, for example. This restriction made it impossible to identify differences between single cells in a whole transcriptome-wide manner (Figure 3). But small subpopulations of cells might potentially play a big role: as we show later in this thesis, only a subset of cardiomyocytes re-enters the cell cycle. But it is precisely this rare cell population that we need to understand better.

In an effort to combine the advantages of single-cell biology with unbiased RNA-sequencing, new techniques have been developed in recent years. Hashimshony and colleagues have shown that, while technically challenging, mRNA sequencing of single cells is possible [53]. This method has been improved upon in recent years. While samples first had to be processed one cell at a time by hand, we now make use of robots in automated processes [54]. This allows the up-scaling to hundreds and thousands of cells to be analyzed by single-cell transcriptomics (Figure 3). Since this method takes cells out of their natural context, computational strategies have been employed to infer cellular localization, with success to a certain extend [55]. *Tomo*-seq, which takes spatial resolution of a tissue into account while providing whole transcriptome information, has been a dramatic improvement upon this (see

Chapter 2 of this thesis).
Altogether, these new techniques allow the identification and analysis of rare cell populations, for example proliferating cardiomyocytes compared to non-proliferating cardiomyocytes during heart regeneration.

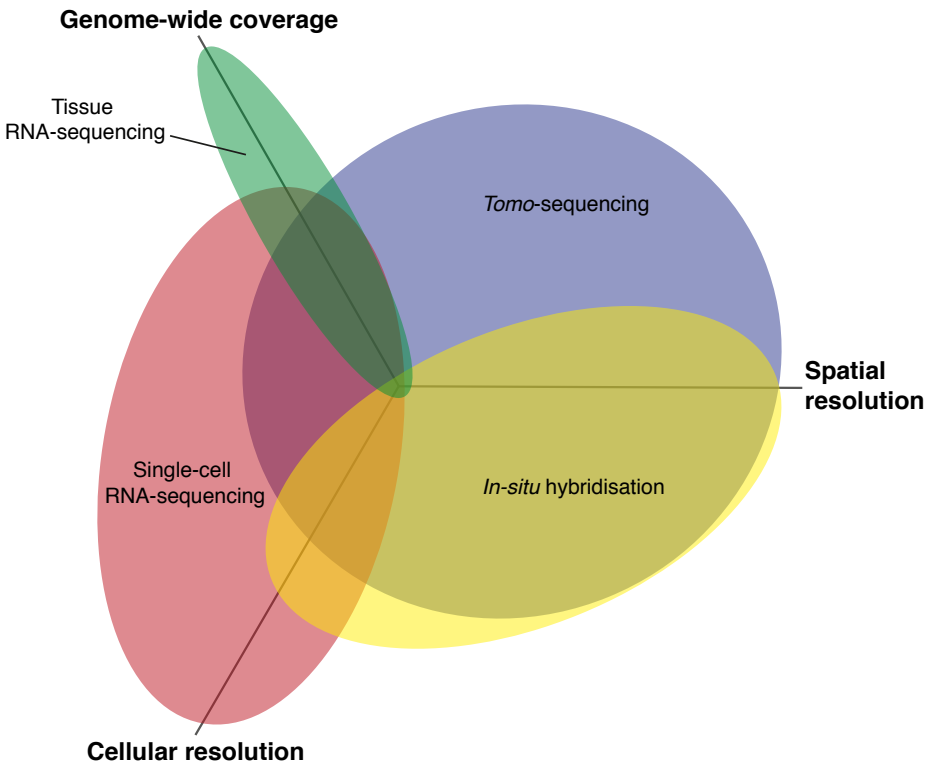

Figure 3: Comparison of methods detecting cell-to-cell transcriptome differences. *Advantages and disavdantages of various methods (Tissue RNA-sequencing, Tomo-sequencing, Single-cell sequencing, In-situ hybridization) are visualized along three parameters: genome-wide coverage, spatial resolution and cellular resolution.*

V. Outline of this thesis

The aim of the work unveiled in this thesis is to find and describe novel mechanisms important for the early phases of heart regeneration in zebrafish. In specific, our focus is on understanding the induction and regulation of cardiomyocyte proliferation.

In **Chapter 2**, *tomo*-seq is described as a technique to acquire whole transcriptome data of a specimen with spatial resolution across one (or more) axis. A step-by-step protocol is supplied for correct and successful generation and analysis of *tomo*-seq data sets.

Chapter 3 builds upon the *tomo*-seq method, applied to the regenerating zebrafish heart. We show how spatially resolved transcriptomics are retrieved for each of the areas in the regenerating heart: injury area, border zone and the remote myocardium. Moreover, we further characterize the borderzone, which we show can be sub-divided into an injury area-related border zone and a myocardial borderzone. Choosing one of the molecular pathways upregulated in the myocardial borderzone, known to harbor the proliferating cardiomyocytes, we describe how bone morphogenetic protein (BMP) signaling is involved in the regenerative process.

Following our special interest in cardiomyocyte proliferation, we go on to perform single-cell sequencing on borderzone cardiomyocytes in **Chapter 4**. Based on the *tomo*-seq data, a transgenic line was generated and used to isolate the border zone cardiomyocytes. We identify a metabolic switch from fatty acid beta-oxidation to glycolysis in the proliferating cardiomyocytes. Moreover, simultaneously with the observed metabolic switch, proliferating cardiomyocytes dedifferentiate and become more embryonic-like, as evidenced by comparison to embryonic single-cell sequencing data.

Investigating upstream initiators of cardiomyocyte dedifferentiation and proliferation, **Chapter 5** focuses on immune cell dynamics during early heart regeneration. First, we established the timeline of macrophage and neutrophil recruitment. Next, based on the expression of several marker genes, we propose that macrophages located in the injury area related borderzone switch to the M2 state. Signifying a conversion to “pro-repair” activity and signaling, we suspect an effect of these M2 macrophages on the neighboring cardiomyocytes, through signaling molecules inducing proliferation.

Chapter 6 aims to put the combined results in perspective, in form of a summarizing discussion.

Bibliography

1. Writing Group, M. *et al*. Executive Summary: Heart Disease and Stroke Statistics--2016 Update: A Report From the American Heart Association. *Circulation* **133**, 447-454 (2016).
2. Laflamme, M.A. & Murry, C.E. Regenerating the heart. *Nat Biotechnol* **23**, 845-856 (2005).
3. Zwetsloot, P.P. *et al*. Cardiac Stem Cell Treatment in Myocardial Infarction: A Systematic Review and Meta-Analysis of Preclinical Studies. *Circ Res* **118**, 1223-1232 (2016).
4. Nigro, P. *et al*. Cell therapy for heart disease after 15 years: Unmet expectations. *Pharmacol Res* (2017).
5. Shiba, Y. *et al*. Allogeneic transplantation of iPS cell-derived cardiomyocytes regenerates primate hearts. *Nature* **538**, 388-391 (2016).
6. Bergmann, O. *et al*. Evidence for cardiomyocyte renewal in humans. *Science* **324**, 98-102 (2009).
7. Senyo, S.E. *et al*. Mammalian heart renewal by pre-existing cardiomyocytes. *Nature* **493**, 433-436 (2013).
8. Porrello, E.R. *et al*. Transient regenerative potential of the neonatal mouse heart. *Science* **331**, 1078-1080 (2011).
9. Heallen, T. *et al*. Hippo pathway inhibits Wnt signaling to restrain cardiomyocyte proliferation and heart size. *Science* **332**, 458-461 (2011).
10. Xin, M. *et al*. Hippo pathway effector Yap promotes cardiac regeneration. *Proc Natl Acad Sci U S A* **110**, 13839-13844 (2013).
11. Heallen, T. *et al*. Hippo signaling impedes adult heart regeneration. *Development* **140**, 4683-4690 (2013).
12. Tao, G. *et al*. Pitx2 promotes heart repair by activating the antioxidant response after cardiac injury. *Nature* **534**, 119-123 (2016).
13. Polizzotti, B.D. *et al*. Neuregulin stimulation of cardiomyocyte regeneration in mice and human myocardium reveals a therapeutic window. *Sci Transl Med* **7**, 281ra245 (2015).
14. Bersell, K., Arab, S., Haring, B. & Kuhn, B. Neuregulin1/ErbB4 signaling induces cardiomyocyte proliferation and repair of heart injury. *Cell* **138**, 257-270 (2009).
15. D'Uva, G. *et al*. ERBB2 triggers mammalian heart regeneration by promoting cardiomyocyte dedifferentiation and proliferation. *Nat Cell Biol* **17**, 627-638 (2015).
16. Nakada, Y. *et al*. Hypoxia induces heart regeneration in adult mice. *Nature* **541**, 222-227 (2017).
17. Wei, K. *et al*. Epicardial FSTL1 reconstitution regenerates the adult mammalian heart. *Nature* **525**, 479-485 (2015).
18. Gemberling, M., Bailey, T.J., Hyde,

D.R. & Poss, K.D. The zebrafish as a model for complex tissue regeneration. *Trends Genet* **29**, 611-620 (2013).

19. Creaser, C.W. The technic of handling the zebra fish (Brachydanio rerio) for the production of eggs which are favorable for embryological research and are available at any specified time throughout the year. *Copeia* **4**, 159-161 (1934).
20. Meunier, R. Stages in the development of a model organism as a platform for mechanistic models in developmental biology: Zebrafish, 1970-2000. *Stud Hist Philos Biol Biomed Sci* **43**, 522-531 (2012).
21. Poss, K.D., Wilson, L.G. & Keating, M.T. Heart regeneration in zebrafish. *Science* **298**, 2188-2190 (2002).
22. Wang, J. *et al*. The regenerative capacity of zebrafish reverses cardiac failure caused by genetic cardiomyocyte depletion. *Development* **138**, 3421-3430 (2011).
23. Chablais, F., Veit, J., Rainer, G. & Jazwinska, A. The zebrafish heart regenerates after cryoinjury-induced myocardial infarction. *BMC Dev Biol* **11**, 21 (2011).
24. Gonzalez-Rosa, J.M., Martin, V., Peralta, M., Torres, M. & Mercader, N. Extensive scar formation and regression during heart regeneration after cryoinjury in zebrafish. *Development* **138**, 1663-1674 (2011).
25. Schnabel, K., Wu, C.C., Kurth, T. & Weidinger, G. Regeneration of cryoinjury induced necrotic heart lesions in zebrafish is associated with epicardial activation and cardiomyocyte proliferation. *PLoS One* **6**, e18503 (2011).
26. Jopling, C. *et al*. Zebrafish heart regeneration occurs by cardiomyocyte dedifferentiation and proliferation. *Nature* **464**, 606-609 (2010).
27. Kikuchi, K. *et al*. Primary contribution to zebrafish heart regeneration by gata4(+) cardiomyocytes. *Nature* **464**, 601-605 (2010).
28. Ahuja, P., Perriard, E., Perriard, J.C. & Ehler, E. Sequential myofibrillar breakdown accompanies mitotic division of mammalian cardiomyocytes. *J Cell Sci* **117**, 3295-3306 (2004).
29. Fan, X. *et al*. Dynamic Alterations to alpha-Actinin Accompanying Sarcomere Disassembly and Reassembly during Cardiomyocyte Mitosis. *PLoS One* **10**, e0129176 (2015).
30. Kikuchi, K. *et al*. Retinoic acid production by endocardium and epicardium is an injury response essential for zebrafish heart regeneration. *Dev Cell* **20**, 397-404 (2011).
31. Wang, J., Cao, J., Dickson, A.L. & Poss, K.D. Epicardial regeneration

is guided by cardiac outflow tract and Hedgehog signalling. *Nature* **522**, 226-230 (2015).

32. Lepilina, A. *et al*. A dynamic epicardial injury response supports progenitor cell activity during zebrafish heart regeneration. *Cell* **127**, 607-619 (2006).
33. Georgijevic, S. *et al*. Spatiotemporal expression of smooth muscle markers in developing zebrafish gut. *Dev Dyn* **236**, 1623-1632 (2007).
34. Kim, J. *et al*. PDGF signaling is required for epicardial function and blood vessel formation in regenerating zebrafish hearts. *Proc Natl Acad Sci U S A* **107**, 17206-17210 (2010).
35. Santoro, M.M., Pesce, G. & Stainier, D.Y. Characterization of vascular mural cells during zebrafish development. *Mech Dev* **126**, 638-649 (2009).
36. Fang, Y. *et al*. Translational profiling of cardiomyocytes identifies an early Jak1/Stat3 injury response required for zebrafish heart regeneration. *Proc Natl Acad Sci U S A* **110**, 13416-13421 (2013).
37. Li, H.S. & Watowich, S.S. Innate immune regulation by STAT-mediated transcriptional mechanisms. *Immunol Rev* **261**, 84-101 (2014).
38. Karra, R., Knecht, A.K., Kikuchi, K. & Poss, K.D. Myocardial NF-kappaB activation is essential for zebrafish heart regeneration. *Proc Natl Acad Sci U S A* **112**, 13255-13260 (2015).
39. Gemberling, M., Karra, R., Dickson, A.L. & Poss, K.D. Nrg1 is an injury-induced cardiomyocyte mitogen for the endogenous heart regeneration program in zebrafish. *Elife* **4** (2015).
40. Lien, C.L., Schebesta, M., Makino, S., Weber, G.J. & Keating, M.T. Gene expression analysis of zebrafish heart regeneration. *PLoS Biol* **4**, e260 (2006).
41. Chablais, F. & Jazwinska, A. The regenerative capacity of the zebrafish heart is dependent on TGFbeta signaling. *Development* **139**, 1921-1930 (2012).
42. Huang, Y. *et al*. Igf Signaling is Required for Cardiomyocyte Proliferation during Zebrafish Heart Development and Regeneration. *PLoS One* **8**, e67266 (2013).
43. Zhao, L. *et al*. Notch signaling regulates cardiomyocyte proliferation during zebrafish heart regeneration. *Proc Natl Acad Sci U S A* **111**, 1403-1408 (2014).
44. Rua, R. & McGavern, D.B. Elucidation of monocyte/macrophage dynamics and function by intravital imaging. *J Leukoc Biol* **98**, 319-332 (2015).
45. Liu, Y.C., Zou, X.B., Chai, Y.F. & Yao, Y.M. Macrophage polarization in inflammatory diseases. *Int J Biol Sci* **10**, 520-529 (2014).
46. Martinez, F.O. & Gordon, S. The M1 and M2 paradigm of

macrophage activation: time for reassessment. *F1000Prime Rep* **6**, 13 (2014).

47. Trial, J., Rossen, R.D., Rubio, J. & Knowlton, A.A. Inflammation and ischemia: macrophages activated by fibronectin fragments enhance the survival of injured cardiac myocytes. *Exp Biol Med (Maywood)* **229**, 538-545 (2004).
48. Aurora, A.B. *et al*. Macrophages are required for neonatal heart regeneration. *J Clin Invest* **124**, 1382-1392 (2014).
49. Epelman, S. *et al*. Embryonic and adult-derived resident cardiac macrophages are maintained through distinct mechanisms at steady state and during inflammation. *Immunity* **40**, 91-104 (2014).
50. Konfino, T., Landa, N., Ben-Mordechai, T. & Leor, J. The type of injury dictates the mode of repair in neonatal and adult heart. *J Am Heart Assoc* **4**, e001320 (2015).
51. Huang, W.C. *et al*. Treatment of Glucocorticoids Inhibited Early Immune Responses and Impaired Cardiac Repair in Adult Zebrafish. *PLoS One* **8**, e66613 (2013).
52. de Preux Charles, A.S., Bise, T., Baier, F., Marro, J. & Jazwinska, A. Distinct effects of inflammation on preconditioning and regeneration of the adult zebrafish heart. *Open Biol* **6** (2016).
53. Hashimshony, T., Wagner, F., Sher, N. & Yanai, I. CEL-Seq: single-cell RNA-Seq by multiplexed linear amplification. *Cell Rep* **2**, 666-673 (2012).
54. Grun, D. *et al*. De Novo Prediction of Stem Cell Identity using Single-Cell Transcriptome Data. *Cell Stem Cell* **19**, 266-277 (2016).
55. Satija, R., Farrell, J.A., Gennert, D., Schier, A.F. & Regev, A. Spatial reconstruction of single-cell gene expression data. *Nat Biotechnol* **33**, 495-502 (2015).

1

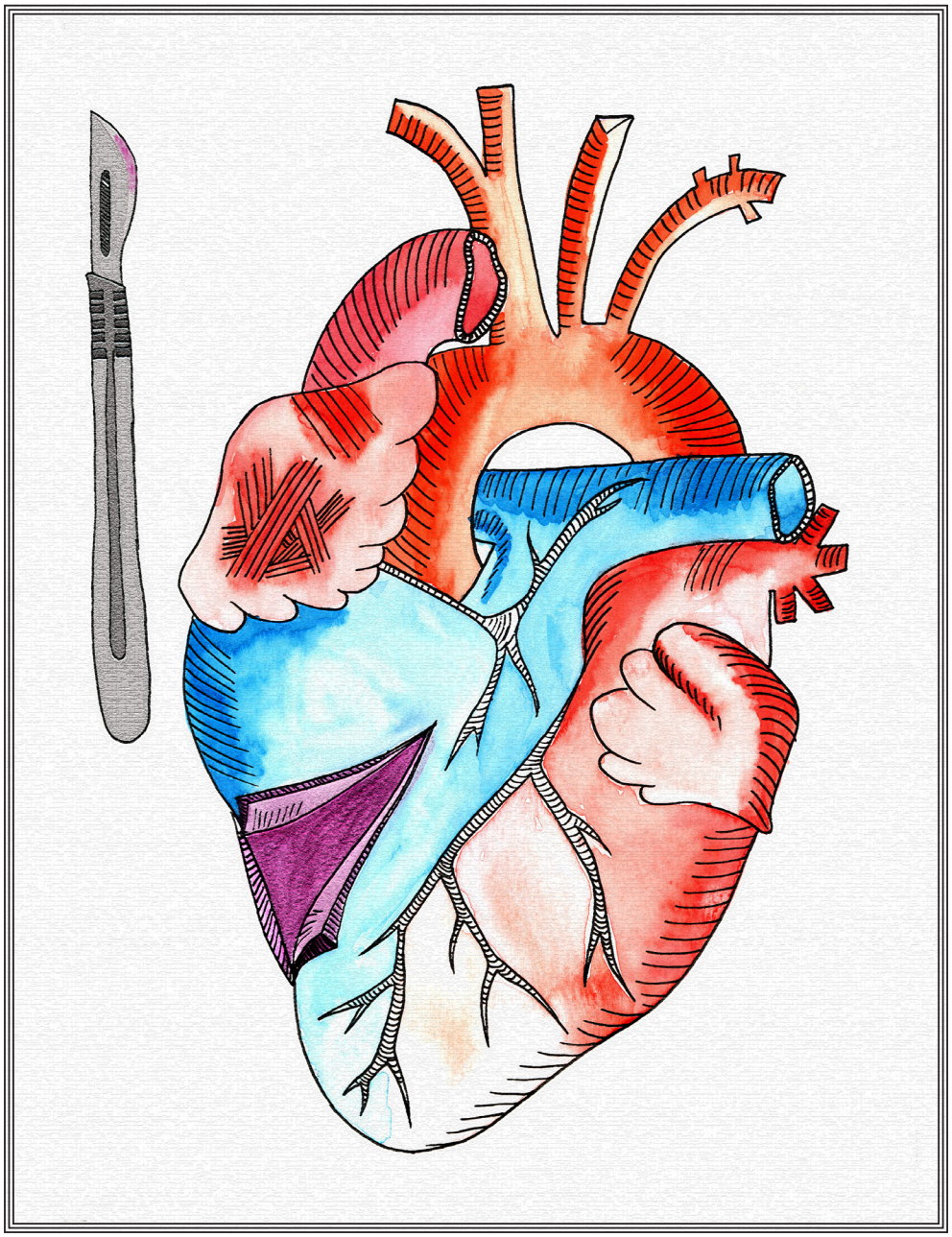

2

Tomo-seq: A method to obtain genome-wide expression data with spatial resolution

Fabian Kruse, Jan Philipp Junker, Alexander van Oudenaarden & Jeroen Bakkers

Hubrecht Institute and University Medical Centre Utrecht, Utrecht, The Netherlands

Adapted with permission from: *Methods in Cell Biology (2016) 135:299-307*

Abstract

To improve our understanding of pattern formation during development and disease we heavily rely on the identification of novel regulators and pathways. While RNA sequencing yields genome-wide expression data that suits this purpose, it lacks spatial resolution. Such spatial resolution can be obtained by microscopy-based methods like *in situ* hybridization, but these fail to provide information on more than a few genes at a time. Here, we describe *tomo*-seq, a technique that combines the advantages of the above-mentioned approaches and provides genome-wide expression data with spatial information. The *tomo*-seq technique is based on cryosectioning of an embryo or tissue of interest and performing RNA-seq on individual sections. Using this method, we have generated genome-wide transcriptomics with high spatial resolution of the whole zebrafish embryo at various stages of development [1] and of adult zebrafish hearts after injury [2].

Key words

RNA-seq, Zebrafish, Embryo, Gene expression, Patterning

I. Introduction

Embryogenesis could not proceed if specific regulators and pathways were not restricted to well-defined regions to ensure asymmetry, directionality and growth into the proper shape. As such, it is fundamental for development that certain genes are expressed in a temporally and spatially restricted domain. Early dorsoventral patterning, for example, requires expression and function of BMP inhibitors such as *chordin* in the dorsal organizer [reviewed in 3]. Thus far, the study of such factors relied on immunohistochemistry or mRNA *in situ* hybridization, which limit the focus to only a few genes per sample. RNA sequencing, on the contrary, provides the power to study the whole transcriptome. While the requirement for high amounts of input material has limited its use for small samples in the past, recent development of strategies to amplify RNA for single-cell sequencing approaches has attenuated this restriction [4-8]. While these techniques have certainly been proven to be very useful, they take cells out of their natural context. Computational strategies are required to infer cellular localization by integrating *in situ* hybridization patterns with single-cell RNA-sequencing data [9].

By adopting protocols for single-cell RNA sequencing, we have established a method to detect spatially resolved genome-wide transcriptomics experimentally, called *tomo*-seq [1]. This method is based on cryosectioning of frozen samples, followed by RNA extraction from individual sections and cDNA synthesis with barcoded primers. In vitro transcription is then used to linearly amplify the cDNA. The addition of barcodes allows identifying which transcript originated from which section. As a result, expression profiles of all detected genes can be generated. Moreover, bioinformatics analysis can generate lists of genes that have a similar expression pattern to a gene of interest. As such, this analysis can identify new factors that are differentially expressed in a region of interest. Moreover, samples taken from multiple embryos or tissues can be pooled in a single sequencing run, reducing the costs for these experiments. In summary, *tomo*-seq provides genome-wide sensitivity with high spatial resolution and can be used to identify genes that are upregulated in a region of interest.

II. Tissue extraction and embedding

The following protocol is very versatile in its applicability. It can be used for a whole (zebrafish) embryo or different organs of various organisms, given a reasonably well annotated genome. To start of with, euthanize the individual animal and directly extract the organ of interest (if applicable). Without any delay, place the tissue in a Tissue-Tek cryomold (Sakura) containing tissue freezing medium (Jung). The tissue can be oriented in the desired position (in relation to the sectioning plane) under a dissection microscope. Affi-Gel Blue Gel beads (100-200 mesh BioRad) can be positioned right in front and behind the tissue. This is helpful during the sectioning process to know when to start and when to stop collecting sections. After proper orientation of the tissue, the mold containing the tissue is placed on dry ice until completely frozen and stored at -80 °C *until further use*.

III. Cryosectioning and Trizol extraction

Before sectioning, labeled LoBind 1.5-ml-tubes (Eppendorf) should be pre-chilled on dry-ice for >30 minutes. Cryosections are made at the desired thickness and intervals, however it is not recommended to section at <10 *μm due to inaccuracy of the cryotome*. The diameter of the tissue that is sectioned may be as small as a few cells, since the protocol was adapted from single-cell RNA-seq methods. Importantly, one should try to cut away large areas of empty tissue freezing medium prior to sectioning. Ideally, the tissue is surrounded by less than 3 mm of tissue freezing medium. Each section is then placed in the bottom of a different tube and kept on dry-ice. The maximum number of sections per sample is 96, due to limitation in barcodes of the primers. Prior to Trizol extraction, the tubes containing the sections should be "warmed up" at -20°C for 10 minutes. In the meantime a master mix containing Trizol (Ambion, for the RNA-extraction), GlycoBlue (Ambion, for visualization of the pellet) and ERCC spike-in RNA (Ambion, to keep track of technical variation) should be prepared: 0.5 ml Trizol, 0.5 μl GlycoBlue, 2 *μl ERCC spike-in (stock 1:5*0,000) per tube. The concentration of the spike-in RNA varies depending on the size of the tissue per section, the above concentration is used for 12 μm sections of zebrafish embryos, where one section contains ~100 cells [1]. Ideally, one would like to end up with ~200 reads spike-in per section. The RNA extraction should not be performed on more than 48 sections at once to ensure sufficient RNA quality. Next, the tubes are taken out of the freezer and RNA-extraction is performed as follows:

1. Add 0.5 ml of the Trizol-mix to each Eppendorf tube and incubate for 3' at RT.
2. Add 0.1 ml Chloroform, vigorously shake all tubes together by hand for 15", incubate 2-3' at RT.
3. Centrifuge at 12.000g for 15'at 4°C, transfer upper aqueous phase to a fresh tube (note: avoid transferring any other phase, as it will interfere with the following steps).
4. Add 250 μl Isopropanol and incubate at -20°C for 1h or o/N.
5. Centrifuge at 12.000g for 10'at 4°C, remove supernatant (the pellet is visible in blue).
6. Add 0.5 ml of ice-cold 75% EtOH and vortex briefly.
7. Centrifuge at 7500g for 5'at 4°C, remove supernatant, air-dry 5-10'.

For all steps, low-bind tubes and pipette-tips should be used. While working with RNA, perform the steps without delay in order to prevent RNA degradation.

IV. cDNA synthesis

Now, the RNA pellets should quickly be resuspended by pipetting in 1.2 *μl* of the barcoded primer mix (at 5 ng/μl). cDNA synthesis and cleanup using the MessageAmpII kit (Ambion) is performed as below. The barcoded-RT primer has several distinct regions: an anchored

polyT, a unique barcode (8 nucleotides, differs for every tube/section), a unique molecule identifier (4 nucleotide random barcode, helps identify amplification biases), the 5' Illumina adapter and a T7 promoter sequences available in [1,2].

1. Incubate primer-RNA-mix 5' at 70*°C*.
2. Add 0.2 µl first strand buffer + 0.4 µl dNTP + 0.1 µl RNase inhibitor + 0.1 µl ArrayScript and incubate for 2h at 42°C.
3. Add 6.3 *µl of water + 1 µl second strand buffer + 0.4 µl dNTP + 0.2 µl DNA pol + 0.1 µl RNase H*
4. Incubate for 2h at 16°C (thermal cycler with unheated lid).
5. Pool all tubes of the same sample in a 1.5-ml-tube (samples can now be stored at -20°) and add 250 µl cDNA binding buffer per 100 µl (volume of 1 section is ~10 *µl*). In case the volume is lower (i.e. less than 10 sections are combined), adjust the volume to 100 *µl*. Load the sample mix onto a cDNA cleanup column.
6. Centrifuge 1' at 10.000g, discard flow-through (if necessary repeat this step until whole sample is loaded).
7. Add 500 *µl wash buffer, Centrifuge 1' at 10.000g, discard flow-through*, spin once more to dry the column.
8. Transfer spin-column to fresh round-bottom 2ml tube.
9. Add 15 *µ*l pre-heated (55°C) nuclease-free water (Ambion), incubate 2' and spin 1.5' at 10.000g.
10. Repeat elution (samples can now be stored at -20°C).

In case of samples with low amounts of input (<20 cells per section) it is advisable to dry the sample in a speedvac and dissolve the pellet in 6.4 *µl* nuclease-free water.

V. In vitro transcription

In order to minimize amplification biases, in vitro transcription is performed for linear amplification of cDNA [4]. To 6.4 *µ*l of sample from the previous step add 1.6 *µ*l of each nucleotide (dATP, dGTP, dCTP and dUTP), 1.6 *µ*l of 10x T7 buffer and 1.6 *µ*l of T7 enzyme (MessageAmpII kit, Ambion) and incubate for 13h at 37°C (thermal cycler lid at 70°C). Next, the amplified RNA (aRNA) is fragmented by adding 4 *µ*l Fragmentation buffer (200mM Tris-acetate, pH 8.1, 500 mM KOAc, 150 mM MgOAc) and incubated for exactly 1'40" at 94°C before quenching on ice and immediately adding 2 *µ*l Fragmentation STOP buffer (0.5 M EDTA). The sample volume is adjusted by adding 8 *µ*l nuclease-free water prior to cleanup (MessageAmpII kit, Ambion). The following steps (loading and binding of aRNA to column) should not be performed for more than one sample at a time. Before loading the sample onto an aRNA spin column, 105 *µ*l aRNA binding buffer is added to the sample, followed by 75 *µ*l EtOH. The sample is immediately mixed by pipetting 3-4 times, loaded onto the column and centrifuged for 1' at 10.000g. Discard the flow-through, add 0.5 ml wash buffer to the column

and proceed with the next sample. When all samples are loaded to the columns, continue with all samples together to perform the wash-step by spinning for 1' at 10.000g. Discard the flow-through and centrifuge again for 1' at 10.000g before transfer of the spin-column to a fresh tube. Elute twice by adding 15 μl pre-heated (55°C) nuclease-free water, incubating for 2' and spinning for 1.5' at 10.000g. Samples can now be stored at -80°C. Check the aRNA amount and quality by loading 1 μl onto Bioanalyzer RNA pico chip (Agilent). The size distribution should peak at 500 bp. If not, the time of the fragmentation should be adjusted accordingly. When starting the in vitro transcription with 0.5 ng total RNA the expected yield is 500-1000 pg/μl.

VI. Library preparation

For a successful library preparation (Illumina TruSeq small RNA sample prep kit, unless otherwise specified), an aRNA concentration of *>1μg/μl is recommended. If the concentration is lower,* it is advisable to concentrate the sample in a speedvac until a sufficient concentration is reached.

First, ligate the 3'adapter to the aRNA from the previous step. To 5 μl of aRNA add 1 μl of 5x diluted RA3 and incubate for 2' at 70°C before quenching on ice. Add 2 μl HML + 1 μl RNase inhibitor + 1 μl truncated T4 RNA ligase (NEB) and incubate for 1h at 28°C. Add 4 μl nuclease-free water to adjust the volume.

Now, the reverse transcription reaction can be set up. To 6 μl of adapter-ligated RNA from previous step (rest can be stored at -80*°C*) add 1 μl RTP and incubate for 2' at 70°C before quenching on ice. Add 2 μl 5x first strand buffer (from superscript kit, Invitrogen), 0.5 μl of 2x diluted dNTPs, 1 μl 100mM DTT (from superscript kit), 1 μl RNase inhibitor, 1 μl Superscript III reverse transcriptase and incubate for 1h at 50°C.

For the following PCR amplification add 8.5 μl ultra pure water, 25 μl PLM and 2 μl RP1. To each library add 2 μl of uniquely indexed RNA PCR primer (RPIX). Run the following PCR program: 98*°C for 30", 14x (*98*°C for 10",* 60*°C for 30",* 72*°C for 30"),* 72*°C for 10',* 4*°C final hold*. Samples can now be stored at -20*°C*.

Clean-up of the libraries is performed using AMPure XP beads (Beckman Coulter). Beads should be pre-warmed at room temperature. Vortex beads until well dispersed before adding 45 μl of beads to 50 μl PCR reaction. Mix well by pipetting and incubate for 15 minutes.

On a magnetic stand that holds 1.5 μ*l* tubes:

1. Place tubes on stand until liquid appears clear (>5') and then remove supernatant.
2. Add 200 μl fresh 80% EtOH (room temperature) and incubate >30" and then remove supernatant.
3. Add 200 μl fresh 80% EtOH and incubate >30" and then remove supernatant.
4. Air-dry for 15' (or until completely dry).

Resuspend with 32.5 μ*l EBT* (10 mM Tris pH8.5, 0.02% Tween-20) and mix by pipetting.

Incubate for 2' to allow the DNA to dissociate from the beads.
On a magnetic stand:

1. Place tubes on stand until liquid appears clear (>5').
2. Transfer 30 μl of supernatant to new tube.

Repeat the bead clean-up, but this time use 35 μl beads and resuspend with 12.5 μl *EBT*. Check the DNA concentration in 1 μl on the Qubit® Fluorometer (Invitrogen) using high sensitivity reagents (dsDNA HS Assay, Invitrogen). The expected concentration should be above 1 ng/μl. Check the size distribution by running 1 μl on a Bioanalyzer (high sensitivity DNA kit, Agilent): expected peak at 300-400 bp. The libraries are now ready to be sequenced by paired-end Illumina sequencing at 50bp read length.

VII. Data Analysis

The obtained paired-end reads can be aligned to the transcriptome using Burrows-Wheeler Aligner's Smith-Waterman Alignment (BWA-SW) [10]. The 5' mate of each pair should be mapped to the reference gene model and reads that map equally well to multiple loci should be discarded. The 3' mate is used for barcode information. Mappability, total number of reads and the number of mapped genes depends on several factors like the origin and amount of input material and the quality of the reference genome. In any case, these parameters should be tracked across different samples to ensure reliable and persistent quality.

The following data analysis can best be performed using the freeware R or MATLAB (MathWorks). Read counts can be normalized either to total counts per section or by linear fit to spike-in RNA reads. The data should afterwards be normalized to the median of total reads across sections to ensure rough correspondence between count numbers and number of mapped reads. Subsequent analyses should be performed on data normalized in such a way.

There are many different ways to analyze the *tomo*-seq data, which will depend on the biological question to be addressed. A good start is a correlation analysis. Here, pairs of sections are compared to each other across all expressed genes. The resulting heatmap plots will show clusters of sections that are similar (or different) to each other, thereby recapitulation the architecture of the tissue that was sectioned and sequenced. For example the correlation plot that was made with *tomo*-seq data of the adult zebrafish heart after cryo-injury showed a distinction between injury area, borderzone and remote/uninjured myocardium [2]. To identify genes with localized expression, clustering of expression traces can be very useful. This analysis can be performed after feature selection (e.g. after filtering for genes with a peak of expression along the sectioning coordinate). The filtered genes are then clustered (e.g. by hierarchical clustering) by similarity of their expression profiles, thereby revealing groups of genes that are possibly co-regulated.

Together, the cluster and correlation analysis provide a good overview of the different zones that are found in the tissue at hand. In most cases it will be very helpful to validate the

tomo-seq data by *in situ* hybridization on selected candidate genes that are predicted to be upregulated in a specific region. As an example we like to point at the *tomo*-seq analysis on the cryo-injured zebrafish heart. The *tomo*-seq analysis predicted the presence of two distinct border zones in the injured heart, which presence we confirmed by *in situ* hybridizations [2].

VIII. Summary and Conclusions

Here, we describe *tomo*-seq, a method to gain whole-genome transcriptomics data in a spatially resolved manner. The protocol described above is easy to implement because it relies on standard laboratory equipment and commercially available reagents. It is very broadly applicable since it can be used on whole organisms (e.g. the zebrafish embryo), but also on isolated organs or tissues (e.g. zebrafish adult heart). We have also successfully used *tomo*-seq on isolated embryonic zebrafish hearts indicating that the method can be downscaled to very small samples. Only few adjustments are necessary to adopt the protocol. The section-size can be varied depending on the research question and the input of spike-in RNA should be adjusted to the amount of input tissue per section (see section III). For very low input of RNA it might be necessary to concentrate the sample before continuation of the reverse transcription (section V) and again before the library preparation (section VI).

In most cases, *tomo*-seq will only be possible in one direction, thus providing 1D data. Since pattern formation often happens along one body axis, this is sufficient in most cases. However, in the case of the zebrafish embryo, which develops in a highly synchronized and staged manner, we had the unique opportunity to perform 3D RNA-tomography [1]. The spatial information provided by 3D RNA-tomography recapitulates the actual zone of expression in the embryo.

Moreover, *tomo*-seq provides several advantages over computational analyses that infer cellular localization of RNA-seq data [9]. This method heavily relies on reference genes for which *in situ* patterns are available. As such, it will have a big disadvantage working with mutants, for example. In mutants, the expression of some reference genes is likely disturbed and computational analyses will have difficulty reconstructing a cellular context. On the contrary, *tomo*-seq will not encounter this problem since it does not rely on *in situ* patterns.

One limitation of *tomo*-seq is that it does not provide the spatial resolution of microscopy-based techniques. We recommend always validating candidate genes by immunohistochemistry or *in situ* hybridization, also because these methods provide additional information like cell-type specificity.

Moreover, *tomo*-seq data can complement single cell RNA-seq results. While single cell RNA-sequencing has the power to identify expression programs in defined cell populations, *tomo*-seq will be able to put these results in the context of the tissue that is under investigation. Vice versa, *tomo*-seq can identify genes that are upregulated in a specific region, which subsequently can be used to genetically mark these cells for more detailed analysis by FACS

sorting and single cell RNA-sequencing.

Openly accessible *tomo*-seq data sets are of tremendous value to the zebrafish community, since searching for a gene-of-interest can be done in a simple manner. Moreover, genes with similar expression traces to a gene-of-interest can easily be identified. Our analysis revealed that over 10% of the differentially expressed genes in the regenerating heart are uncharacterized, highlighting the potential of *tomo*-seq to identify novel players during development and disease.

Bibliography

1. Junker, J.P. *et al*. Genome-wide RNA Tomography in the zebrafish embryo. *Cell* **159**, 662-675 (2014).
2. Wu, C.C. *et al*. Spatially Resolved Genome-wide Transcriptional Profiling Identifies BMP Signaling as Essential Regulator of Zebrafish Cardiomyocyte Regeneration. *Dev Cell* **36**, 36-49 (2016).
3. Langdon, Y.G. & Mullins, M.C. Maternal and zygotic control of zebrafish dorsoventral axial patterning. *Annual review of genetics* **45**, 357-377 (2011).
4. Hashimshony, T., Wagner, F., Sher, N. & Yanai, I. CEL-Seq: single-cell RNA-Seq by multiplexed linear amplification. *Cell reports* **2**, 666-673 (2012).
5. Islam, S. *et al*. Characterization of the single-cell transcriptional landscape by highly multiplex RNA-seq. *Genome research* **21**, 1160-1167 (2011).
6. Picelli, S. *et al*. Smart-seq2 for sensitive full-length transcriptome profiling in single cells. *Nature methods* **10**, 1096-1098 (2013).
7. Ramskold, D. *et al*. Full-length mRNA-Seq from single-cell levels of RNA and individual circulating tumor cells. *Nature biotechnology* **30**, 777-782 (2012).
8. Tang, F. *et al*. mRNA-Seq whole-transcriptome analysis of a single cell. *Nature methods* **6**, 377-382 (2009).
9. Satija, R., Farrell, J.A., Gennert, D., Schier, A.F. & Regev, A. Spatial reconstruction of single-cell gene expression data. *Nature biotechnology* **33**, 495-502 (2015).
10. Li, H. & Durbin, R. Fast and accurate long-read alignment with Burrows-Wheeler transform. *Bioinformatics* **26**, 589-595 (2010).

2

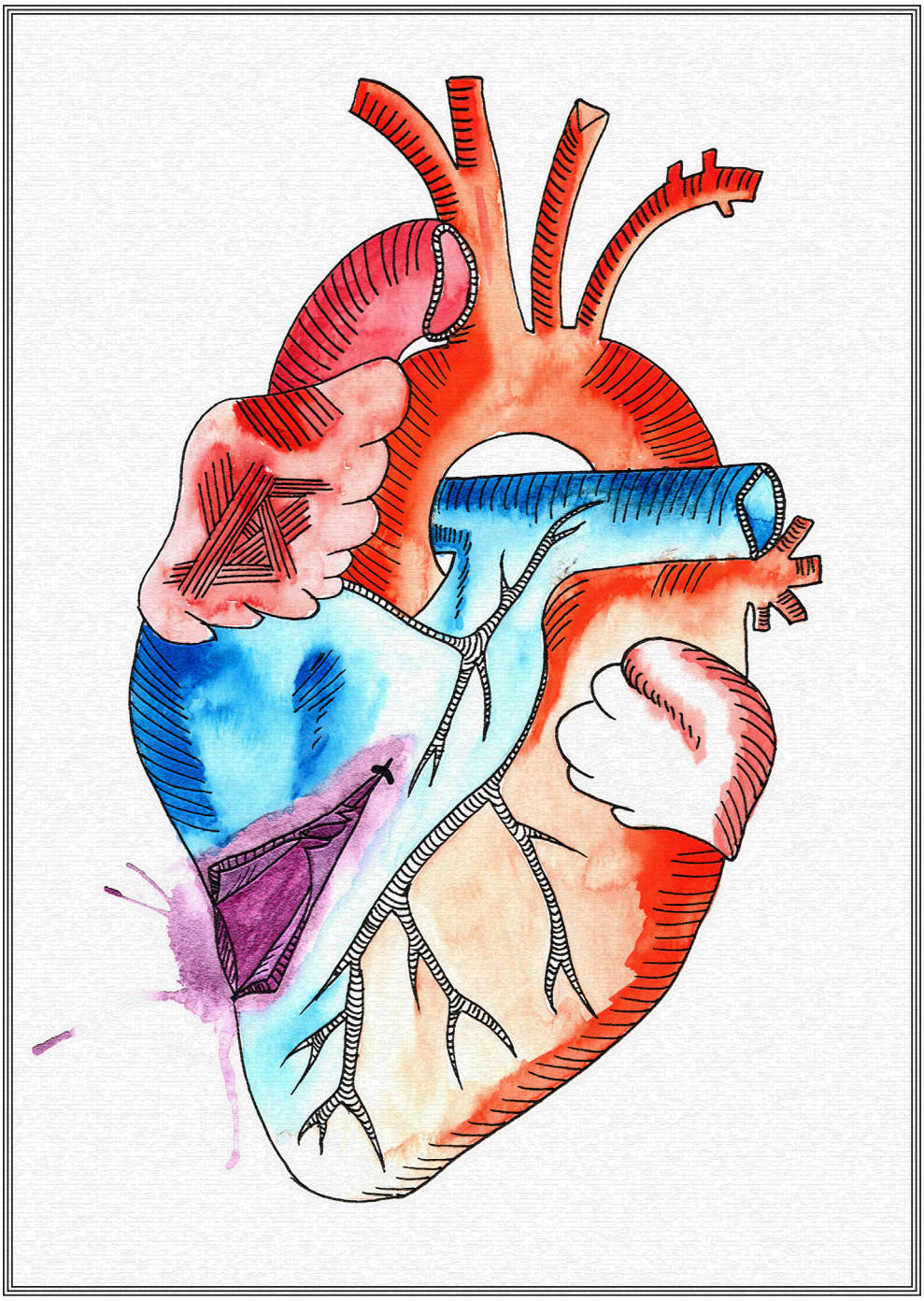

3

Spatially-resolved genome-wide transcriptional profiling identifies Bone Morphogenetic Protein signaling as essential regulator of zebrafish cardiomyocyte regeneration

Chi-Chung Wu[1,*], **Fabian Kruse[2,*]**, Mohankrishna Dalvoy Vasudevarao[1], Jan Philipp Junker[2], David C. Zebrowski[3], Kristin Fischer[4], Emily S. Noël[2], Dominic Grün[2], Eugene Berezikov[5,6], Felix B. Engel[3], Alexander van Oudenaarden[2], Gilbert Weidinger[1,$] and Jeroen Bakkers[2,$]

[1] Institute for Biochemistry and Molecular Biology, Ulm University, Ulm, Germany

[2] Hubrecht Institute and University Medical Centre Utrecht, Utrecht, The Netherlands

[3] Exp. Renal and Cardiovasc. Research, Friedrich-Alexander-Universität Erlangen-Nürnberg, Erlangen, Germany

[4] Institute of Clinical Genetics, Technische Universität Dresden, Dresden, Germany

[5] ERIBA, University of Groningen, University Medical Center Groningen, Groningen, the Netherlands

[6] Skolkovo Institute of Science and Technology, Skolkovo Moscow Region, Russia

* These authors contributed equally

$ Co-senior and joint corresponding authors

Adapted with permission from: *Developmental Cell (2016) 36(1):36-49*

Summary

In contrast to mammals, zebrafish regenerate heart injuries via proliferation of cardiomyocytes located near the wound border. To identify regulators of cardiomyocyte proliferation we applied spatially resolved RNA-seq (tomo-seq) and generated a high-resolution genome-wide atlas of gene expression in the regenerating zebrafish heart. Interestingly, we identified two wound border zones with distinct expression profiles including the re-expression of embryonic cardiac genes and targets of Bone Morphogenetic Protein (BMP) signaling. Endogenous BMP signaling has been reported to be detrimental to mammalian cardiac repair. In contrast, we find that genetic or chemical inhibition of BMP signaling in zebrafish reduces cardiomyocyte dedifferentiation and proliferation, ultimately compromising myocardial regeneration, while *bmp2b* overexpression is sufficient to enhance it. Our results provide a resource for further studies on the molecular regulation of cardiac regeneration and reveal intriguing differential cellular responses of cardiomyocytes to a conserved signaling pathway in regenerative versus non-regenerative hearts.

Highlights

- Tomo-seq reveals genome-wide spatial gene expression profiles of regenerating zebrafish hearts.
- The wound border zone expresses regulators and targets of BMP signaling.
- BMP signaling is activated in cardiomyocytes and promotes their proliferation.
- Heart regeneration requires BMP signaling and is enhanced by pathway activation.

Introduction

Myocardial infarction (MI) is a leading cause of death worldwide. In adult mammals, most cardiomyocytes lost after infarction are not replaced and infarcted hearts develop permanent scars. In contrast, zebrafish display complete scar resolution and regeneration of lost cardiomyocytes after various insults, namely ventricular resection [1], genetic cardiomyocyte ablation [2] and cryoinjury-induced necrotic lesions [3-5]. Genetic fate-mapping experiments have revealed that zebrafish cardiomyocyte regeneration relies primarily on proliferation of spared cardiomyocytes, which show signs of dedifferentiation including disassembled sarcomeric structures and activation of regulatory sequences of the cardiac transcription factor *gata4* [6, 7]. While adult mammalian cardiomyocytes have long been considered to be post-mitotic, there is increasing evidence for low, yet significant cardiomyocyte turnover via proliferation in adult mammalian hearts [8, 9]. Although the rate of natural adult cardiomyocyte proliferation is too low for effective cardiac repair in mammals, its discovery fosters the hope to heal hearts via therapeutic activation of endogenous cardiomyocyte proliferation. A thorough understanding of the mechanisms controlling cardiomyocyte regeneration in zebrafish will be instrumental towards achieving this goal. While several signaling pathways have been implicated in zebrafish myocardial regeneration, including Fibroblast growth factor (Fgf), Retinoic acid (RA), Transforming growth factor-ß (Tgf-ß), Insulin growth factor (Igf), Jak1/Stat3, Notch and Neuregulin signaling [reviewed in 10, 11], little is known about how these signaling pathways regulate cardiomyocyte replacement. Moreover, with the exception of the Jak1/Stat3 pathway [12], it is unclear whether these signals act cell-autonomously in cardiomyocytes or whether they are indirectly required for cardiomyocyte regeneration.

BMP signaling plays several well studied roles during vertebrate cardiovascular development [reviewed in 13], while its role after cardiac injury is less clear. In mouse hearts BMP signaling appears to be activated within hours after MI, as indicated by expression of BMP ligands and accumulation of phosphorylated Smad1/5/8, a readout for active BMP signaling [14]. However, the cell types upregulating BMP signaling in response to injury have not been identified [14, 15]. BMP gain-of-function experiments *in vivo* or in cardiomyocyte culture have revealed little about the endogenous function of BMP signaling in the injured mammalian heart, since several studies have reported contradictory results. BMP2 protein has been shown to induce cardiomyocyte cell cycle re-entry *in vitro* and to reduce cardiomyocyte apoptosis both *in vivo* and *in vitro* [16-18], while BMP4 protein is able to enhance apoptosis and hypertrophy of cultured cardiomyocytes [19]. Thus, it appears that exogenously supplied BMP ligands can elicit opposing responses in mammalian cardiomyocytes [20]. On the other hand, loss-of-function data point towards a detrimental role for endogenous BMP signaling in the injured mammalian heart. Noggin binds to and blocks the function of several BMP ligands, with a preference for BMP2 and 4, but not the related Tgfß ligands [21]. *In vivo* treatment of mice with Noggin or the small molecule BMP type I receptor antagonist Dorsomorphin reduces cardiomyocyte apoptosis as well as infarct size, and improves functional recovery after MI

[14]. These results indicate that endogenous BMP signaling limits mammalian cardiomyocyte survival and regeneration.

Cellular injury responses occurring in cardiomyocytes at the wound border appear to be central for zebrafish heart regeneration. Further progress towards a mechanistic understanding of naturally occurring heart regeneration will thus be aided by a comprehensive view of molecular responses to injury in this border zone. To identify genes that are expressed in specific regions of a tissue of interest we developed tomo-seq, a method providing spatially resolved genome-wide expression profiles [22]. Tomo-seq combines traditional histological techniques with low-input RNA sequencing to generate a high-resolution genome-wide atlas of spatially resolved gene expression. Importantly, tomo-seq data can be easily searched for genes that satisfy any desired spatial expression criteria.

Here we have applied tomo-seq to the regenerating zebrafish heart, which allowed us to identify genes enriched in the injury area, border zone and uninjured myocardium. The border zone is characterized by the re-expression of embryonic cardiac genes, smooth muscle genes and regulators of growth, such as BMP pathway genes. We found that BMP signaling is activated in border zone cardiomyocytes and that it is required for myocardial regeneration. Interestingly, the requirement of BMP signaling for cardiomyocyte proliferation appears to be regeneration-specific since it did not regulate physiological cardiomyocyte proliferation during cardiogenesis, but was required for injury-specific cellular responses of cardiomyocytes, namely dedifferentiation and cell cycle re-entry. Our findings reveal BMP signaling as essential regulator of zebrafish heart regeneration and they indicate that the difference in the capacity to regenerate the heart in fish and mammals could be related to differential responses of cardiomyocytes to activation of the same signaling pathway.

Results

Tomo-seq reveals distinct molecular regions within the injured heart

Zebrafish myocardial regeneration occurs via proliferation of differentiated cardiomyocytes, which in response to ventricular resection have been shown to dedifferentiate and re-enter the cell cycle [6, 7]. The location of dedifferentiating cardiomyocytes has however not been well characterized following cryoinjury-induced necrotic lesions. At 7 days post cryoinjury (dpi), we observed that cardiomyocytes within about 50 μm of the wound border displayed reduced expression of the *myl7*:GFP transgene, a marker of differentiated cardiomyocytes (Figure 1A). Information on sample numbers for this and other experiments is shown in Table S1. These GFP^{low} cardiomyocytes also displayed other signs of dedifferentiation, namely disassembled sarcomeric structures (Figure S1A), reduced expression of the contractile protein Myomesin (Figure S1B), and activation of regulatory sequences of the *gata4* gene (Figure S1C) [23, 24]. In addition, GFP^{low} cardiomyocytes also upregulated markers of cell cycle activity and mitosis (Figures 1A, 1B and S1D).

To identify molecular signatures specific to this zone of dedifferentiating cardiomyocytes, we applied tomo-seq [22]. For this purpose, cryoinjured hearts (at 3 and 7 dpi) were cryosectioned starting from the injury area into the healthy, uninjured myocardium (Figure 1C) and isolated RNA from each section was subjected to RNA-seq. 3-5 million reads were sequenced, which mapped to ~15,000 genes (Supplementary File S1). To investigate global patterns of gene expression in our dataset, Pearson's correlation analysis was performed across all genes for each pairwise combination of sections. Interestingly, we observed several blocks of contiguous sections that are positively correlated to each other (3 dpi data presented in Figure 1D, 7 dpi data not shown), suggesting that the injured heart can be subdivided into regions with specific molecular profiles based on gene expression patterns. To identify such regions we performed hierarchical clustering of genes that show a clear expression peak (z-score > 1 in > 4 consecutive sections). The resulting plot confirmed that at least three distinct zones are present in the regenerating heart at 3 dpi: zone I (sections 1-6), zone II (sections 7-18) and zone III (sections 19-40) (Figure 1E). Next, we sought to verify these zones and analyze them in more detail. By calculating the log2-transformed fold change of the z-score for every gene between a zone-of-interest and the other zones, ranked lists of spatially upregulated genes were generated (Supplementary Files S2, S3, S4). Analysis of the ranked lists of the different zones (by visual analysis of the gene-expression traces) indicated that at 3 dpi more than 1000 genes have enriched expression in one of the three zones (408 genes in zone I, 261 genes in zone II and 362 genes in zone III). Interestingly, 10% of the genes with spatially enriched expression (114 genes) have not been functionally annotated in any system. GO-term analysis of the genes expressed in the different regions revealed that genes with an expression peak in zone I were associated with "translation", "embryo development" and "immune response". Interestingly, genes with expression peaks in zone II were most significantly linked to "regeneration", "protein folding" and "developmental growth", while genes with an expression peak in zone III were associated with "ATP metabolic process", "ventricular cardiac myofibril assembly" and "heart contraction" (Figure 1F). This indicates that zone I, II and III correspond to the injury area, the wound border zone, where a regenerative program is activated, and the uninjured myocardium, respectively. To validate expression patterns identified by tomo-seq we performed *in situ* hybridizations for top-ranked genes in each list on sections of cryoinjured hearts at 3 dpi. The 8 selected genes upregulated in zone I indeed showed restricted expression in the wound including the epicardium overlaying it (Figure 2A and data not shown), confirming that zone I corresponds to the injury area. Amongst the tested genes are several wound healing response genes, e.g. *thymosinβ4* (*tmsb4x*), *granulin* (*grn1, grn2*) and *cathepsin D* (*ctsd*). For zone II the 8 selected genes showed expression in between the injury area and the uninjured myocardium confirming that zone II represents the wound border zone ("BZ", Figure 2B and data not shown). Most prominent in the list of BZ genes is *natriuretic peptide B* (*nppb*), a cardiac hormone that is induced in response to myocardial stress in the mammalian heart and after ventricular resection in zebrafish [24, 25].

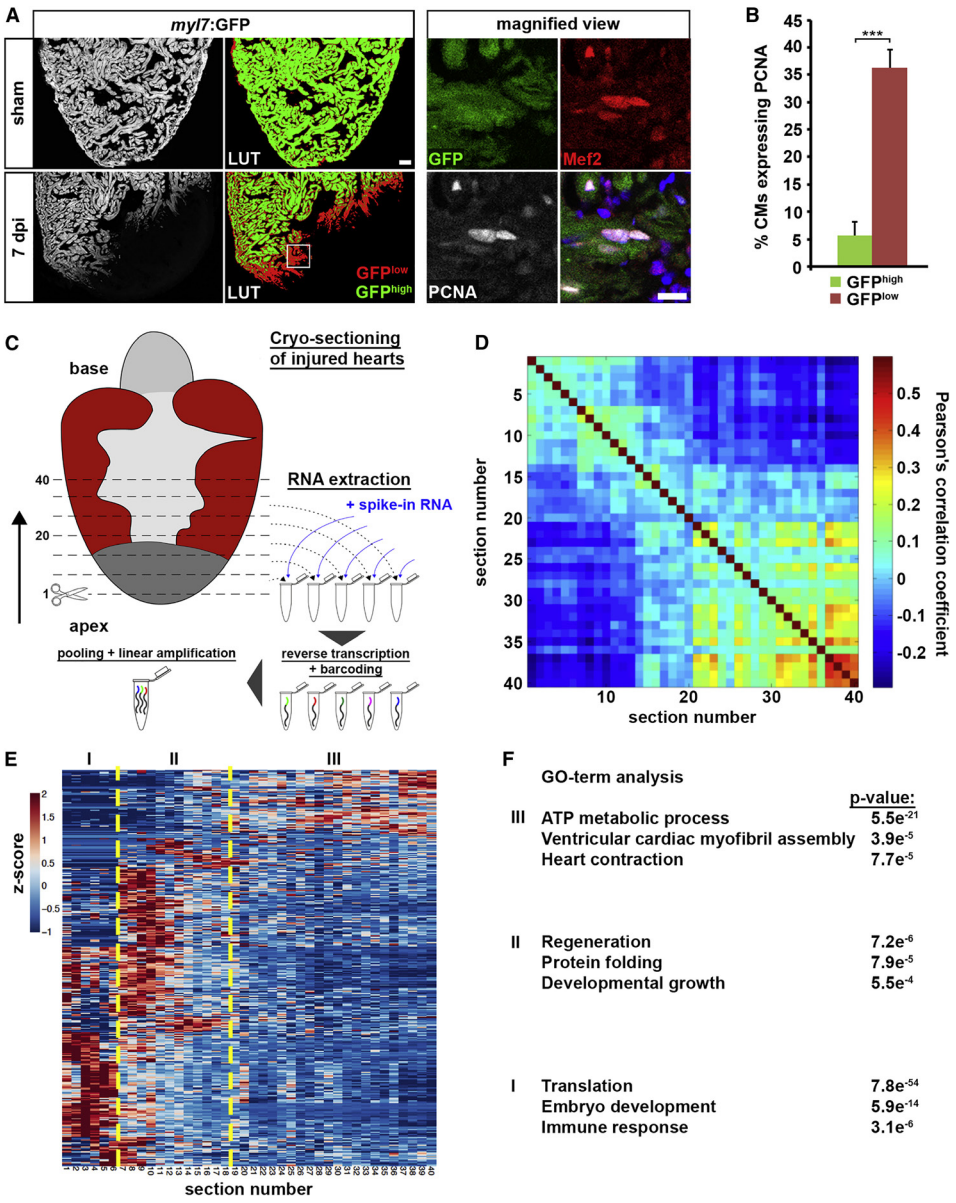

Figure 1. Tomo-seq identifies genes with spatially restricted expression in the regenerating heart

(A) Ventricular myl7:GFP expression is reduced at the wound border at 7 days post cryoinjury (dpi). In LUT images, GFP intensity below a threshold of 30% of signal intensity is displayed in red (GFP^{low}) while the rest is displayed in green (GFP^{high}). Magnified view shows examples of Mef2+, GFP^{low} cardiomyocytes expressing PCNA. Scale bar, 50 µm (overview) and 25 µm (magnified view). (B) Average percentage of PCNA expressing GFP^{low} and GFP^{high} cardiomyocytes. Error bars represent SEM. Student's t test p = 0.0003.

(C) Cartoon summarizing the tomo-seq procedure. Cryoinjured zebrafish ventricles were sectioned from apex to base. RNA from single sections was extracted, followed by reverse transcription and barcoding after which the samples were pooled for linear amplification and sequence library preparation. (D) Pairwise correlation between individual sections across all genes detected at more than 4 reads in more than 1 section of the 3 dpi heart. (E) Hierarchical clustering of z-score transformed expression profiles of all genes with expression peak (z-score > 1 in > 4 consecutive sections) in the 3 dpi heart. Zone I to III are marked by dashed yellow lines. (F) Results of gene ontology term analysis using GOrilla for genes with spatially restricted expression in zones I, II and III in the 3 dpi heart.

Of the 8 tested genes upregulated in zone III, 6 showed a restricted expression in the uninjured myocardium by *in situ* hybridization (Figure 2C), while the remaining 2 genes (*acta1b* and *atp5b*) showed strong expression in the uninjured myocardium and weaker expression in the entire epicardium (data not shown). These results indicate that zone III represents the uninjured area. This is consistent with the observation that many genes expressed in this region have a known role in muscle function (*ckmt2b, fabp3, cox7a1, acta1b, pgam2, casq2* and *ckma*).

In summary, tomo-seq can identify the wound area, border zone and uninjured myocardium in an unbiased manner simply based on spatially resolved genome-wide gene expression data. The resulting molecular profiles specific for these domains should facilitate identification of regulators of heart regeneration. The analyzed data for 3 and 7 dpi are available on our web page http://zebrafish.genomes.nl/heart/, providing a database that allows for easy searching of gene-expression traces.

Spatially restricted gene expression reveals two distinct border zone regions

Careful inspection of the hierarchical gene cluster analysis suggested the presence of sub-clusters in the border zone (region II in Figure 1E). Clustering of genes with a z-score > 1 in > 3 consecutive sections identified two sub-clusters, one corresponding to genes expressed in the border zone further apically near the injury area (BZinj), and the other in the border zone further basally near the uninjured myocardium (BZmyo) (Figure 3A). Lists of genes upregulated in these two zones were generated in the same manner as above (Supplementary files S5, S6). *In situ* hybridization with the top-rated genes of both the BZinj and the BZmyo on consecutive sections of the same injured heart confirmed their expression in two spatially distinct regions (Figure S2A). Expression of the BZinj genes *crip2* and *ywhabl* overlapped with the endothelial marker *kdrl*, suggesting an endothelial character of BZinj cells. Furthermore, the BZinj showed upregulation of genes known for their expression in vascular endothelium (*vwa1, cldn5b* and *mmrn2b*) and of smooth muscle cell markers (e.g. *myl6, junbb, crip2* and *tagln*, encoding SM22a) (Figure 3B and S2B). Importantly, smooth muscle markers are known to be upregulated in myofibroblasts, which form in response to

tissue injury and contribute to the wound repair process [reviewed in 26].

Interestingly, the BZmyo was enriched with genes that are highly expressed in the embryonic myocardium (e.g. *nppb, vmhc, actc1* and *desma*), which regulate cardiac hypertrophy in mammals (e.g. *igf2b*) or control the cell cycle (e.g. *cyclinE* [*ccne2*], *brcc3, psmd14*, and *E2F1*) (Figure 2B, 3C and S2B). Moreover, we observed that while *vmhc-like* the orthologue of mammalian MYH7, [27] is expressed throughout the myocardium, *vmhc* (the MYH6 orthologue) is upregulated in the BZmyo (Figure 3D). Immunofluorescence confirmed that Vmhc is expressed in embryonic, but not adult hearts, yet is upregulated specifically in dedifferentiating cardiomyocytes at the wound border in cryoinjured hearts (Figure 3E). These findings indicate that expression switching from adult to embryonic myosins occurs in the injured zebrafish heart, as it does in mammals.

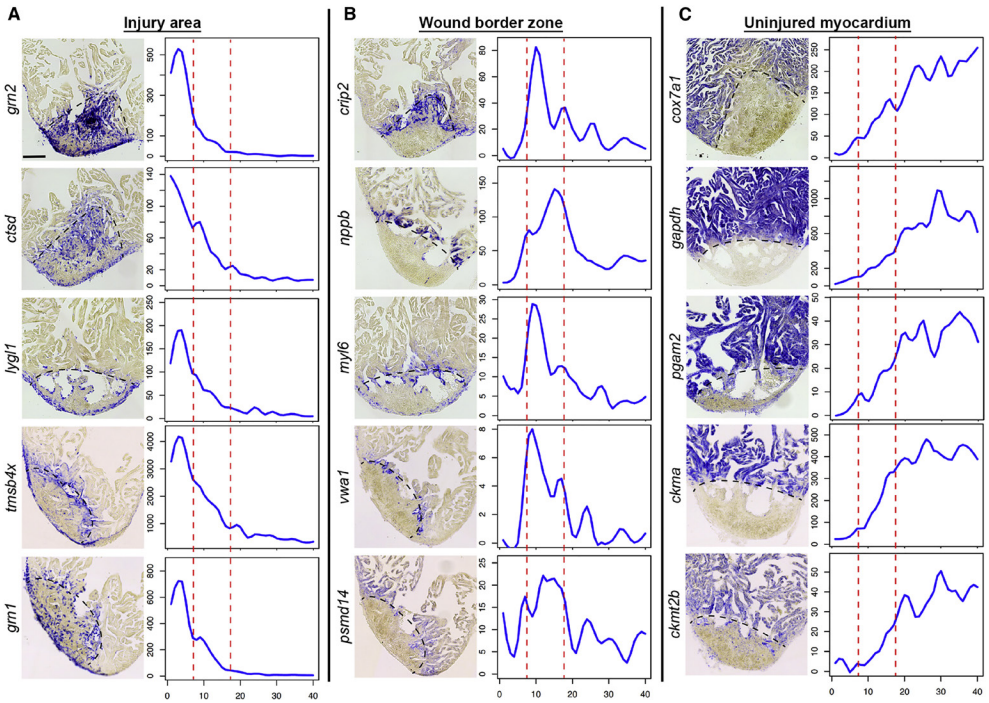

Figure 2. In situ hybridization validates tomo-seq results.

In situ hybridization for genes identified by tomo-seq to be enriched in the injury area (zone I) (A), wound border zone (zone II) (B) or in the uninjured myocardium (zone III) (C)at 3 dpi (n=3). Left, representative in situ staining, right, expression traces from tomo-seq data. y-axis, read counts, x-axis, section number. Scale bar, 100 µm. Dashed black line indicates wound boundary on sections. Red lines in plots surround the border zone.

Together these results suggest that two border zone regions with distinct gene expression profiles can be identified in the cryoinjured zebrafish heart. While the apical, injury-abutting border zone shows profiles characteristic of fibrosis and vasculogenesis, the myocardial border zone is characterized by the induction of embryonic myocardial genes, growth factors and genes controlling the cell cycle.

BMP signaling is specifically activated in the border zone

Interestingly, several genes with known roles in BMP signaling or known BMP target genes were enriched in the two border zones (e.g. *acvr1l* [*alk8*], *smad1, id1, id2b, junbb, sall1b* and *rgma*) (Figure 4A and data not shown). *In situ* hybridization confirmed the upregulation of the BMP target genes *id1* and *id2b*, the BMP ligands *bmp2b* and *bmp7*, and the type I BMP receptor *bmpr1aa* (*alk3a*) in multiple cell types located in the border zone at 3 dpi (Figure 4B and data not shown). Expression of *bmp2b*, *bmp7* and *bmpr1aa* continued to be enhanced at the wound border zone at 7 dpi, but was also upregulated in the epicardium covering the wound at this stage. Using accumulation of phosphorylated Smad1/5/8 in the nucleus as readout, we observed that BMP signaling was inactive in sham-operated adult zebrafish hearts but was activated in cardiomyocytes in the BZmyo from 1 dpi, where it increased by 3 dpi and persisted until at least 7 dpi (Figures 4C and 4D). Additionally, BMP signaling activity was also observed in both the endocardium and the epicardium at 3 dpi (Figure S3A). Taken together, these results suggest that BMP signaling activation is an injury response in the zebrafish heart, as it is in the injured mammalian heart. Interestingly however, pathway activation appears to occur later after injury and/or to persist longer than in mammalian hearts [14].

Heart regeneration depends on BMP signaling and is enhanced by BMP overactivation

We next investigated whether BMP signaling is detrimental to or required for zebrafish heart regeneration. To block BMP signaling, we overexpressed the secreted BMP antagonist *noggin3* in heat-shock inducible *hsp70l*:nog3 transgenic fish [28], which was sufficient to drastically reduce nuclear pSmad1/5/8 expression in cardiomyocytes within 6 hours (Figure 5A). In zebrafish, cryoinjury-induced lesions of about 15 - 20% of the ventricle are regenerated within 60 to 120 days, and the wound shrinks to about ¼ of its size within 21 days [3, 5]. To assess whether BMP signaling is required for heart regeneration, we continuously inhibited BMP signaling via daily heat-shock of *hsp70l*:nog3; *myl7*:GFP double transgenic fish and quantified the *myl7*:GFP negative wound area at 21 dpi. Interestingly, *noggin3*-expressing fish displayed significantly larger wounds than *myl7*:GFP single transgenic siblings that underwent the same heat-shock regime (Figure 5B). Assessment of wound size based on collagen and fibrin detection showed similar results in *hsp70l*:nog3 transgenics, which were heat-shocked daily from 3 to 21 dpi (Figure 5C). In addition, the healthy myocardial tissue expressing the *myl7*:GFP transgene was smaller in *noggin3*-expressing hearts (Figure S3B).

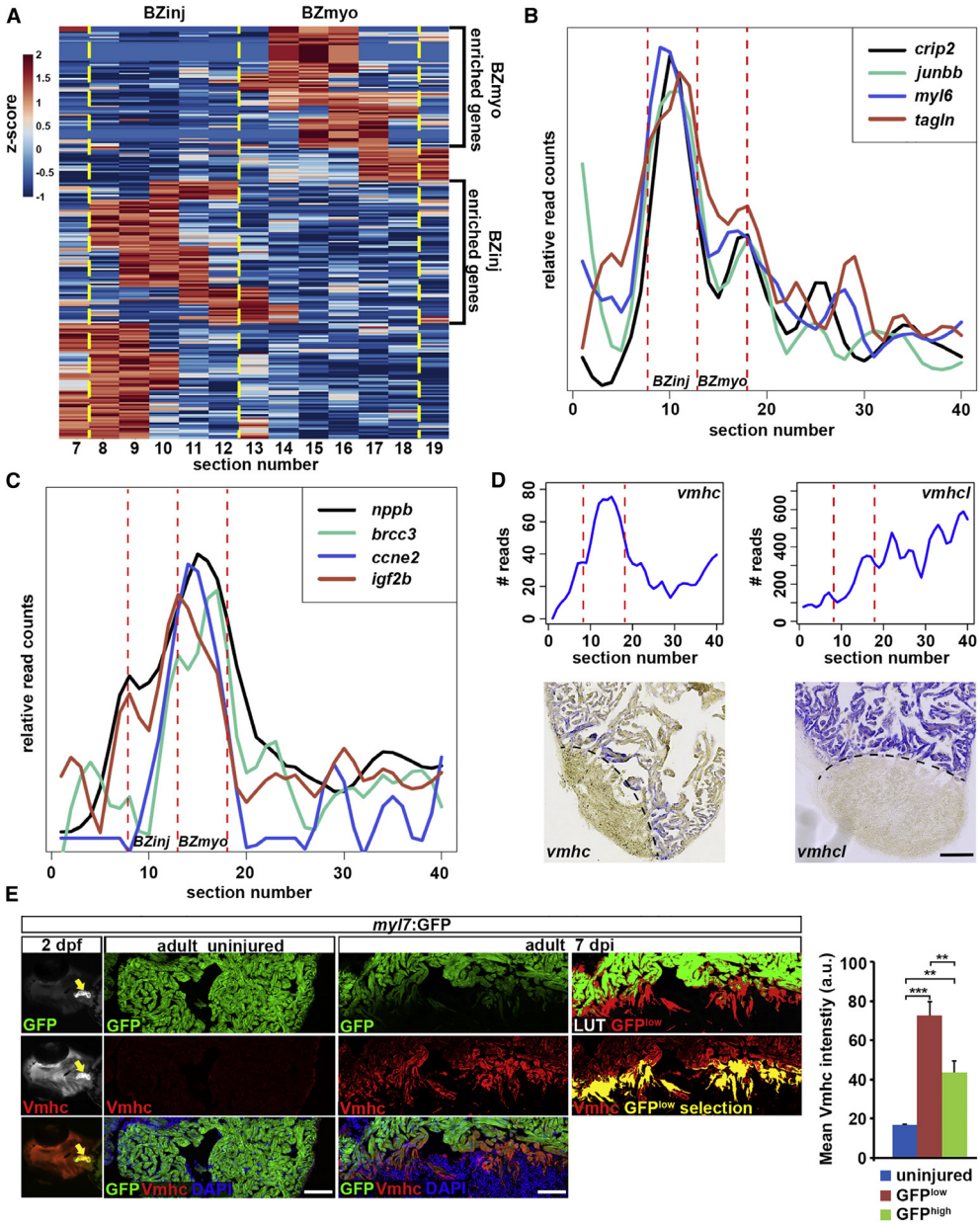

Figure 3. The wound border zone can be subdivided based on distinct expression profiles.
(A) Cluster analysis on all genes with expression peaks in greater than 3 consecutive sections in the border zone (sections 8-18) of the 3 dpi heart identifies two sub-regions showing different expression patterns. Color spectrum indicates z-score. BZinj and BZmyo are marked by dashed yellow line. (B+C) Expression traces from tomo-seq data on cryoinjured heart (3 dpi) for selected genes showing peak expression in the BZinj and BZmyo region.

(D) Expression traces from tomo-seq data and in situ hybridization on cryoinjured heart (3 dpi) for the MHC genes vmhc and vmhc-like (vmhcl). Scale bar, 100 µm. (E) Ventricular myosin heavy chain (Vmhc) immunostaining in embryonic (2dpf) and adult (uninjured and 7dpi) myl7:GFP transgenic zebrafish hearts. In LUT (lookup table) images, GFP intensity below 30% of signal intensity is displayed in red (GFP^{low}) while the rest is displayed in green (GFP^{high}). Note the overlapping expression pattern between GFP^{low} area (depicted as GFP^{low} selection) and Vmhc. Average Vmhc signal intensity in uninjured, GFP^{low} and GFP^{high} cardiomyocytes at 7 dpi is plotted on the right. Error bars represent SEM. Scale bar, 50 µm. Student's t test, p = 0.0008 (uninjured vs GFP^{low}), p = 0.002 (uninjured vs GFP^{high}), p = 0.004 (GFP^{low} vs GFP^{high}).

We conclude that endogenous BMP signaling is required for zebrafish heart regeneration.
Next, we asked whether overactivation of BMP signaling can enhance heart regeneration. Heat-shock-induced overexpression of *bmp2b* in *hsp70l*:bmp2b transgenics [28] was sufficient to induce accumulation of nuclear pSmad1/5/8 in uninjured hearts (Figure S3C) and to enhance the expression of the BMP target gene *id1* in injured hearts (Figure S3D). We continuously overexpressed *bmp2b* via daily heat-shock starting at 1 dpi. At 7 dpi, no differences in wound size between *hsp70l*:bmp2b; *myl7*:GFP double transgenics and heat-shocked *myl7*:GFP single transgenic siblings could be detected, confirming that the cryoinjury-induced lesions were of similar size in both groups (Figure S3E). In contrast, at 21 dpi the *myl7*:GFP negative area in hearts overexpressing *bmp2b* was 60% of the size of that observed in siblings (Figure 5B), and collagen and fibrin-containing wound tissue likewise was massively reduced (Figure 5C). In addition, *bmp2b* overexpression increased the size of healthy myocardial tissue (Figure S3B). Thus, prolonged overexpression of *bmp2b* is sufficient to enhance zebrafish heart regeneration.

BMP signaling promotes cardiomyocyte dedifferentiation

To understand how BMP signaling regulates heart regeneration, we assessed the cellular responses of different cardiac tissues to BMP inhibition. Re-activation of developmental gene programs in the endocardium and the epicardium has been identified as early responses to heart injury [4,5,29]. However, treatment with the BMP type I receptor antagonist Dorsomorphin interfered neither with endocardial expression of *aldh1a2,* the rate-limiting enzyme in the synthesis of retinoic acid, which regulates cardiomyocyte proliferation [29], nor with *wt1b*:GFP expression, a marker for the activated epicardium [4,5] (Figures S4A and S4B). These results suggest that BMP signaling is not required for activation of the regenerative response in the endo- and epicardial layers.
We then concentrated on putative functions of BMP signaling in cardiomyocyte regeneration. Since BMP signaling has been implicated both positively [16] and negatively [14,30] in mammalian cardiomyocyte survival following insults, we asked whether BMP pathway activity is required for cardiomyocyte survival in regenerating zebrafish hearts. While we detected only

few TUNEL-positive apoptotic cardiomyocytes at the wound border at 1, 3 and 7 dpi (Figure 6A), *bmp2b* overexpression was sufficient to reduce their number even further (Figure 6B). In contrast, BMP inhibition by *noggin3* overexpression from 1 to 7 dpi did not enhance cardiomyocyte apoptosis (Figure 6B), arguing against an essential role of endogenous BMP signaling in protecting zebrafish cardiomyocytes from injury-induced cell death.

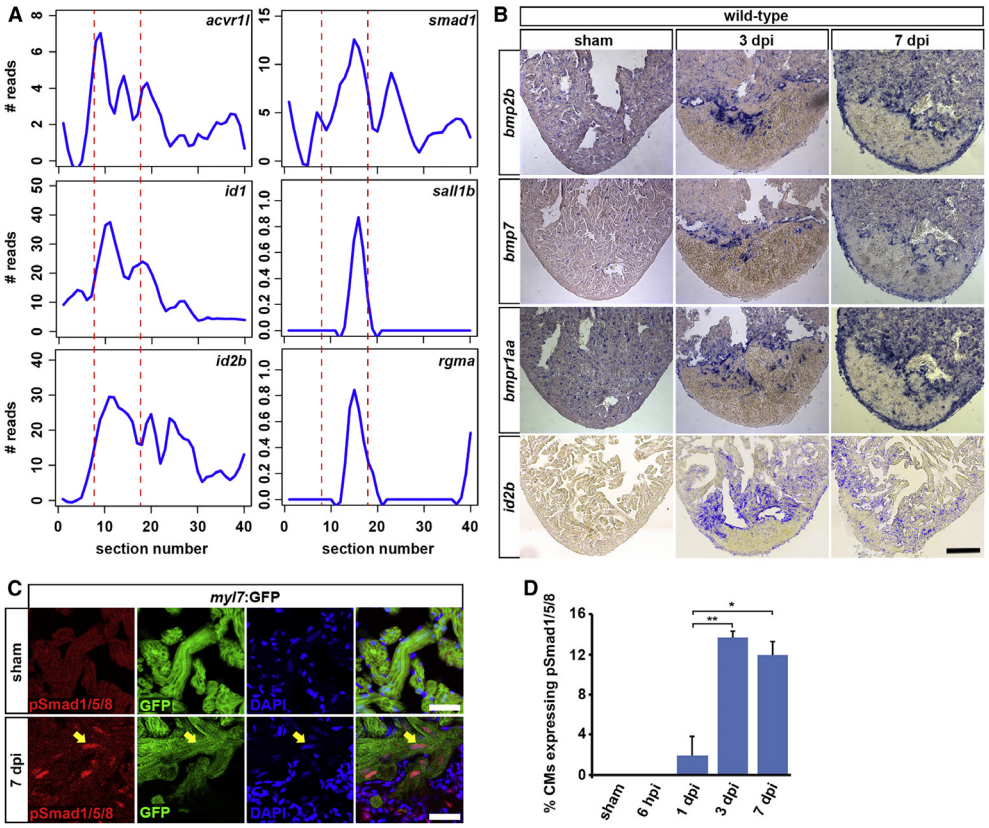

Figure 4. BMP signaling is activated in border zone cardiomyocytes. *(A) Expression traces from tomo-seq data on cryoinjured heart (3 dpi) for BMP signaling-related genes reveal peak expression in the wound border zone. (B) In situ hybridizations on sham-operated and 3 and 7 dpi hearts for the BMP ligands bmp2b and bmp7, the BMP receptor bmpr1aa (alk3a) and the BMP target gene id2b. (C) At 7 dpi, nuclear pSmad1/5/8 expression (arrow) is detected in myl7:GFP-positive cardiomyocytes at the wound border. Scale bar, 25 µm. (D) Average percentage of cardiomyocytes at the wound border expressing nuclear pSmad1/5/8 at different time points after cryoinjury. Error bars represent SEM. Student's t test, * p = 0.011, ** p = 0.004.*

Since we found that BMP signaling is activated in cardiomyocytes of the BZmyo, we asked whether it is required for cardiomyocyte dedifferentiation, a cellular response to injury in

this region, which has been suggested to contribute to heart regeneration [2, 6, 7]. A significantly higher fraction of cardiomyocytes with low *myl7*:GFP expression (GFP^{low}) (25%) than with high *myl7*:GFP expression (GFP^{high}) (9%) was positive for nuclear pSmad1/5/8, indicating that BMP signaling activation is correlated with cardiomyocyte dedifferentiation (Figure 6C). We then investigated a potential function of BMP signaling in cardiomyocyte dedifferentiation by examining *myl7*:GFP downregulation and fetal myosin re-expression in the BZmyo. Both overexpression of *noggin3* and treatment with Dorsomorphin from 3 to 7 dpi, which significantly suppressed nuclear pSmad1/5/8 accumulation in cardiomyocytes (Figure 6D), reduced the area of GFP^{low} cardiomyocytes in *myl7*:GFP transgenics at the wound border by half (Figures 6E). In contrast, wound size was not significantly altered by BMP signaling inhibition within this time frame (Figure S5A), showing that the reduced cardiomyocyte dedifferentiation was not a consequence of different extents of injury. Similarly, the re-expression of fetal myosin was also significantly reduced upon Dorsomorphin treatment (Figure S5B). These results indicate that BMP signaling is required for dedifferentiation of cardiomyocytes at the wound border after injury.

BMP signaling is required for injury-induced - but not physiological - cardiomyocyte proliferation

Cardiomyocyte dedifferentiation is a process which presumably occurs only early - within about one week – post injury. To test whether BMP signaling regulates heart regeneration primarily because it is required for cardiomyocyte dedifferentiation, we inhibited or overactivated signaling in *hsp70l*:nog3 and *hsp70l*:bmp2b transgenics from 1 to 7 dpi and allowed them to further regenerate without heat-shocks till 21 dpi. We found that BMP signaling modulation within the first week after injury was not sufficient to significantly alter wound size at 21 dpi (Figure S5C), suggesting that BMP signaling activity beyond the first week after injury is required for heart regeneration. We thus looked for additional cellular processes regulated by BMP signaling. Proliferation of cardiomyocytes is key for zebrafish heart regeneration [reviewed in 31]. Thus, we examined whether BMP signaling activation correlates with cell cycle re-entry of cardiomyocytes. We looked for co-localization of PCNA and the cardiomyocyte marker Mef2 with a transcriptional reporter for BMP signaling (*BRE*:GFP) [32], and found that the number of GFP-positive cardiomyocytes was five-fold higher among PCNA-positive cardiomyocytes than in the entire cardiomyocyte population (35% compared to 7%) (Figure 7A). Furthermore, throughout the early phase of regeneration (1, 2, 3, 5 and 7 dpi), the percentage of *BRE*:GFP-positive cardiomyocytes was positively correlated with the percentage of proliferating cardiomyocytes (Pearson's correlation coefficient: 0.76) (Figure S6A). These results show that BMP pathway activity is correlated with cell cycle activity in cardiomyocytes.

Next, we tested whether BMP signaling is required for cardiomyocyte cell cycle re-entry. Short-term (6 h) inhibition of BMP signaling by either *noggin3* overexpression or

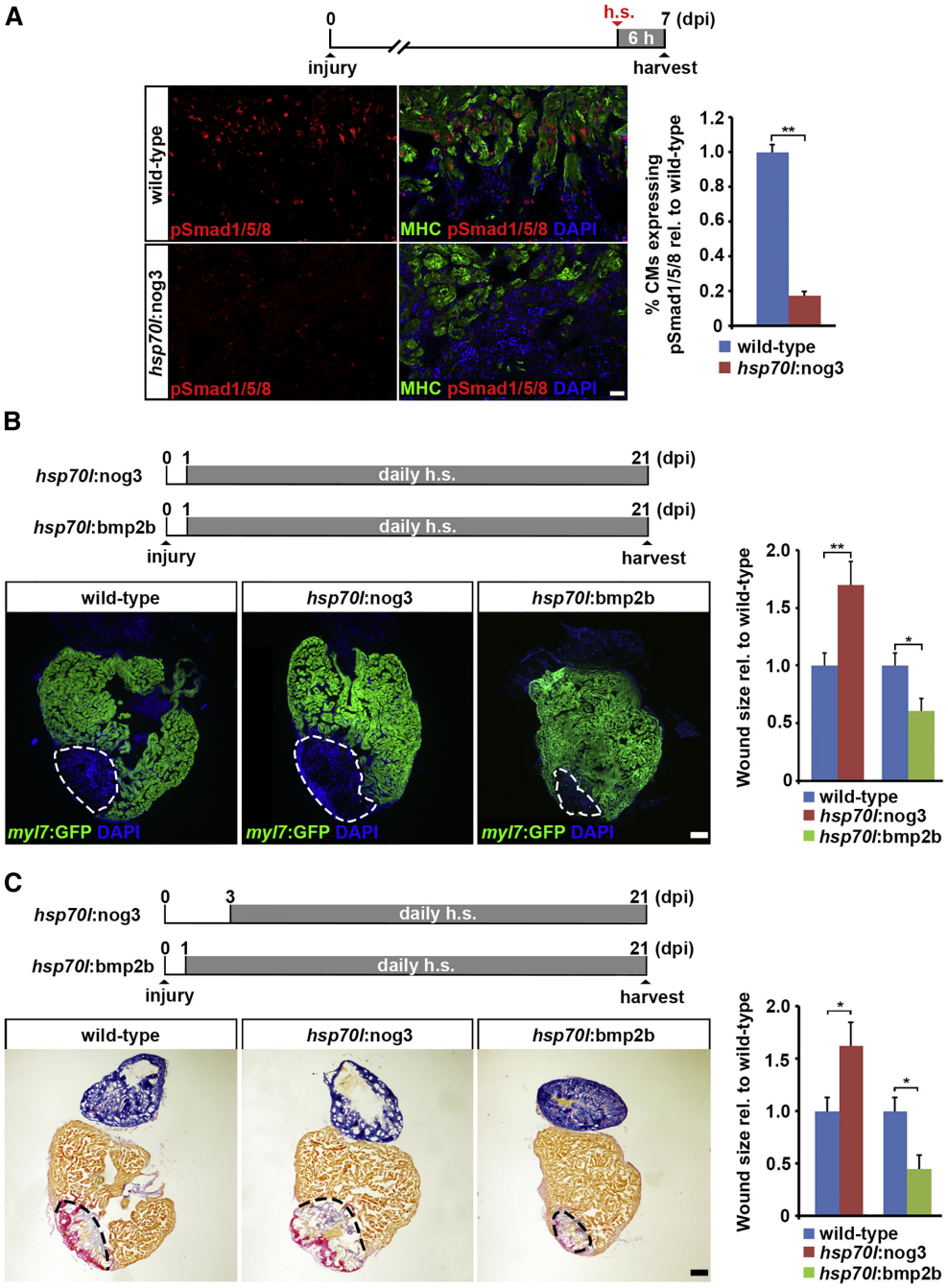

Figure 5. BMP signaling is required for myocardial regeneration and is sufficient to enhance it. *(A) Expression of noggin3 in hsp70l:nog3 transgenics for 6 h is sufficient to significantly reduce nuclear pSmad1/5/8 accumulation in cardiomyocytes (positive for myosin heavy chain, MHC) at*

the wound border at 7 dpi. Average percentage of cardiomyocytes expressing pSmad1/5/8 relative to that in wild-type hearts is plotted. Error bars represent SEM. Scale bar, 25 µm. Student's t test, p = 0.003. (B) GFP immunofluorescence analysis reveals wound size (dashed lines) at 21 dpi on heart sections of hsp70l:nog3; myl7:GFP and hsp70l:bmp2b; myl7:GFP double transgenics and their respective myl7:GFP-only siblings subjected to the depicted heat-shock regime. Size of the GFP-negative area relative to the whole ventricle and normalized to heat-shocked myl7:GFP-only siblings is plotted. Error bars represent SEM. Scale bar, 100 µm. Student's t test, p = 0.0081 (nog3), p = 0.018 (bmp2b). (C) Acid fuchsin orange G (AFOG) staining reveals wound size (dashed lines) at 21 dpi on heart sections of hsp70l:nog3, hsp70l:bmp2b transgenics and wild-type siblings subjected to the depicted heat-shock regime. Size of the wound tissue (red and purple staining) relative to the whole ventricle and normalized to heat-shocked wild-type siblings is plotted on the right. Error bars represent SEM. Scale bar, 100 µm. Student's t test, p = 0.002 (nog3), p = 0.016 (bmp2b).

Dorsomorphin treatment at 7 dpi significantly reduced PCNA expression in cardiomyocytes (Figures 7B and S6B). To validate these findings in a genetic model, we studied injury-induced cardiomyocyte proliferation in fish homozygous for a loss-of-function mutation in the BMP receptor *bmpr1aa* [33], which is expressed in the wound border zone in injured hearts (Figure 4B). While in double mutant embryos lacking both *bmpr1aa* and *bmpr1ab* cardiomyocyte specification is entirely lost, mutant embryos lacking only *bmpr1aa* display only mild larval defects in organ laterality and dorsoventral patterning and survive to adulthood without any discernible cardiac defects. In contrast, *bmpr1aa* function is required for heart regeneration, since *bmpr1aa* mutants showed fewer PCNA-positive cardiomyocytes than heterozygous control fish at 3 and 7 dpi (Figure 7C). On the other hand, overexpression of *bmp2b* from 1 to 7 dpi in *hsp70l*:bmp2b transgenics significantly enhanced PCNA expression in cardiomyocytes, particularly within 50 μm from the wound border (Figures 7D and S6C). Finally, we asked whether BMP signaling is also required for cardiomyocyte mitosis. Since the number of cardiomyocytes expressing phosphorylated histone H3 (PH3) at any particular time point during heart regeneration is very low [34], which makes it difficult to attain statistically sound data on modulators of mitosis, we inhibited cytokinesis using nocodazole treatment and thus arrested cardiomyocytes in a PH3-positive state. Short-term inhibition (24 h) of BMP signaling by *noggin3* overexpression (together with nocodazole treatment) strongly reduced the mitotic index of cardiomyocytes at 7 dpi (Figure 7E). Treatment with Dorsomorphin for 1 or 4 days suppressed cardiomyocyte mitosis at 7 dpi as well (Figure S6D). Altogether, these data strongly indicate that BMP signaling promotes proliferation of spared cardiomyocytes following injury.

This finding prompted us to examine whether BMP signaling activity is also required for cardiomyocyte proliferation during physiological heart growth in juvenile zebrafish [35]. While many cardiomyocytes were PCNA-positive in the juvenile heart at 8-9 weeks of age, we could not detect any nuclear pSmad1/5/8 expression in these hearts (Figure 7F). In addition,

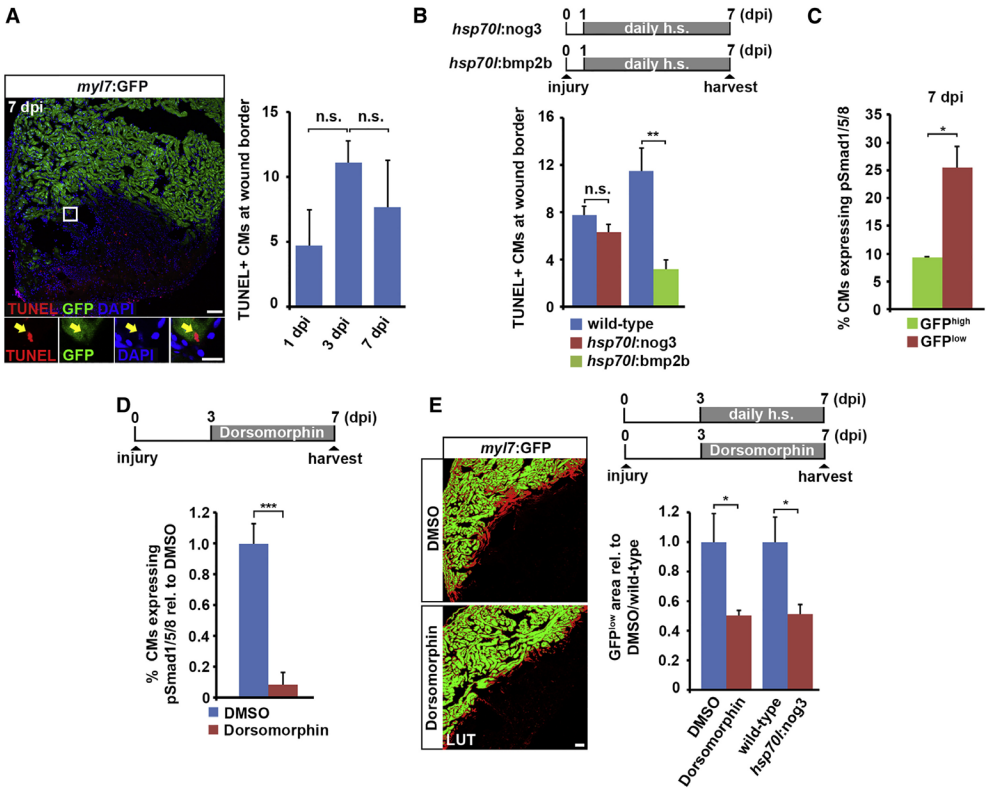

Figure 6. BMP signaling is required for cardiomyocyte dedifferentiation but not survival.

(A) TUNEL staining on sections of myl7:GFP hearts at 7 dpi. Magnified view shows an example of an apoptotic cardiomyocyte. Average absolute number of TUNEL+ cardiomyocytes per section found at the wound border at different time points post injury is plotted. Error bars represent SEM. Scale bars, 50 µm (overview), 12.5 µm (inset). Student's t test, p = 0.13 (1 vs 3 dpi), p = 0.45 (3 vs 7 dpi). (B) The number of TUNEL+ cardiomyocytes at the wound border at 7 dpi does not significantly change in hsp70l:nog3 transgenics relative to heat-shocked wild-type siblings, while it is reduced in hsp70l:bmp2b transgenics. Error bars represent SEM. Scale bars, 50 µm (overview), 12.5 µm (inset). Student's t test, p = 0.38 (nog3), p = 0.004 (bmp2b). (C) Average percentage of pSmad1/5/8 expressing GFP^{low} and GFP^{high} cardiomyocytes in myl7:GFP transgenic hearts at 7 dpi. Error bars represent SEM. Student's t test, p = 0.014. (D) Treatment of myl7:GFP transgenic fish with 5 µM Dorsomorphin for 4 days significantly reduces nuclear pSmad1/5/8 accumulation in cardiomyocytes at the wound border at 7 dpi. Average percentage of cardiomyocytes expressing pSmad1/5/8 relative to DMSO control is plotted. Error bar represents SEM. Student's t test, p = 0.0002. (E) Cardiomyocyte dedifferentiation, as monitored by the size of the GFP^{low} area in myl7:GFP transgenic hearts at 7 dpi, is reduced upon BMP signaling inhibition either by treatment with 5 µM Dorsomorphin or by noggin3 overexpression for 4 days. Error bars represent SEM. Scale bar, 50 µm. Student's t test, p = 0.013 (Dorsomorphin), p = 0.025 (nog3).

neither *noggin3* overexpression nor Dorsomorphin treatment reduced the percentage of PCNA-positive cardiomyocytes in juvenile hearts (Figure 7G and S6E). Furthermore, while overexpression of *bmp2b* in *hsp70l*:bmp2b transgenics was sufficient to activate BMP signaling in uninjured adult hearts (Figure S3C), it did not induce cardiomyocyte proliferation in the absence of injury (Figure S6F). Together with the observation that *bmpr1aa* mutant hearts have normal morphology and size, these data reveal that BMP signaling specifically regulates injury-induced cardiomyocyte proliferation.

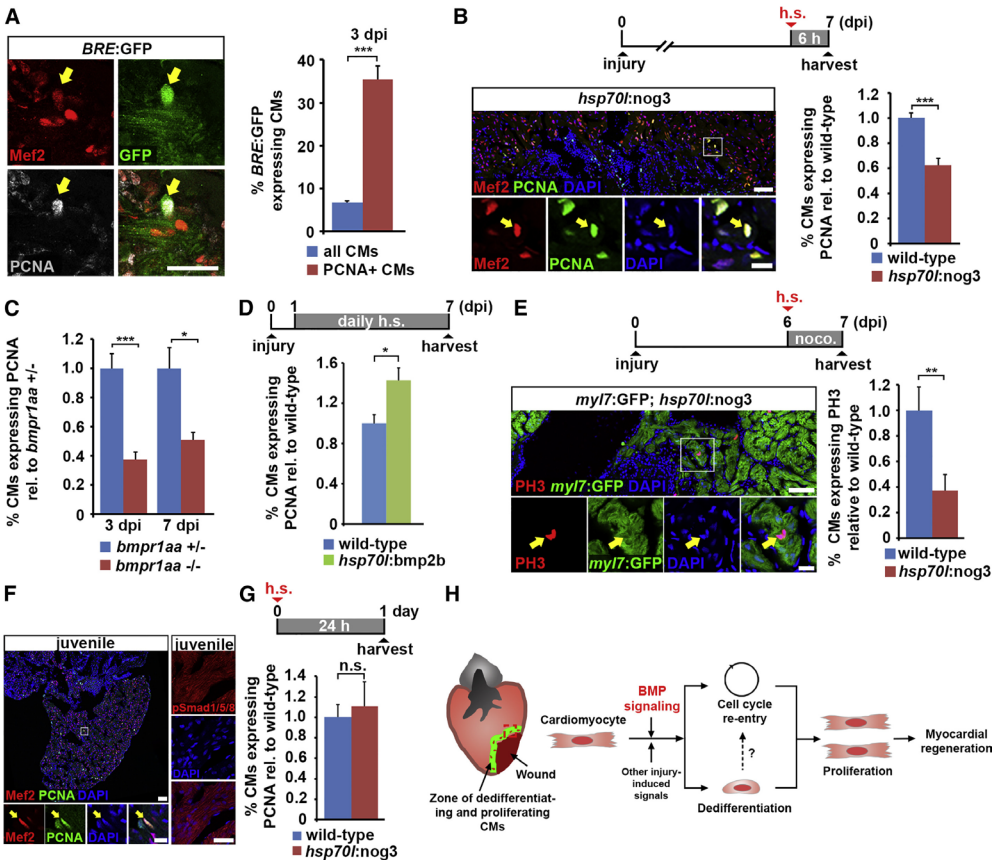

Figure 7. BMP signaling is required for injury-induced but not physiological cardiomyocyte proliferation. *(A) Co-localization of Mef2 and PCNA with GFP (arrow), which reports BMP-mediated transcriptional activity in BRE:GFP transgenic hearts, at 3 dpi. Average percentage of PCNA+ or all cardiomyocytes that express GFP is plotted. Error bars represent SEM. Student's t test, p = 0.000023. (B) Expression of noggin3 in hsp70l:nog3 transgenics for 6 h is sufficient to reduce PCNA expression in cardiomyocytes (identified by nuclear Mef2, arrow) at the wound border at 7 dpi. Average percentage of cardiomyocytes expressing PCNA relative to wild-type is plotted. Error bars represent SEM. Scale bar, 50 µm. Student's t test, p = 0.00095.*

(C) Hearts homozygous for a loss-of-function mutation of the BMP type I receptor bmpr1aa display reduced expression of PCNA in cardiomyocytes (identified by nuclear Mef2) at the wound border at 3 and 7 dpi compared to bmpr1aa +/- hearts. Average percentage of cardiomyocytes expressing PCNA relative to bmpr1aa +/- control is plotted. Error bars represent SEM. Student's t test, p = 0.0002 (3dpi), p = 0.01 (7 dpi). (D) Overexpression of bmp2b for 6 days via daily heat-shock is sufficient to increase PCNA expression in cardiomyocytes at the wound border in hsp70l:bmp2b transgenics relative to heat-shocked wild-type siblings at 7 dpi. Average percentage of cardiomyocytes expressing PCNA relative to wild-type is plotted. Error bars represent SEM. Student's t test, p = 0.011. (E) Expression of noggin3 for 24 h in hsp70l:nog3; myl7:GFP double transgenics that were treated with 5 µM nocodazole reduces the percentage of phospho-Histone 3 (PH3)+ mitotic cardiomyocytes (arrow). Average percentage of cardiomyocytes expressing PH3 relative to wild-type is plotted. Error bars represent SEM. Scale bar, 50 µm (overview) and 25 µm (magnified view). Student's t test, p = 0.0068. (F) Many Mef2+ cardiomyocytes are also PCNA positive (arrow) in 9 weeks old juvenile fish hearts, but no nuclear pSmad1/5/8 can be detected. (G) Expression of noggin3 in juvenile hsp70l:nog3 transgenics for 24 h does not reduce the expression of PCNA in cardiomyocytes. Average percentage of cardiomyocytes expressing PCNA relative to wild-type is plotted. Error bars represent SEM. Student's t test, p = 0.67. (H) Model for BMP function during zebrafish heart regeneration. BMP signaling is activated in cardiomyocytes at the wound border and is required for cellular responses to injury in these cells, namely dedifferentiation and cell cycle re-entry, and thus for cardiomyocyte proliferation and myocardial regeneration.

Discussion

Here we applied tomo-seq, a technique we have recently established to obtain genome-wide RNA-seq data from embryos or tissues with spatial resolution, to the regenerating zebrafish heart. We could distinguish distinct regions in the regenerating heart solely based on their expression profiles. Most importantly, we have identified two wound border zones with distinct expression profiles where processes essential for heart regeneration, namely cardiomyocyte dedifferentiation and proliferation, occur. This led to the discovery that BMP signaling is specifically activated in the border region. Our results suggest the following model for BMP signaling function during heart regeneration (Figure 7H). Physiological cardiomyocyte proliferation during heart growth in juvenile fish does not require BMP signaling. However, in injured hearts BMP signaling is activated in resident cardiomyocytes at the wound border. This pathway is essential for myocardial regeneration via regulating cardiomyocyte dedifferentiation and cell cycle re-entry, cellular processes that are specifically activated after injury and do not occur in growing hearts. Experimental activation of BMP signaling in uninjured hearts is however not sufficient to induce cardiomyocyte cell cycle re-entry, indicating that it acts with other injury-induced signals (Figure 7H). Thus, BMP

signaling is an essential and injury-specific regulator of cardiomyocyte regeneration in the naturally regenerating zebrafish heart.

We show that the tomo-seq technique, which has thus far only been applied to embryos, works well to identify regions with specific expression profiles in isolated adult tissues. Several previous studies have used RNA-seq or micro-array technology to identify expression profiles of entire regenerating zebrafish hearts [36, 37] and one study has used translational profiling to identify injury-responses specifically in cardiomyocytes [12]. Although these techniques are useful for differential gene expression analysis within a rather homogenous tissue, they are of limited use to identify genes that are specifically regulated in a small region of the tissue. Furthermore, conventional methods for obtaining spatial information of gene expression like *in situ* hybridization or immunohistochemistry can only be applied to a limited set of candidates. We believe that the tomo-seq data generated for the regenerating heart will be useful for future studies into the mechanisms driving heart regeneration. In addition, our data show that there are many uncharacterized genes with spatially restricted expression in the injured heart that might have important functions.

While most signaling pathways that have been implicated in zebrafish heart regeneration are mainly active in the endocardium and/or epicardium [reviewed in 10], BMP signaling is activated in proliferating cardiomyocytes after injury. Thus, together with Jak1/Stat3 signaling [12], BMP signaling is a good candidate for a pathway that directly affects cardiomyocyte regeneration. However, the cellular sources of BMP ligands remain to be identified. Our tomo-seq data and *in situ* hybridization analyses showed that expression of BMP ligands (*bmp2b* and *bmp7*) and the type 1 BMP receptor (*bmpr1aa*) localizes to the border zone and appears to include both endocardial cells and cardiomyocytes. Further studies will be required to determine which BMP ligands are responsible for Smad1/5/8 signaling activation in cardiomyocytes and whether they act in a paracrine and/or autocrine fashion.

In zebrafish, cardiomyocytes modulate their differentiation state in response to heart injury, which includes upregulation of the regulatory sequence of *gata4* our data and [7] and other cardiac transcription factors like *tbx20* and *nkx2.5* [38]. Since expression of these transcription factors is regulated by BMP signaling during heart development [39-41], it is possible that the pathway promotes cardiomyocyte dedifferentiation via regulation of these factors. Moreover, activated BMP signaling leads to the induction of *id* gene expression, encoding negative regulators of basic helix-loop-helix (bHLH) transcription factors [42]. Expression of Id proteins is typically high in stem- and progenitor cells suggesting that they play a role in maintenance of the undifferentiated state [43, 44]. In addition, Id proteins can promote cell proliferation by regulating the expression of cell cycle genes [45]. Our tomo-seq and *in situ* hybridization data demonstrate the upregulation of *id1* and *id2b* in the border zone, suggesting that BMP-mediated upregulation of Id proteins could play a role in the dedifferentiation and proliferation of cardiomyocytes possibly via the inhibition of bHLH transcription factors.

In cultured mammalian cardiomyocytes, exogenous BMP2 protein is able to induce cell cycle activity [17] while BMP4 protein has been shown to enhance apoptosis and hypertrophy [19]. To clarify the role of BMP signaling in mammalian cardiomyocytes, we also compared the effects of BMP2 and BMP4 on neonatal rat cardiomyocyte *in vitro*. Addition of either protein did not induce cardiomyocyte proliferation, but caused hypertrophic responses including expression of *Nppa* (ANP) and increases in cell size (Figure S7A and S7B). Thus, we could not confirm the previously reported pro-proliferative role of BMP2 or a differential effect of BMP2 and BMP4 on cultured neonatal mammalian cardiomyocytes. However, such discrepancies could be attributed to different experimental setups, e.g. different ways of measuring cardiomyocyte proliferation (Ki67 vs. BrdU incorporation).

While *in vivo* Noggin injection in mice reduces apoptosis and infarct size and improves functional recovery after MI, transgenic overexpression of *noggin3* in the zebrafish heart has no effect on cardiomyocyte apoptosis but significantly compromises cardiomyocyte regeneration [14]. These findings indicate that endogenous BMP signaling is activated by cardiac injury in both mammals and zebrafish but has opposite effects on cardiac repair. Whether these different outcomes can be attributed to different spatial and temporal activation profiles of BMP signaling or to different downstream effectors and transcriptional targets in cardiomyocytes remains to be elucidated. Nonetheless, our result indicate that in search for molecular reasons for the differential ability of fish and mammals to regenerate the heart, it could be equally important to look for differentially regulated pathways as well as to identify how the heart reacts to signals that are regulated in response to injury in both fish and mammals.

In summary, we show that the spatial gene expression information provided by tomo-seq allows for the identification of molecular signals that regulate essential regenerative processes in the zebrafish heart. We anticipate that our detailed characterization of the border zone in the regenerating heart and the identification of BMP signaling as an important regulator of cardiomyocyte proliferation will help to find strategies for stimulating regenerative capacities of the mammalian heart in the future.

Experimental Procedures

Transgenic fish lines, cryoinjury, heat-shocks and Dorsomorphin treatment

All procedures involving animals were approved by the local animal experiments committees and performed in compliance with animal welfare laws, guidelines and policies, according to national and European law.

Zebrafish of ~ 4 to 18 months of age were used, except for experiments with juvenile fish which were 8-9 weeks old. The following fish lines were used: *hsp70l*:nog3^{fr14Tg} [28], *hsp70l*:bmp2b^{fr13tg} [28], *wt1b*:GFP^{li3Tg} [46], *BRE*:GFP^{pt510Tg} [32], *myl7*:GFP^{twu34Tg} [47], *fli1a*:eGFP^{y1Tg} [48], *-14.8gata4*:GFP^{ae1} [49], *bmpr1aa*^{hu4087} [33], Et(*krt4*:eGFP)^{sqet27} [50] and *myl7*:DsRed2-NLS^{f2Tg} [51]. Cryoinjuries were performed as previously described [5], except that a liquid nitrogen-cooled copper filament of 0.3 mm diameter was used instead of dry ice. For experiments involving heat-shock inducible gene expression, fish were heat-shocked at 37˚C for 1 h, after which the water temperature was reduced back to 27˚C within 15 minutes. For short-term experiments hearts were harvested 5 h after the end of the heat-shock, for long-term experiments fish were heat-shocked once daily.

For drug treatment, Dorsomorphin (Sigma P5499) or nocodazole (Sigma M1404) were applied at 5 μM in fish system water while DMSO was used as a solvent control.

Histological methods, immunofluorescence and TUNEL assay

For immunofluorescence and histological staining, hearts were extracted, fixed in 4% PFA (in Phosphate buffer with 4% sucrose) at room temperature for 1 h and cryosectioned into 10 μm sections. Heart sections were equally distributed onto seven serial slides so each slide contained sections representing all areas of the ventricle.

Acid fuchsin-orange G (AFOG) staining was performed on cryosections as previously described [1]. Measurements of the size of ventricular areas (the wound area based on AFOG staining, the GFP^{low} cardiomyocyte area and the area of fetal myosin expression) were performed manually with ImageJ (NIH) software on 2 - 4 sections containing the biggest wound [52]. Measurements of the size of the wound area and of the regenerated myocardium on sections of *myl7*:GFP hearts or on myosin heavy chain-immunostained sections on wild-type or transgenics hearts were performed manually with ImageJ software on all sections of one serial slide, representing approximately one-seventh of the total ventricle.

Primary antibodies used were anti-PCNA (Dako #M0879), anti-GFP (Abcam #ab13970), anti-PH3 (Cell-Signaling #9706), anti-pSmad1/5/8 (Cell-Signaling #9511), anti-Vmhc (Sigma #SAB2701875), anti-Aldhla2 (Abmart #P30011), anti-α-actinin (Sigma #A7811), anti-MF20 (Developmental Studies Hybridoma Bank), anti-Myomesin B4 (Developmental Studies Hybridoma Bank) and anti-Mef2c (Santa Cruz #SC313). For PCNA and Mef2c, antigen retrieval was performed by heating slides containing heart sections at 85˚C in 10 mM sodium citrate buffer (pH 6) for 10 minutes. Secondary antibodies conjugated to Alexa

488, 555 or 633 (Invitrogen) were used at a dilution of 1:1000. Nuclei were shown by DAPI (4',6-diamidino-2-phenylindole) staining. All images of immunofluorescence stainings are single optical planes acquired with Leica Sp5 or Sp8 confocal microscopes. For quantifications, 2 to 3 sections displaying the biggest wounds were analyzed per heart. Quantifications of PCNA, Mef2, PH3 and TUNEL expression were performed in cardiomyocytes situated within 150 μm from the wound border unless otherwise specified.
For cardiomyocyte mitotic index estimation, the number of PH3-positive cardiomyocytes situated within 150 μm from the wound border in all sections from each heart containing an obvious wound area was counted. In those sections, the total number of cardiomyocytes was estimated by determining the average density of cardiomyocytes per μm^2 in three separate areas (size: 70 μm^2), and by multiplying this number with the total area size.
TUNEL staining was performed using ApoTag Red in-situ kit (Millipore) on heart cryosections as per the manufacturer´s instructions.

In situ hybridization

After o/n fixation in 4% PFA, hearts were washed in PBS twice, dehydrated in EtOH, and embedded in paraffin. Serial sections were made at 10 μm. *In situ* hybridization was performed on paraffin-sections as previously described [53] except that the hybridization buffer used did not contain heparin and yeast total RNA.

Tomo-seq and data analysis

Cryoinjured zebrafish hearts were extracted at 3 dpi or 7 dpi and directly embedded in Jung tissue freezing medium (Leica). Hearts were cryosectioned starting from the injury area into the uninjured myocardium at 12 μm thickness and collected in separate tubes. RNA was extracted using Trizol (Ambion) after adding a defined amount of spike-in RNA to correct for technical variations during the downstream processing. RNA-seq was performed as previously described [22] and is described in detail in the supplemental experimental procedures. For correlation analysis, all genes expressed at > 4 reads in > 1 section were selected prior to total-read-normalization. Based on the log2-transformed-fold-change (zlfc) of the z-score (number of standard deviations above the mean) of all genes, the Pearson correlation was calculated across all genes for each pairwise combination of sections. Hierarchical cluster analysis on the entire dataset (after z-score transformation) was performed on all genes with a peak in > 4 consecutive sections (z-score > 1). All genes with a peak in > 3 consecutive sections were used for cluster analysis of the border zone (sections 8-18). Ranked lists of spatially upregulated genes were generated by calculating the zlfc for every gene between a zone-of-interest and the remaining zones. GO-term analysis on ranked lists was performed using the online tool GOrilla by submitting whole lists for GO-term analysis [54]. Bioinformatic analyses were largely performed with R software using custom written code [55]. The correlation analysis and plot were generated in MATLAB (MathWorks).

Author contributions

F.K. performed Tomo-Seq, *in situ* hybridizations and experiments on the *alk3* mutant and *BRE*:GFP fish. J.P.J, D.G and A.v.O. assisted with the bioinformatic analysis. E.B. created the searchable database. D.C.Z. performed experiments on cultured mammalian cardiomyocytes. M.D.V. performed experiments on cardiomyocyte apoptosis All other experiments were performed by C-C.W. All authors designed experiments and analyzed data. C-C.W., F.K., J.B. and G.W. wrote the paper.

Acknowledgements

J.B. acknowledges support from the Netherlands Cardiovascular Research Initiative, the Dutch Heart Foundation, Dutch Federation of University Medical Centres, the Netherlands Organisation for Health Research and Development and the Royal Netherlands Academy of Sciences. G.W. thanks Doris Weber and Brigitte Korte for fish care and technical help. This work was supported by a CVON grant (CVON2011-12 HUSTCARE) to J.B., a "Klaus-Georg und Sigrid Hengstberger-Forschungsstipendium" by the German Cardiac Society to G.W. and a EuFishBioMed Short Term Fellowship to C.-C. W.

Bibliography

1. Poss, K.D., Wilson, L.G. & Keating, M.T. Heart regeneration in zebrafish. *Science* **298**, 2188-2190 (2002).
2. Wang, J. *et al*. The regenerative capacity of zebrafish reverses cardiac failure caused by genetic cardiomyocyte depletion. *Development* **138**, 3421-3430 (2011).
3. Chablais, F., Veit, J., Rainer, G. & Jazwinska, A. The zebrafish heart regenerates after cryoinjury-induced myocardial infarction. *BMC developmental biology* **11**, 21 (2011).
4. Gonzalez-Rosa, J.M., Martin, V., Peralta, M., Torres, M. & Mercader, N. Extensive scar formation and regression during heart regeneration after cryoinjury in zebrafish. *Development* **138**, 1663-1674 (2011).
5. Schnabel, K., Wu, C.C., Kurth, T. & Weidinger, G. Regeneration of cryoinjury induced necrotic heart lesions in zebrafish is associated with epicardial activation and cardiomyocyte proliferation. *PloS one* **6**, e18503 (2011).
6. Jopling, C. *et al*. Zebrafish heart regeneration occurs by cardiomyocyte dedifferentiation and proliferation. *Nature* **464**, 606-609 (2010).
7. Kikuchi, K. *et al*. Primary contribution to zebrafish heart regeneration by gata4(+) cardiomyocytes. *Nature* **464**, 601-605 (2010).
8. Bergmann, O. *et al*. Evidence for cardiomyocyte renewal in humans. *Science* **324**, 98-102 (2009).
9. Senyo, S.E. *et al*. Mammalian heart renewal by pre-existing cardiomyocytes. *Nature* **493**, 433-436 (2013).
10. Gemberling, M., Bailey, T.J., Hyde, D.R. & Poss, K.D. The zebrafish as a model for complex tissue regeneration. *Trends Genet* **29**, 611-620 (2013).
11. Gemberling, M., Karra, R., Dickson, A.L. & Poss, K.D. Nrg1 is an injury-induced cardiomyocyte mitogen for the endogenous heart regeneration program in zebrafish. *Elife* **4** (2015).
12. Fang, Y. *et al*. Translational profiling of cardiomyocytes identifies an early Jak1/Stat3 injury response required for zebrafish heart regeneration. *Proceedings of the National Academy of Sciences of the United States of America* **110**, 13416-13421 (2013).
13. van Wijk, B., Moorman, A.F. & van den Hoff, M.J. Role of bone morphogenetic proteins in cardiac differentiation. *Cardiovasc Res* **74**, 244-255 (2007).
14. Pachori, A.S. *et al*. Bone morphogenetic protein 4 mediates myocardial ischemic injury through JNK-dependent signaling pathway. *J Mol Cell Cardiol* **48**,

1255-1265 (2010).
15. Zaidi, S.H., Huang, Q., Momen, A., Riazi, A. & Husain, M. Growth differentiation factor 5 regulates cardiac repair after myocardial infarction. *J Am Coll Cardiol* **55**, 135-143 (2010).
16. Ebelt, H. *et al*. Treatment with bone morphogenetic protein 2 limits infarct size after myocardial infarction in mice. *Shock* **39**, 353-360 (2013).
17. Chakraborty, S., Sengupta, A. & Yutzey, K.E. Tbx20 promotes cardiomyocyte proliferation and persistence of fetal characteristics in adult mouse hearts. *J Mol Cell Cardiol* **62**, 203-213 (2013).
18. Izumi, M. *et al*. Bone morphogenetic protein-2 inhibits serum deprivation-induced apoptosis of neonatal cardiac myocytes through activation of the Smad1 pathway. *The Journal of biological chemistry* **276**, 31133-31141 (2001).
19. Sun, B. *et al*. Bone morphogenetic protein-4 mediates cardiac hypertrophy, apoptosis, and fibrosis in experimentally pathological cardiac hypertrophy. *Hypertension* **61**, 352-360 (2013).
20. Lu, J. *et al*. Bone morphogenetic protein-2 antagonizes bone morphogenetic protein-4 induced cardiomyocyte hypertrophy and apoptosis. *J Cell Physiol* **229**, 1503-1510 (2014).
21. Zimmerman, L.B., De Jesus-Escobar, J.M. & Harland, R.M. The Spemann organizer signal noggin binds and inactivates bone morphogenetic protein 4. *Cell* **86**, 599-606 (1996).
22. Junker, J.P. *et al*. Genome-wide RNA Tomography in the zebrafish embryo. *Cell* **159**, 662-675 (2014).
23. Szibor, M., Poling, J., Warnecke, H., Kubin, T. & Braun, T. Remodeling and dedifferentiation of adult cardiomyocytes during disease and regeneration. *Cell Mol Life Sci* **71**, 1907-1916 (2014).
24. Gupta, V. *et al*. An injury-responsive gata4 program shapes the zebrafish cardiac ventricle. *Current biology : CB* **23**, 1221-1227 (2013).
25. Sergeeva, I.A. *et al*. A transgenic mouse model for the simultaneous monitoring of ANF and BNP gene activity during heart development and disease. *Cardiovasc Res* **101**, 78-86 (2014).
26. Hinz, B. *et al*. The myofibroblast: one function, multiple origins. *Am J Pathol* **170**, 1807-1816 (2007).
27. Shih, Y.H. *et al*. The Cardiac Transcriptome and Dilated Cardiomyopathy Genes in Zebrafish. *Circ Cardiovasc Genet* (2015).
28. Chocron, S., Verhoeven, M.C., Rentzsch, F., Hammerschmidt, M. & Bakkers, J. Zebrafish Bmp4 regulates left-right asymmetry at two distinct developmental time points. *Developmental biology*

305, 577-588 (2007).

29. Kikuchi, K. *et al*. Retinoic acid production by endocardium and epicardium is an injury response essential for zebrafish heart regeneration. *Dev Cell* **20**, 397-404 (2011).
30. Mungrue, I.N. *et al*. Abcc6 deficiency causes increased infarct size and apoptosis in a mouse cardiac ischemia-reperfusion model. *Arterioscler Thromb Vasc Biol* **31**, 2806-2812 (2011).
31. Kikuchi, K. & Poss, K.D. Cardiac regenerative capacity and mechanisms. *Annu Rev Cell Dev Biol* **28**, 719-741 (2012).
32. Laux, D.W., Febbo, J.A. & Roman, B.L. Dynamic analysis of BMP-responsive smad activity in live zebrafish embryos. *Dev Dyn* **240**, 682-694 (2011).
33. Smith, K.A. *et al*. Bmp and nodal independently regulate lefty1 expression to maintain unilateral nodal activity during left-right axis specification in zebrafish. *PLoS Genet* **7**, e1002289 (2011).
34. Sallin, P., de Preux Charles, A.S., Duruz, V., Pfefferli, C. & Jazwinska, A. A dual epimorphic and compensatory mode of heart regeneration in zebrafish. *Dev Biol* **399**, 27-40 (2015).
35. Wills, A.A., Holdway, J.E., Major, R.J. & Poss, K.D. Regulated addition of new myocardial and epicardial cells fosters homeostatic cardiac growth and maintenance in adult zebrafish. *Development* **135**, 183-192 (2008).
36. Lien, C.L., Schebesta, M., Makino, S., Weber, G.J. & Keating, M.T. Gene expression analysis of zebrafish heart regeneration. *PLoS Biol* **4**, e260 (2006).
37. Sleep, E. *et al*. Transcriptomics approach to investigate zebrafish heart regeneration. *J Cardiovasc Med (Hagerstown)* **11**, 369-380 (2010).
38. Lepilina, A. *et al*. A dynamic epicardial injury response supports progenitor cell activity during zebrafish heart regeneration. *Cell* **127**, 607-619 (2006).
39. de Pater, E. *et al*. Bmp signaling exerts opposite effects on cardiac differentiation. *Circ Res* **110**, 578-587 (2012).
40. Mandel, E.M. *et al*. The BMP pathway acts to directly regulate Tbx20 in the developing heart. *Development* **137**, 1919-1929 (2010).
41. Liu, Y. *et al*. CHD7 interacts with BMP R-SMADs to epigenetically regulate cardiogenesis in mice. *Human molecular genetics* **23**, 2145-2156 (2014).
42. Ling, F., Kang, B. & Sun, X.H. Id proteins: small molecules, mighty regulators. *Current topics in developmental biology* **110**, 189-216 (2014).
43. Liu, H. *et al*. p53 regulates neural stem cell proliferation and differentiation via BMP-Smad1

signaling and Id1. *Stem cells and development* **22**, 913-927 (2013).
44. Ying, Q.L., Nichols, J., Chambers, I. & Smith, A. BMP induction of Id proteins suppresses differentiation and sustains embryonic stem cell self-renewal in collaboration with STAT3. *Cell* **115**, 281-292 (2003).
45. Prabhu, S., Ignatova, A., Park, S.T. & Sun, X.H. Regulation of the expression of cyclin-dependent kinase inhibitor p21 by E2A and Id proteins. *Molecular and cellular biology* **17**, 5888-5896 (1997).
46. Perner, B., Englert, C. & Bollig, F. The Wilms tumor genes wt1a and wt1b control different steps during formation of the zebrafish pronephros. *Developmental biology* **309**, 87-96 (2007).
47. Huang, C.J., Tu, C.T., Hsiao, C.D., Hsieh, F.J. & Tsai, H.J. Germ-line transmission of a myocardium-specific GFP transgene reveals critical regulatory elements in the cardiac myosin light chain 2 promoter of zebrafish. *Dev Dyn* **228**, 30-40 (2003).
48. Lawson, N.D. & Weinstein, B.M. In vivo imaging of embryonic vascular development using transgenic zebrafish. *Developmental biology* **248**, 307-318 (2002).
49. Heicklen-Klein, A. & Evans, T. T-box binding sites are required for activity of a cardiac GATA-4 enhancer. *Developmental biology* **267**, 490-504 (2004).
50. Parinov, S., Kondrichin, I., Korzh, V. & Emelyanov, A. Tol2 transposon-mediated enhancer trap to identify developmentally regulated zebrafish genes in vivo. *Dev Dyn* **231**, 449-459 (2004).
51. Mably, J.D., Mohideen, M.A., Burns, C.G., Chen, J.N. & Fishman, M.C. heart of glass regulates the concentric growth of the heart in zebrafish. *Curr Biol* **13**, 2138-2147 (2003).
52. Schneider, C.A., Rasband, W.S. & Eliceiri, K.W. NIH Image to ImageJ: 25 years of image analysis. *Nat Methods* **9**, 671-675 (2012).
53. Moorman, A.F., Houweling, A.C., de Boer, P.A. & Christoffels, V.M. Sensitive nonradioactive detection of mRNA in tissue sections: novel application of the whole-mount in situ hybridization protocol. *J Histochem Cytochem* **49**, 1-8 (2001).
54. Eden, E., Navon, R., Steinfeld, I., Lipson, D. & Yakhini, Z. GOrilla: a tool for discovery and visualization of enriched GO terms in ranked gene lists. *BMC Bioinformatics* **10**, 48 (2009).
55. R Core Team (R Foundation for Statistical Computing, Vienna, Austria; 2013).

Supplementary Figures

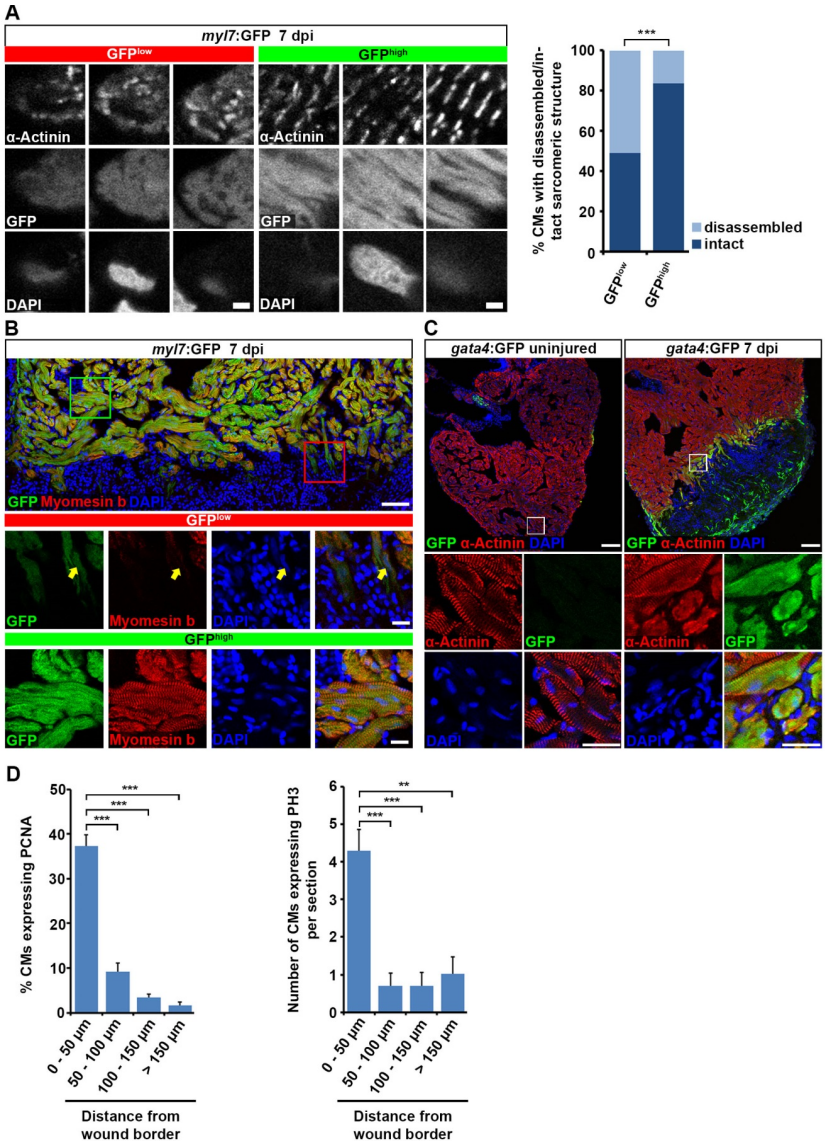

Figure S1. Cardiomyocytes at the wound border dedifferentiate and re-enter the cell cycle. *(A) Individual GFPlow and GFPhigh cardiomyocytes were randomly picked on sections of myl7:GFP transgenic hearts and their sarcomeric structure was categorized according to α-Actinin protein arrangement. Striated and disorganized pattern of α-Actinin protein expression was categorized as intact and disassembled sarcomeric structure, respectively. A higher fraction of GFPlow cardiomyocytes display disassembled sarcomeric structures than GFPhigh cardiomyocytes at 7 dpi. Scale bar, 12.5 µm. Fisher's exact test, p = 0.0002. (B) GFPlow cardiomyocytes show reduced Myomesin b expression (arrow) in myl7:GFP transgenic hearts at*

7 dpi. Scale bar, 50 μm (overview) and 25 μm (inset). (C) GFP expression in gata4:GFP transgenic hearts is activated in α-Actinin+ cardiomyocytes at the wound border at 7 dpi. Scale bar, 50 μm (overview) and 12.5 μm (inset). (D) Proliferating cardiomyocytes, as revealed by PCNA and PH3 expression, are mainly localized within 50 μm of the wound border. Average percentage of PCNA and average number of PH3 positive cardiomyocytes at various distances from the wound border is plotted. Error bars represent SEM. Student's t test, PCNA: p = 0.00002 (0 – 50 μm vs 50 – 100 μm), p = 0.000001 (0 – 50 μm vs 100 – 150 μm), p = 0.0000008 (0 – 50 μm vs >150 μm); PH3: p = 0.0006 (0 – 50 μm vs 50 – 100 μm), p = 0.0006 (0 – 50 μm vs 100 – 150 μm), p = 0.0019 (0 – 50 μm vs >150 μm).

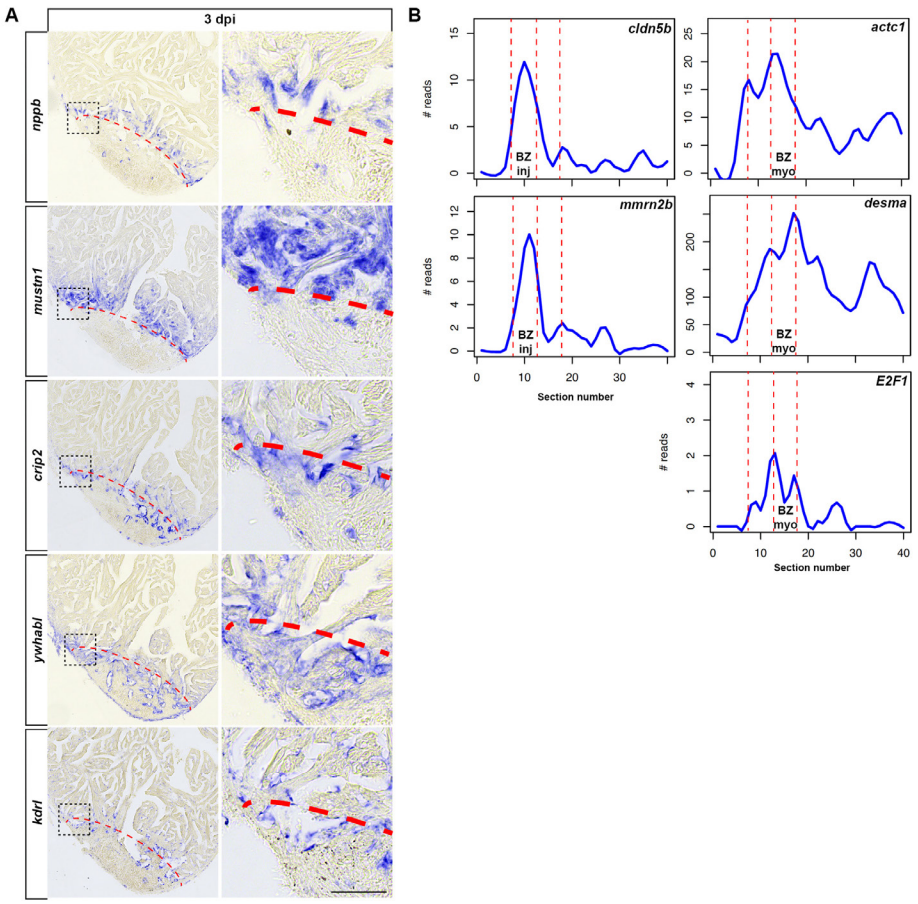

Figure S2. Spatially restricted gene expression reveals two distinct border zone regions. *(A) In situ hybridization on consecutive heart sections (3 dpi) for genes identified by Tomo-seq to be upregulated in the BZmyo (nppb and mustn1) and BZinj (crip2 and ywhabl). Expression of crip2 and ywhabl overlapped with endothelial kdrl. Scale bar, 50 μm. Dashed red line outlines the injury area. (B) Tomo-seq expression traces (3 dpi) for genes involved in embryonic vascular endothelium development (cldn5b and mmrn2b), myocardial development (actc1 and desma) and cell cycle control (E2F1).*

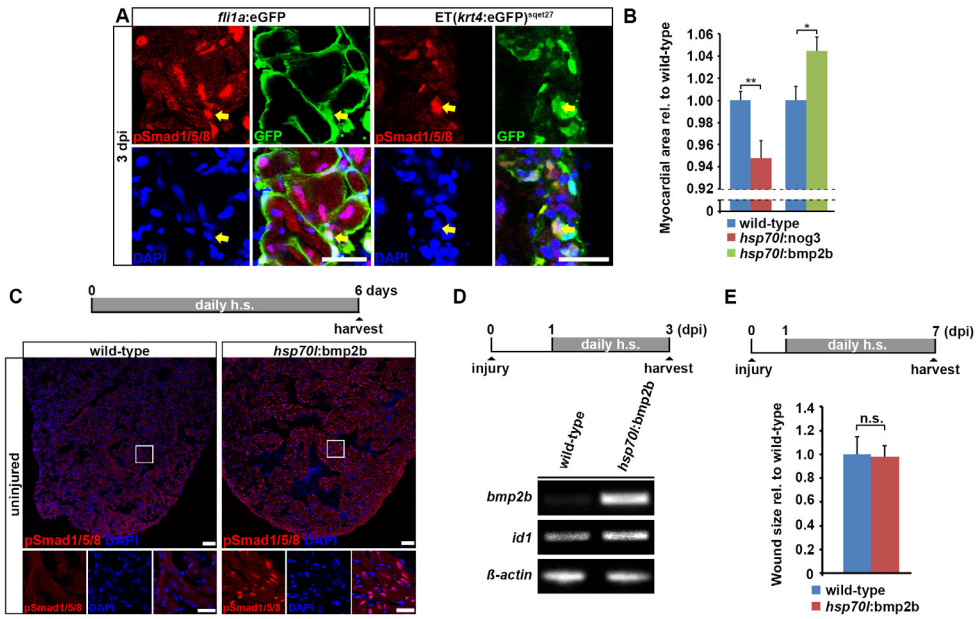

Figure S3. BMP signaling is activated in endocardial and epicardial cells after injury and transgenic overexpression of bmp2b is sufficient to induce accumulation of nuclear pSmad1/5/8 and expression of the BMP target gene id1. *(A) BMP signaling, as revealed by expression of nuclear pSmad1/5/8, is activated in endocardial cells (marked by fli1a:eGFP expression, arrow) and epicardial cells (marked by ET(krt4:eGFP) expression, arrow) at 3 dpi. Scale bar, 25 µm. (B) At 21 dpi, hsp70l:nog3; myl7:GFP double transgenic fish heat-shocked using the same regime as shown in Figure 5B display a smaller area of ventricular myocardial tissue (positive for myl7:GFP) than heat-shocked myl7:GFP-only siblings. In contrast, hsp70l:bmp2b; myl7:GFP double transgenics contain more myocardial tissue than myl7:GFP-only controls. Size of the myocardial tissue relative to the whole ventricle normalized to myl7:GFP-only siblings is plotted. Error bars represent SEM. Student's t test, p = 0.0081 (nog3), p = 0.018 (bmp2b). (C) Overexpression of bmp2b for 6 days via daily heat-shock is sufficient to induce expression of nuclear pSmad1/5/8 in uninjured hsp70l:bmp2b transgenic hearts but not in heat-shocked wild-type hearts. Scale bar, 50 µm. (D) RT-PCR reveals that overexpression of bmp2b for 2 days via daily heat-shock is sufficient to enhance the expression of bmp2b and id1, a conserved BMP target gene, in hsp70l:bmp2b transgenic hearts compared to heat-shocked wild-type siblings at 3 dpi. β-actin serves as loading control. (E) hsp70l:bmp2b transgenic hearts and respective wild-type siblings heat-shocked daily for 6 days do not show different wound sizes at 7 dpi. Error bars represent SEM. Student's t test, p = 0.9.*

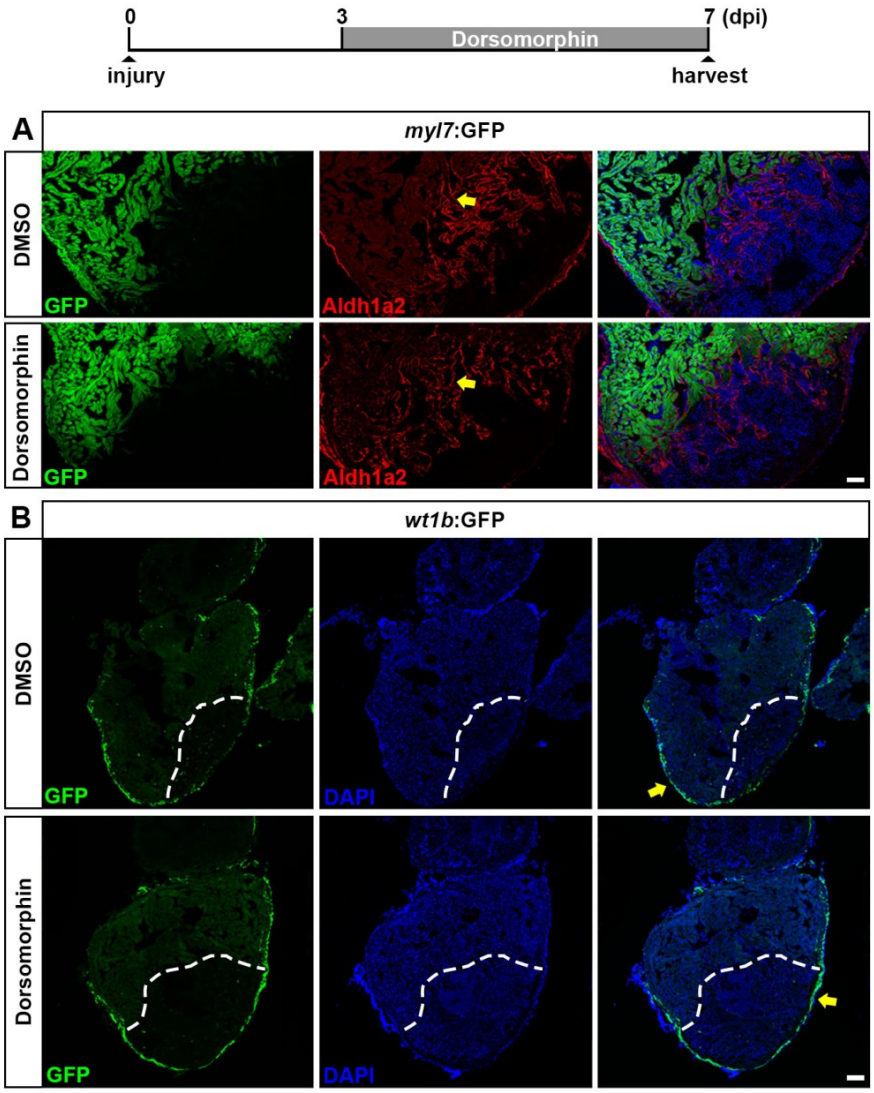

Figure S4. BMP signaling inhibition does not interfere with re-activation of aldhla2 and wt1b in the endocardium and epicardium. *(A) Treatment of myl7:GFP transgenic fish with 5 μM Dorsomorphin for 4 days does not interfere with expression of Aldh1a2 in endocardial cells (arrow) at 7 dpi. Scale bar, 50 μm. (B) Treatment of wt1b:GFP transgenic fish with 5 μM Dorsomorphin for 4 days does not interfere with epicardial expression of GFP (arrow) at 7 dpi. Dashed lines, wound boundary. Scale bar, 100 μm.*

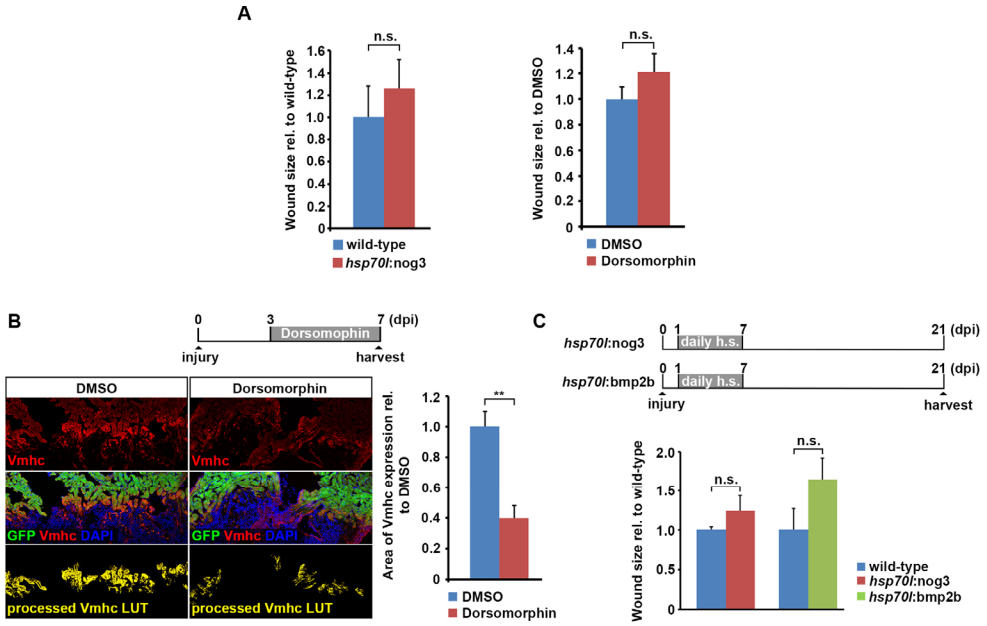

Figure S5. Inhibition of BMP signaling interferes with loss of cardiomyocyte differentiation markers and re-expression of a fetal form of myosin heavy chain. *(A) Inhibition of BMP signaling either by treatment with 5 µM Dorsomorphin in myl7:GFP transgenic hearts or by noggin3 overexpression for 4 days in myl7:GFP; hsp70l:nog3 double transgenic hearts does not alter wound size (the ventricular area lacking GFP expression) at 7 dpi. Error bars represent SEM. Student's t test, p = 0.49 (wild-type vs hsp70l:nog3), p = 0.23 (DMSO vs Dorsomorphin). (B) Treatment of myl7:GFP transgenic fish with 5 µM Dorsomorphin for 4 days reduces the area of ventricular myosin heavy chain (Vmhc) expression in cardiomyocytes at 7 dpi. In processed Vmhc LUT images, all Vmhc signal with pixel intensity lower than 65 (8-bit image) were considered background. Error bars represent SEM. Scale bar, 50 µm. Student's t test, p = 0.006. (C) Immunofluorescence analysis reveals wound size at 21 dpi on heart sections of hsp70l:nog3; myl7:GFP (GFP+) and hsp70l:bmp2b (positive for myosin heavy chain staining) transgenics and their respective wild-type siblings subjected to the depicted heat-shock regime. Size of the wound tissue relative to the whole ventricle normalized to wild-type siblings is plotted. Error bars represent SEM. Student's t test, p = 0.25 (nog3), p = 0.14 (bmp2b).*

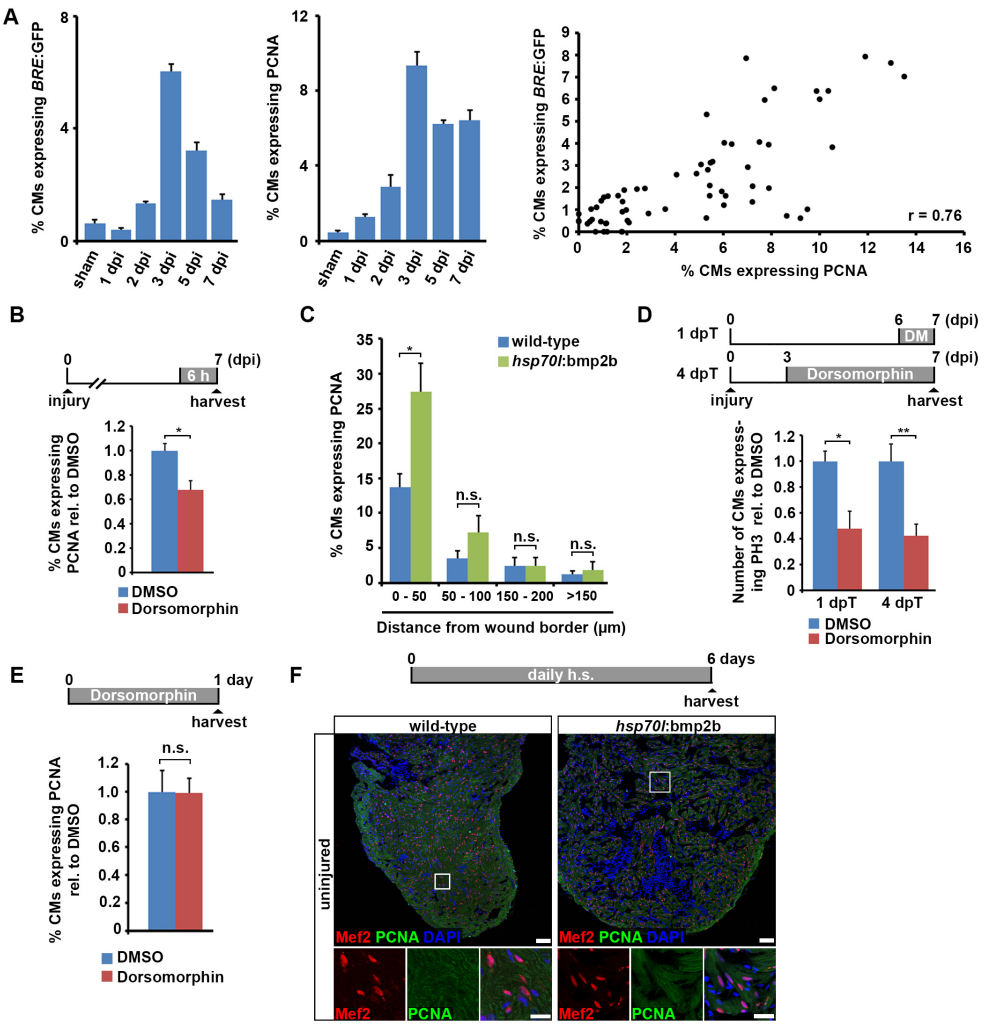

Figure S6. BMP signaling is required for cardiomyocyte cell cycle re-entry. *(A) BMP signaling activation, as revealed by BRE:GFP expression, positively correlates with PCNA expression in cardiomyocytes. Average percentage of cardiomyocytes expressing BRE:GFP and PCNA in sham and injured hearts at 1, 2, 3, 5 and 7 dpi is plotted. Percentage of cardiomyocytes expressing BRE:GFP is then plotted against percentage of cardiomyocytes expressing PCNA to determine the Pearson's correlation coefficient (r = 0.76). Each data point represents one analyzed section. (B) Treatment of wild-type fish with 5 µM Dorsomorphin for 6 h reduces the expression of PCNA in cardiomyocytes at 7 dpi. Average percentage of cardiomyocytes expressing PCNA relative to DMSO control is plotted. Error bars represent SEM. Student's t test, p = 0.015. (C) Overexpression of bmp2b for 6 days via daily heat-shock increases the expression of PCNA in cardiomyocytes within 50 µm of the wound border, but not further away, in hsp70l:bmp2b transgenics relative to heat-shocked wild-type siblings at 7 dpi. Average percentage of cardiomyocytes expressing PCNA at different distances from the wound border*

*is plotted. Error bars represent SEM. Student's t test, *, p = 0.02 (0 - 50 µm), p = 0.25 (50 – 100 µm), p = 0.98 (100 – 150 µm), p = 0.66 (> 150µm). (D) Treatment of myl7:GFP transgenic fish with 5 µM Dorsomorphin for 1 or 4 days reduces the number of phospho-Histone 3 (PH3)+ mitotic cardiomyocytes. Average number of cardiomyocytes expressing PH3 relative to DMSO control is plotted. Error bars represent SEM. Student's t test, p = 0.028 (1 dpT), p = 0.0014 (4 dpT). (E) In juvenile fish, treatment with 5 µM Dorsomorphin for 24 h does not reduce the expression of PCNA in cardiomyocytes. Average percentage of cardiomyocytes expressing PCNA relative to wild-type is plotted. Error bars represent SEM. Student's t test, p = 0.96. (F) Overexpression of bmp2b for 6 days via daily heat-shock is not able to induce expression of PCNA in cardiomyocytes in uninjured hsp70l:bmp2b transgenic hearts. Scale bar, 50 µm.*

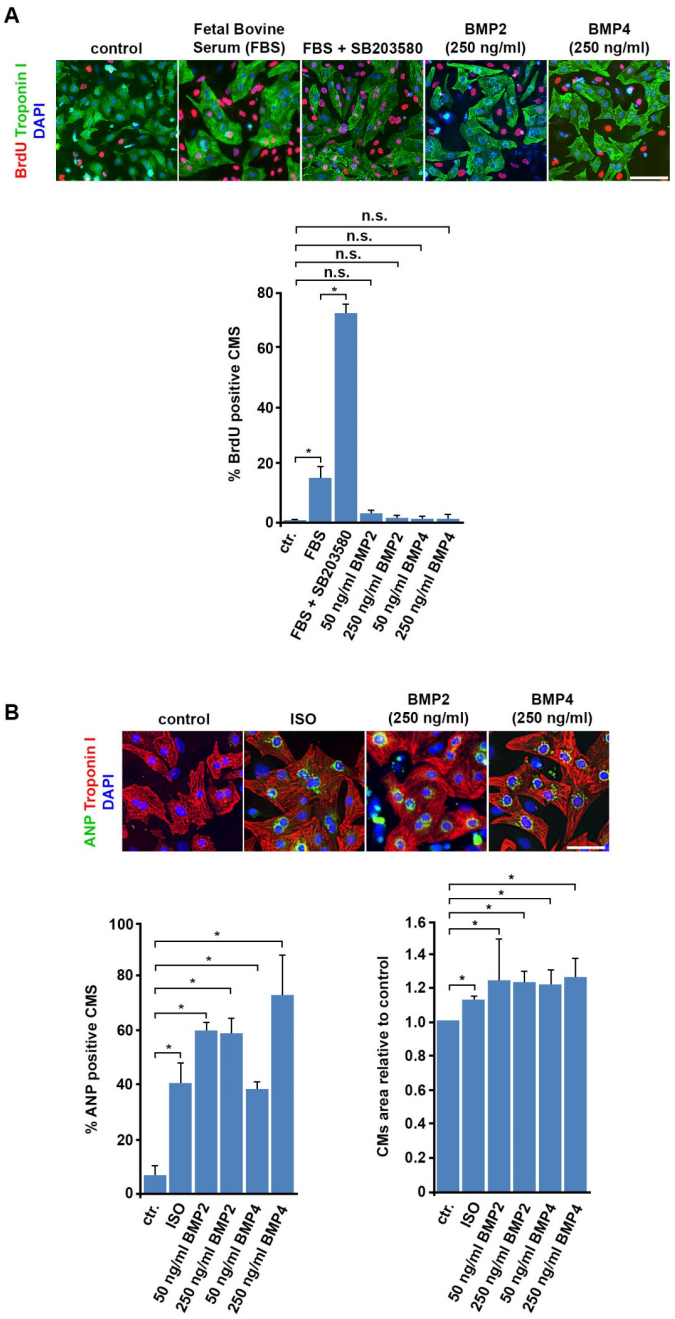

Figure S7. BMP2 and BMP4 induce hypertrophy but not proliferation in cultured neonatal rat cardiomyocytes. *(A) Addition of fetal bovine serum (FBS) or FBS plus 5 μM SB203580 p38 MAPK inhibitor for 48 h induces BrdU incorporation in cultured neonatal rat cardiomyocytes (isolated at P3), while addition of neither BMP2 nor BMP4 recombinant protein at 50 or 250 ng/ml does. Error bars represent SD. Scale bar, 100 μm. Student's t test, * $p < 0.05$. (B) Addition of either 10 μM Isoproterenol (ISO) or 50 or 250 ng/ml of BMP2 or BMP4 recombinant protein for 48 h induces cultured neonatal rat cardiomyocytes hypertrophic responses including atrial natriuretic peptide (ANP) expression and increases in cell size. Error bars represent SD. Scale bar, 50 μm. Student's t test, $p < 0.05$.*

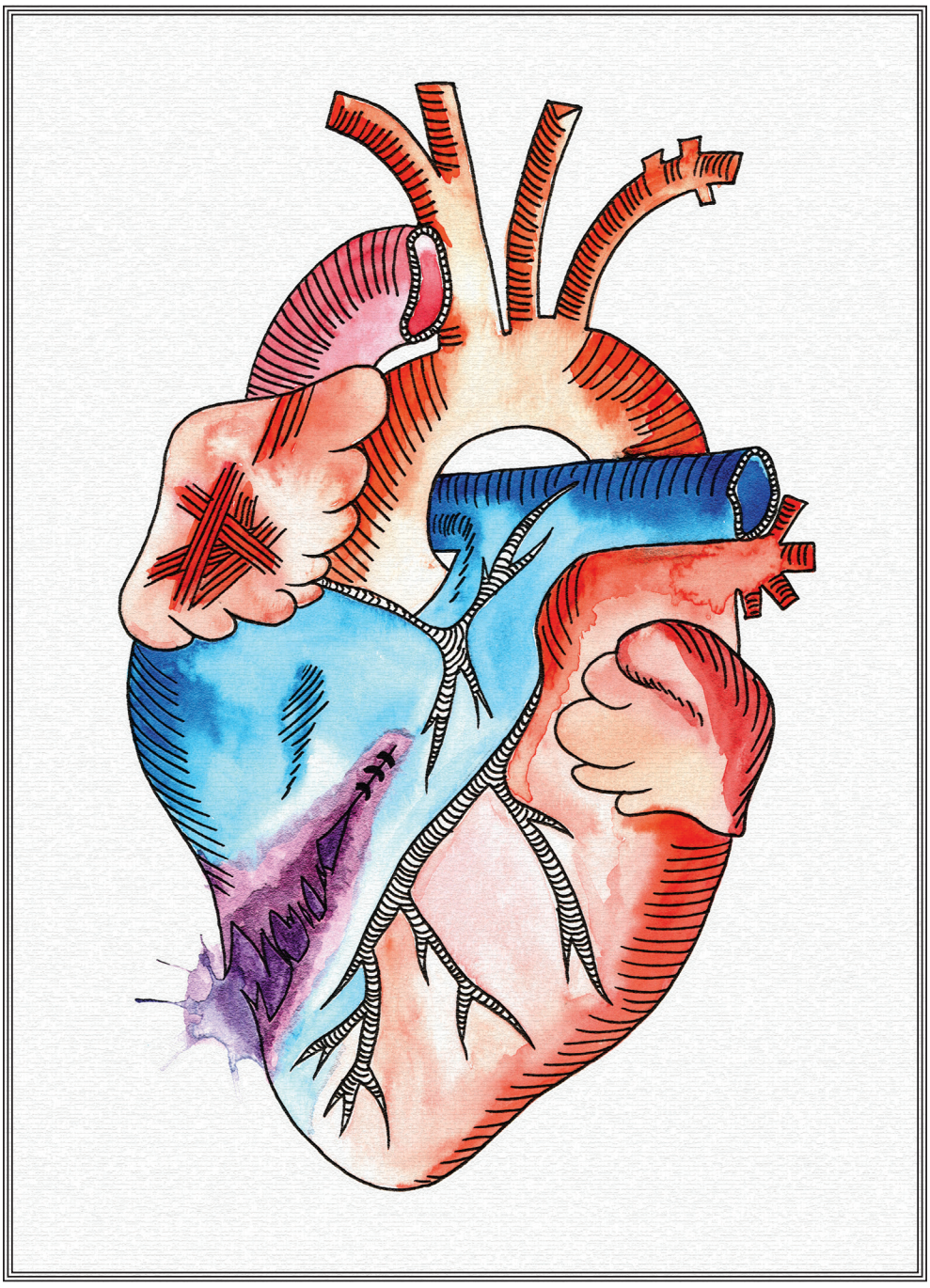

4

Single-cell transcriptomics identifies a cardiac progenitor cell with a distinct metabolism in the regenerating zebrafish heart

Fabian Kruse[1], Cecilia de Heus[2], Laurence Garric[1], Mauro J Muraro[1], Federico Tessadori[1], Joshua C. Peterson[4], Wendy Noort[3], Dennis E.M. de Bakker[1], George Posthuma[2], Dominic Grün[5], Willem J. van der Laarse[6], Judith Klumperman[2], Richard T. Jaspers[3], Alexander van Oudenaarden[1,8] and Jeroen Bakkers[1,7,8]

[1] *Hubrecht Institute and University Medical Center Utrecht, Utrecht, The Netherlands*

[2] *Department of Cell Biology and Institute of Biomembranes, UMC Utrecht, Utrecht, The Netherlands*

[3] *Laboratory for Myology, Department of Human Movement Sciences, Faculty of Behavioural and Movement Sciences, Vrije Universiteit Amsterdam, Amsterdam, The Netherlands.*

[4] *Leiden University Medical Centre, Department of Anatomy and Embryology, Leiden, The Netherlands*

[5] *Max Planck Institute of Immunobiology and Epigenetics, Freiburg, Germany*

[6] *Department of Physiology, VU University Medical Center, Amsterdam, The Netherlands*

[7] *Department of Medical Physiology, Division of Heart and Lungs, UMC Utrecht, Utrecht, the Netherlands.*

[8] *Shared senior authors*

Manuscript under review

Summary

Myocardial infarction is a major cause of death worldwide. It causes permanent scarring due to the irreversible loss of heart muscle tissue, which can lead to heart failure. Recent findings in the adult mammalian heart suggest that a rare population of endogenous cardiomyocytes retains the capacity to proliferate, and has the potential to repair the damaged myocardium [1-5]. However, their identification and characterization have been hampered by the lack of genetic markers, and technical difficulties dissociating and sorting heart muscle cells. Endogenous cardiomyocytes in zebrafish also proliferate in response to injury, and can fully regenerate the damaged heart [6-8]. Here we established a zebrafish *nppa:mCitrine* line to mark proliferating cardiomyocytes in the regenerating adult zebrafish heart to enable their characterization using single-cell transcriptome analysis. While differentiated cardiomyocytes are known to rely on mitochondrial oxidative phosphorylation (OXPHOS) for energy production, in contrast, in proliferating adult cardiomyocytes we found upregulation of transcripts encoding glycolytic enzymes, accompanied by increased glycolytic activity, decreased OXPHOS activity, and altered mitochondrial morphology. The proliferating adult cardiomyocytes had uniform transcriptomes enriched in genes expressed in the embryonic heart, indicative of a dedifferentiated phenotype. Indeed, single-cell mRNA-sequencing revealed strong similarities between embryonic cardiomyocytes and proliferating adult cardiomyocytes. Thus, proliferating cardiomyocytes in the regenerating heart have unique metabolic features and resemble embryonic cardiomyocytes. These features could be used to develop therapeutic interventions to increase the regenerative capacity of the mammalian heart.

Results

After injury, the zebrafish heart regenerates by proliferation of a small population of existing cardiomyocytes located mostly adjacent to the injury site, also known as the border zone [6-8]. These cycling cardiomyocytes exist within a heterogeneous cell population including non-proliferating cardiomyocytes, endothelial cells and immune cells. Thus, a single cell approach is required to isolate them for detailed analysis. We generated a transgenic zebrafish *nppa* reporter line (*TgBAC(nppa:mCitrine)*) in which mCitrine expression recapitulates endogenous expression of the border zone stress gene *nppa* (which encodes a natriuretic peptide) (Fig. 1a, b and Extended Data Fig. 1a-d). Histochemical analysis of injured adult hearts revealed that ~90% of the *nppa:mCitrine* expressing cells were cardiomyocytes, of which ~70% were also positive for the cell proliferation marker PCNA (Extended Data Fig. 2). To isolate these proliferating border zone cardiomyocytes, *nppa:mCitrine* hearts were cryo-injured, followed by cell dissociation and FACS sorting of mCitrine^{high} (border zone) and mCitrine^{low} (remote zone) cells (Fig. 1c and Extended Data Fig. 3). Individual, living cells were sorted onto 384-well plates, followed by single-cell mRNA-sequencing using the SORT-seq (SOrting and Robot-assisted Transcriptome SEQuencing) platform [9] (Supplementary Data 1). To identify the cardiomyocytes amongst the other cell types, we first identified the different cell types based on their transcriptomes. k-medoids clustering of the single cell transcriptomes by the StemID clustering algorithm was used [10] (Supplementary Data 2), and visualized in two dimensions using *t*-distributed stochastic neighbor embedding (*t*-SNE) (Fig. 1d, e). Based on the expression of marker genes for specific cell types (Extended Data Fig. 4a), we identified a large group of cardiomyocytes, a smaller group of endothelial cells, and some fibroblasts and immune cells (Fig. 1e). Based on the transcriptome clustering, the cardiomyocytes fell into four main transcriptionally-related clusters (1, 2, 4 and 7). Comparison of the mCitrine fluorescence intensity (recorded during FACS sorting) of the cardiomyocyte clusters revealed an increase along the vertical axis of the t-SNE map (cluster 2<1<4<7) (Fig. 1f). Thus cardiomyocytes in cluster 7 had on average the highest levels of the *nppa* stress marker. In order to identify specifically the proliferating border zone cardiomyocytes, we also analyzed expression of additional border zone genes (*nppb* and *mustn1b*) and cell cycle-related genes (*cyclin I, ywhaba* and *mycb*). Again, the highest expression was observed in cells from cardiomyocyte cluster 7 and the lowest in cardiomyocyte cluster 2 (Fig. 1g and Extended Data Fig. 4b, c). Together, these results indicate two things: first, the proliferating border zone cardiomyocytes (grouped in cluster 7) can be identified as a separate group in the single-cell seq data. Secondly, these proliferating cardiomyocytes are transcriptionally distinct from non-proliferating cardiomyocytes (grouped in cluster 2), while two intermediate cardiomyocyte clusters lie inbetween.

To identify the molecular characteristics that define the proliferating border zone cardiomyocytes we compared the transcriptomes between the opposing cardiomyocyte clusters 2 and 7 (Fig. 2a, Supplementary Data 3). 771 genes were differentially expressed ($p <$

Figure 1

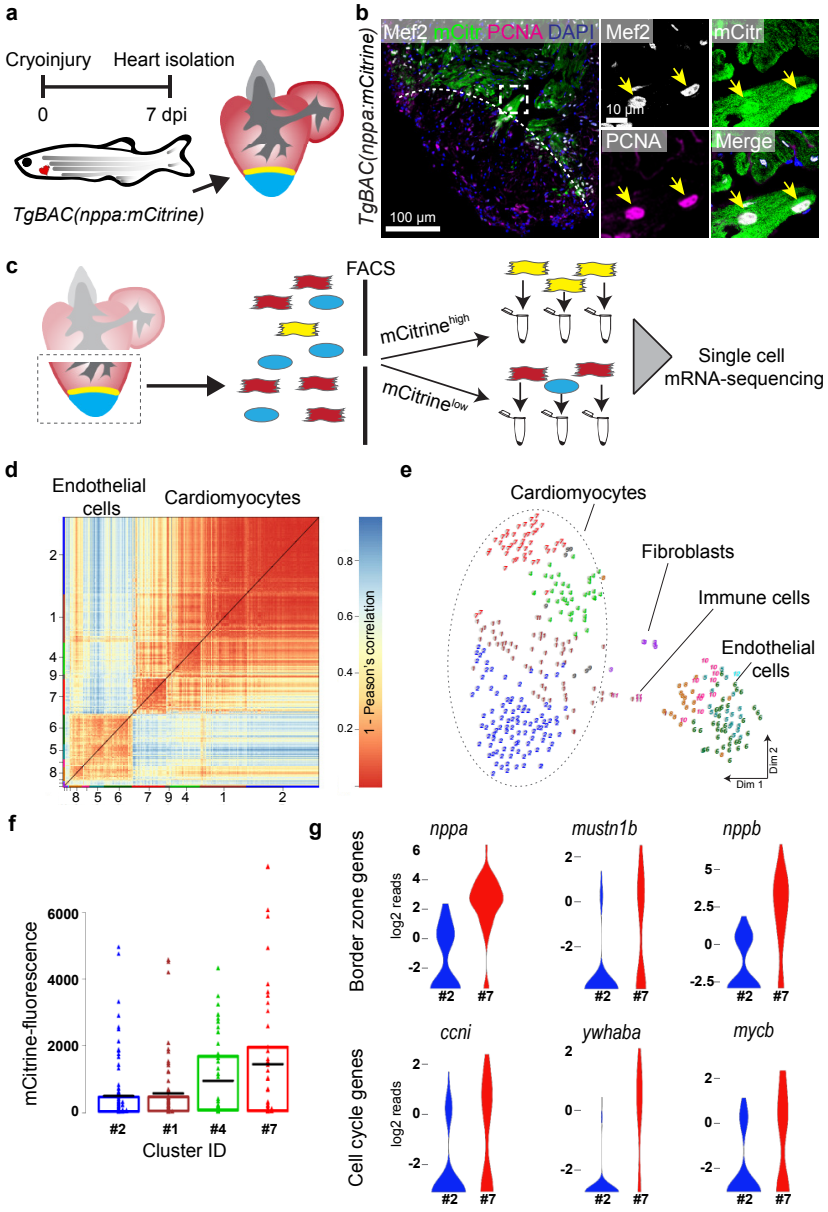

Figure 1: Single-cell mRNA sequencing identifies different cardiomyocyte-populations in the injured zebrafish heart. *(a) Schematic of cryoinjury procedure on adult TgBAC(nppa:mCitrine) fish, followed by heart isolation 7 days post injury (dpi). Injury area depicted in blue, border zone in yellow. (b) Immunostaining on section of injured TgBAC(nppa:mCitrine) heart. Mef2 detects cardiomyocytes, YFP shows nppa expression, and PCNA marks proliferating cells.*

Arrows indicate triple-positive cells. (c) Experimental outline of the single-cell mRNA-sequencing: dissociation of injured hearts into cell suspension followed by FACS sorting for high and low mCitrine fluorescence and single-cell mRNA-sequencing. (d) Pairwise correlation between individual cells across all genes detected. Colour-code indicates cell-to-cell distances measured by [1 – Pearson's correlation coefficient]. StemID clusters are indicated by colour and number on the x- and y-axis. (e) t-distributed stochastic neighbor embedding (tSNE) map representation of transcriptome similarities between individual cells. Colours and numbers indicate StemID clusters as shown in (d). Cell types were identified based on the expression of known marker genes. (f) mCitrine fluorescence levels of the cells sorted into the four cardiomyocyte clusters. The box indicates the 25-75% quartiles, black lines indicate mean-fluorescence per cluster and single measurements are shown by triangles. (g) Violin plots visualizing log2-transformed transcript counts of the border zone genes nppa, mustn1b and nppb, as well as cell cycle related genes ccni, ywhaba and mycb in cluster 2 (mCitrine^{low} cardiomyocytes) and cluster 7 (mCitrine^{high} cardiomyocytes).

0.05; adjusted p-value after Benjamini-Hochberg correction), of which 752 were specifically upregulated in cluster 7 cardiomyocytes, including the border zone genes, *nppa*, *nppb* and *mustn1b* (Fig. 2a). Gene ontology analysis of the differentially expressed genes revealed enrichment in *translation, glycolysis, tricarboxylic acid cycle, OXPHOS, oxidation reduction* and *heart development* genes (Fig. 2a, Supplementary Data 4). The GO-term *translation* is indicative of active cell proliferation, confirming that proliferating cardiomyocytes are grouped in cluster 7. Adult cardiomyocytes rely on fatty acid metabolism and aerobic mitochondrial OXPHOS rather than glycolysis for their energy production [11]. It was therefore surprising that cluster 7 cardiomyocytes upregulated expression of glycolysis genes. Strikingly, genes encoding for all the enzymes required for glycolysis were upregulated, including rate-limiting enzymes such as hexokinase (*hk1*), phospho-fructokinase (*pfkmb*) and pyruvate kinase M2 (*pkm2a* and *pkm2b*) (Fig. 2b). In addition, genes encoding glucose importers (*glut1a*/*slc2a1a* and *glut1b*/*slc2a1b*) and enzymes diverting pyruvate away from the TCA cycle such as pyruvate dehydrogenase kinase (*pdk2a*) and lactate dehydrogenase (*ldha*) were specifically upregulated in the proliferating border zone cardiomyocytes (Fig. 2b). To verify this upregulation in the border zone cardiomyocytes we performed *in situ* hybridization on sections from injured hearts. Consistent with our single cell analyses, we observed specific upregulation of glycolysis genes in border zone cardiomyocytes and their absence in remote cardiomyocytes (Fig. 3a). Furthermore, glucose-6 phosphate dehydrogenase (G6PD), an enzyme participating in the pentose phosphate pathway, was activated in border zone cardiomyocytes (Fig. 3b). Known inducers of glycolysis are the energy-sensing AMP-activated protein kinases (AMPKs)[12], including the AMPK-related *nuak1*. *Nuak1* expression was also induced, both in the isolated border zone cardiomyocytes and *in situ* (Fig. 2b and 3a). Both the upregulated as well as the downregulated genes in cluster 7 cardiomyocytes were enriched in OXPHOS genes (Fig. 2a, b). Strikingly, all 19

downregulated genes are transcribed from mitochondrial DNA with functions in OXPHOS and ATP metabolism (Fig. 2a, b), suggesting altered mitochondrial OXPHOS activity in border zone cardiomyocytes. Corroborating this, a 40% reduction in succinate dehydrogenase (SDH) enzymatic activity, located in the inner mitochondrial membrane that functions in both the citric acid cycle and electron transport chain, was observed specifically in the border zone cardiomyocytes as compared to the remote cardiomyocytes (Fig. 3c,d). In agreement with the reduced mitochondrial OXPHOS activity, transmission electron microscopy (TEM) imaging revealed more immature mitochondria in border zone cardiomyocytes evidenced by their altered morphology and reduced cristae density (Fig. 3e-g), which is consistent with previous reports linking mitochondrial function with morphology [13-15]. Together these results indicate that proliferating cardiomyocytes located in the border zone have a distinct metabolism compared to non-proliferating cardiomyocytes located in the remote region. *In situ*, we also observed altered mitochondrial morphology and a reduction in mitochondrial OXPHOS activity restricted to the border zone cardiomyocytes, with simultaneous induction of glycolysis gene expression, which were not observed in the remote zone or in sham-operated hearts (Extended Data Fig. 5). These observations suggest that, upon cardiac injury, a small population of cardiomyocytes located in the border zone switch their metabolism from aerobic mitochondrial OXPHOS to glycolysis when entering the cell cycle.

Interestingly, a similar metabolic shift from aerobic OXPHOS to glycolysis occurs in tumor cells, known as the Warburg effect [16]. Glycolysis, while yielding less ATP compared to aerobic OXPHOS, does produce essential nutrients that are needed in proliferating cells to produce more biomass [17]. Furthermore, progenitor cells in the developing embryo as well as induced pluripotent stem cells, also depend on glycolysis to maintain proliferation and their potency [18, 19]. This link between cellular metabolism, proliferation and differentiation is interesting in the light of earlier studies speculating that cardiomyocytes in the border zone dedifferentiate [6, 7, 20-22]. This prompted us to compare the transcriptomes of proliferating cardiomyoytes and non-proliferating cardiomyocytes to find indications for (de)differentiation. To do this, we used part of the StemID algorithm that uses the single cell transcriptome data and cell clustering to derive a branched lineage tree [10]. Thereby, this approach proposes the lineage of the sequenced single cells based on their transcriptomes, and in turn, the most likely differentiation route (Extended Data Fig. 6). The algorithm is based on the premise that stem cells and less differentiated cells tend to exhibit more uniform transcriptomes than differentiated cells, which express smaller numbers of genes at higher rates [23]. Moreover, the algorithm assumes that stem cells have the potential to differentiate into a variety of cell types, ergo the transcriptomes of stem cells are related to more cell types than differentiated cells [10]. Thus, the number of branches within the derived lineage tree (i.e., how many links can be made from each cluster to the other clusters, which would represent potential differentiation from one to another) and the transcriptome uniformity (entropy) of the cell cluster are used as features that correlate with the degree of potency. Using this approach, we

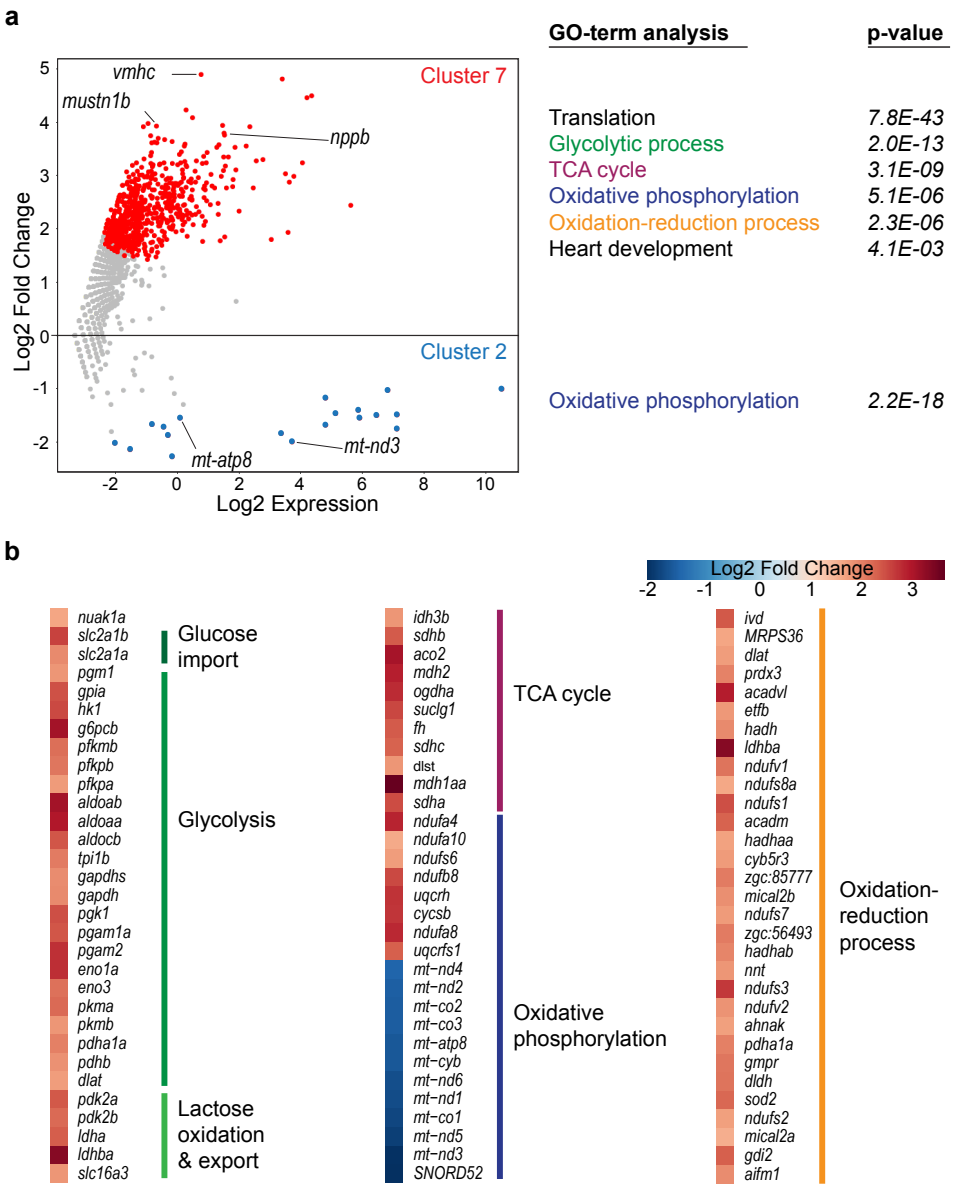

Figure 2: Metabolism genes are differentially expressed between proliferating and non-proliferating cardiomyocytes. *(a) Plot showing differentially expressed genes between cluster 7 versus cluster 2 cells. Differentially expressed genes (p-value<0.05) are highlighted in red (upregulated in cluster 7 cells) and blue (upregulated in cluster 2 cells). Gene ontology (GO) term analysis of significantly differentially expressed genes (p-value<0.05). (b) Log2 fold change of differentially expressed genes (cluster 7 vs cluster 2) selected from GO-terms correlated with metabolism. High relative expression in cluster 7 depicted in red, high expression in cluster 2 depicted in blue.*

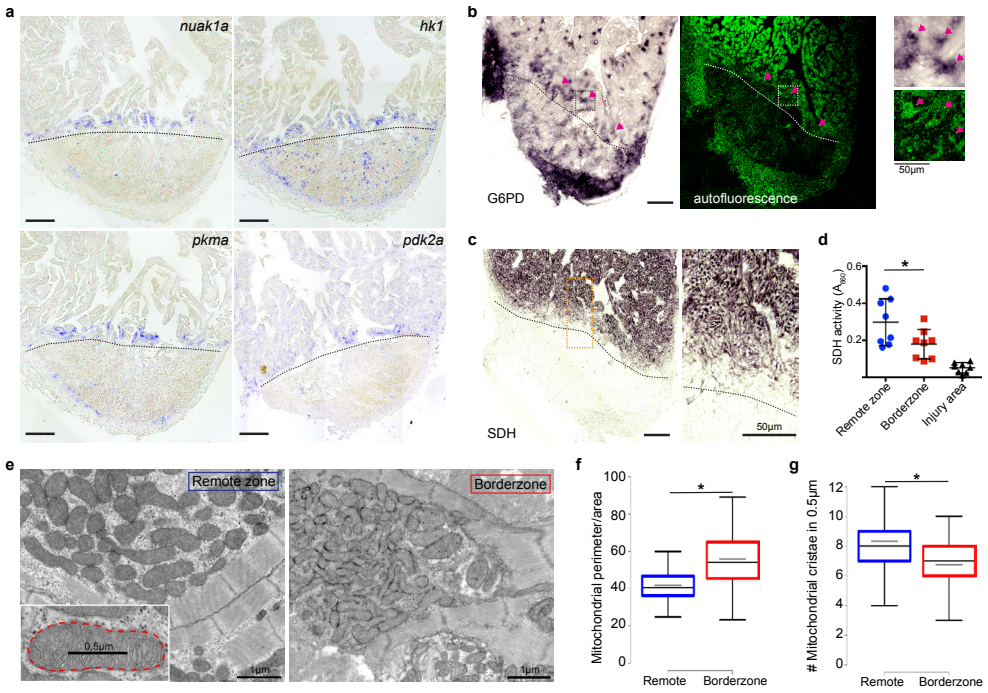

Figure 3: Border zone cardiomyocytes switch metabolism from mitochondrial OXPHOS to glycolysis. *(a) In situ hybridizations on sections from injured hearts (7 dpi) for metabolic genes differentially expressed in cluster 7 cells: NUAK family SNF1-like kinase 1 (nuak1a), hexokinase (hk1), pyruvate kinase (pkma), pyruvate dehydrogenase kinase (pdk2a). Scale bar 100 µm. Injury area is separated by dashed line. (b) Glucose-6-phosphate-dehydrogenase (G6PD) enzymatic staining and autofluorescence marking cardiomyocytes of the same section (7 dpi). Injury area is separated by dashed line and G6PD positive areas are highlighted by magenta arrows. Boxed areas are shown in higher magnification. (c) Succinate dehydrogenase (SDH) enzyme staining on serial section of the same heart, injury area separated by dashed line. Boxed area shown in magnification. (d) Quantification of SDH activity in injury area, border zone and remote zone (n=8 hearts). Scale bar 100 µm (50 µm in magnification). (e) Transmission electron microscopy images of mitochondria in cardiomyocytes from the remote zone and the border zone of the injured heart (7 dpi). Note the smaller and irregular shaped mitochondria in the border zone cardiomyocyte. Box shows mitochondrion with delineated perimeter (dotted red line) and 0.5 um measurement across cristae, as used for quantification in d and e. Scale bar 1 µm. (f) Quantification of mitochondrial perimeter-to-area ratio in 100 remote and border zone mitochondria, taken from three hearts. (g) Quantification of mitochondrial cristae density in 40 remote and border zone mitochondria, taken from three hearts. * P-value<0.05.*

found a similar number of links between the four clusters, suggesting similar differentiation potentials. However, there were large differences in transcriptome entropy, resulting in low (cluster 2), intermediate (clusters 1 and 4) and high (cluster 7) StemID scores (Fig. 4a). This gradual increase suggests a dedifferentiation axis from non-proliferating to proliferating cardiomyocytes.

While cardiomyocytes undergo a well defined sequence of morphological and transcriptional changes during differentiation, very little is known about the reverse process. Ordering whole-transcriptome profiles of single cells with an unsupervised algorithm can improve the temporal resolution during differentiation by identifying intermediate stages of differentiation without a priori knowledge of marker genes [24]. In this manner, the single-cell mRNA-seq experiment will constitute an in silico time series, with each cell representing a distinct state of differentiation along a continuum. To analyze the transcriptional changes occurring during this apparent dedifferentiation, the most likely dedifferentiation path, based on the StemID scores, was choosen starting at cluster 2 and progressing through clusters 1, 4 and 7. StemID infers the position of each cell on the link connecting two cluster centres based on how much a cell is biased towards either one of these clusters (Extended Data Fig. 6). The relative position of all cells on a given link reflects a pseudo-temporal order of the differentiation progress. Next, gene expression profiles along this pseudo-temporal order were computed for all detected genes using the single-cell transcriptomes. These gene expression profiles were grouped into modules of co-expressed genes using self-organizing maps (SOMs), resulting in 14 modules (Fig. 4b, Supplementary Data 5). Corroborating our hypothesis of varying differentiation states, we observed that gene expression within these modules changed smoothly over pseudo time. We next analyzed the temporally-ordered expression profiles and identified four groups of genes that shared the same dynamics of expression during this differentiation trajectory. The first group (modules 1, 2) contained genes that were most highly expressed only in cells at the very beginning of the pseudo time line and their expression rapidly declined in cells that were positioned later. This group contained many genes transcribed from mitochondrial DNA, which indicates that the cells at the start of the pseudo time line are mature cardiomyocytes. The second group (modules 3-5 and 11) contained genes with a low expression in cells both at the start and the end of the pseudo-temporal line and a high expression in cells halfway, suggestive of an early role during the dedifferentiation process. Interestingly this group contained many glycolytic genes. The third group (modules 6 and 12-14) also contained genes that were induced early (like group 2 genes), but stayed constant in cells further along the pseudo time line. Many ribosomal genes followed this expression pattern. The fourth group (module 10) contained genes that showed an exponential increase in expression starting when genes from the second group, containing the glycolytic genes, had reached a peak in their expression. Their late induction suggests that these genes mark the most dedifferentiated cells. GO-term analysis of module 10 genes revealed an enrichment in genes with a function in *cardiac muscle fiber development* (p =

3,97E-06) and *actin binding* (p = 1,45E-08) including genes encoding titin (*ttna* and *ttnb*), myomesin (*myom2*), nebulin-related anchoring protein (*nrap*), smooth muscle actin (*acta2*), non-muscle myosin (*myh10*) and xin actin binding repeat containing 1 (*xirp1*). Importantly, *in situ* hybridization on sections of injured hearts confirmed their expression in the border zone (Extended Data Fig. 5). Interestingly, many of these genes are also highly expressed in embryonic cardiomyocytes where they are required for sarcomere assembly [25, 26]. These data indicate that the proliferating border zone cardiomyocytes are embryonic-like and have a distinct metabolic state. Importantly, the SOM analysis confirmed the dedifferentiation axis between the cardiomyocyte cell clusters and suggested an immature character of the proliferating cardiomyocytes in cluster 7.

To test this dedifferentiation hypothesis in a more direct manner, we compared the transcriptomes of adult cardiomyocytes in the regenerating heart with embryonic cardiomyocytes. To obtain embryonic cardiomyocytes we performed FACSorting on embryos expressing the cardiomyocyte specific marker *Tg(myl7:GFP)* (Fig. 4c). Embryos at 2 days post fertilization were chosen since glycolytic metabolism genes were strongly expressed (Extended Data Fig. 10). Single-cell mRNA-sequencing was performed (Supplementary Data 6) and combined with the single-cell data from the injured adult hearts (Supplementary Data 7). The StemID algorithm identified two embryonic cardiomyocyte clusters and three adult cardiomyocyte clusters (Extended Data Fig. 8a, b, c). The two embryonic cardiomyocyte clusters were composed of ventricular and atrial cardiomyocytes, as evidenced by *vmhc* and *myh6* expression, respectively (Extended Data Fig. 8d). Importantly, the proliferating cardiomyocytes identified in cluster 7 of the adult data analysis had a transcriptome that was highly similar to embryonic cardiomyocytes, as shown by pairwise correlation of the differentially expressed genes between the cardiomyocyte clusters: only 184 genes (p-value <0.01), out of 23,707 total detected genes, were differentially expressed between the embryonic and the proliferating adult cardiomyocytes (Fig. 4d). In contrast, over 1800 genes (p-value <0.01) were differentially expressed between embryonic and non-proliferating adult cardiomyocytes, including many genes with a role in cellular metabolism (Fig. 4d and Extended Data Fig. 9, Supplementary Data 8). Together, these results indicate that proliferating adult cardiomyocytes located in the border zone of the regenerating heart closely resemble embryonic cardiomyocytes.

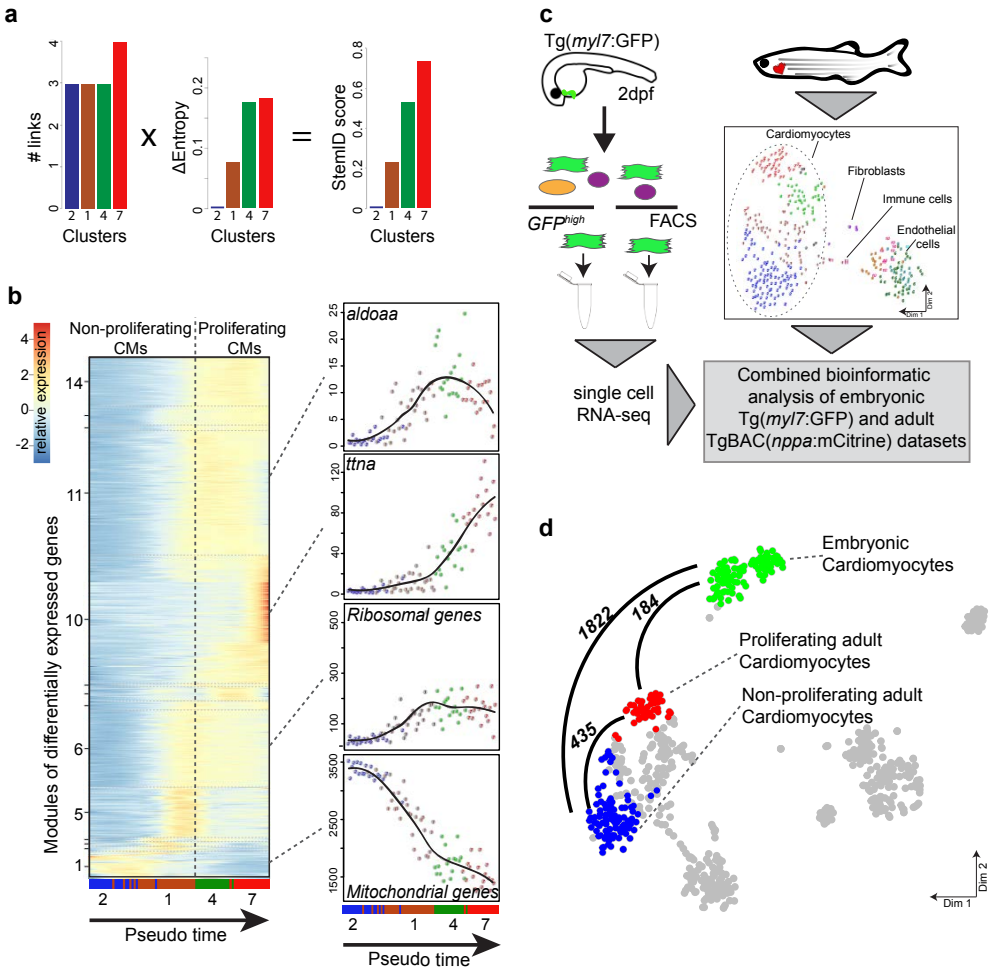

Figure 4: Proliferating cardiomyocytes resemble embryonic cardiomyocytes. *(a) Bar plot of StemID scores for the cardiomyocyte clusters (clusters #2, 1, 4 and 7) calculated by the formula: number of significant links for each cluster multiplied by the median transcriptome entropy across all cells in a cluster. (b) One-dimensional SOM of z-score transformed expression profiles along the differentiation trajectory incurred by StemID analysis. Y-axis represents the fourteen modules with differentially expressed genes. X-axis represents the pseudo time in which the cells were ordered. Expression profiles of representative genes of the major modules are shown on the right. Y-axis shows transcript counts. Running mean with a window size of 25 is shown by a black line. (c) Experimental outline: 2-day old myl7:GFP embryos were dissociated and FACS sorted for GFP^{high} cardiomyocytes, followed by single cell mRNA sequencing. Single-cell transcriptomics data from embryonic and adult injured heart cells (shown in Fig. 1) were combined for StemID analysis. (d) tSNE map visualizing embryonic (green), adult proliferating (red, previously cluster 7) and adult non-proliferating (blue, previously cluster 2) cardiomyocyte populations. The number of pairwise differentially expressed genes between the various cardiomyocyte clusters is indicated.*

In conclusion, we provide evidence that proliferating cardiomyocytes in the regenerating zebrafish heart dedifferentiate towards embryonic-like cardiomyocytes. Our analysis goes beyond earlier studies examining sarcomere structures and signaling factors that have also suggested that proliferating cardiomyocytes may have dedifferentiated [6, 7, 8, 20-22]. By isolating this rare population of cardiomyocytes at the single cell level, we have now been able to show that dramatic changes occur across the whole transcriptome of the proliferating cardiomyocytes such that they essentially become embryonic-like. A model in which these embryonic-like cardiomyocytes are already present in the undamaged heart is less likely since we were unable to detect such cells in sham operated hearts. Somehow, this metabolic switch and dedifferentiation induced in the injured zebrafish heart is restricted to cardiomyocytes in the border zone. The signal driving the metabolic switch and reprogramming of border zone cardiomyocytes needs to be determined and could be related to a change in cell-cell interactions or physiological condition, such as availability of oxygen, caused by the injury.
One important difference in the repair mechanisms between zebrafish and mammalian hearts is that in zebrafish a natural response to cardiac injury results in efficient heart regeneration. This is absent in the adult mammalian heart either due to the lack of appropriate signals or the inability to respond to these signals. However, like the zebrafish heart, the neonatal mouse and human heart can regenerate very efficiently[27, 28]. Mammalian cardiomyocytes also undergo a metabolic switch from glycolysis to OXPHOS during the transition from an embryonic- to a postnatal environment, which exposes cells to higher oxygen levels, while differentiating into mature cardiomyocytes [11, 29, 30]. Thus, there appears to be a conserved link between the proliferative/regenerative capacity of cardiomyocytes, their metabolic phenotype, and their maturity. Importantly, hypoxia, which reduces mitochondrial activity and aerobic respiration, can induce cardiomyocyte proliferation in adult mice [3, 31]. Whether cellular metabolism in the proliferating mammalian cardiomyocytes switches from OXPHOS to glycolysis, like we show here in zebrafish, remains to be determined. If it does, determining the cellular metabolic state could be used to identify proliferating cardiomyocytes and determine the regenerative capacity of the heart. This will aid the search for interventions to promote regeneration of the mammalian heart.

Methods:

Transgenic fish lines and cryoinjury

All procedures involving animals were approved by the local animal experiments committees and performed in compliance with animal welfare laws, guidelines and policies, according to national and European law.

The TgBAC(*nppa*:mCitrine) line was generated essentially as described previously [32, 33]. In short, an iTOL2_amp cassette for pTarBAC was inserted in the vector sequence of bacterial artificial chromosome (BAC) CH211-70L17, which contains the full *nppa* locus. Subsequently, a mCitrine_kan cassette was inserted at the ATG start codon of the first exon of the nppa gene. Amplification from a pCS2+mCitrine_kanR plasmid was achieved with primers :

FWD_NPPA_HA1_GFP_5'-gagccaagccagttcagagggcaagaaaacgcattcagagacactcagagACCA TGGTGAGCAAGGGCGAGG-3' and REV_NPPA_HA2_NEO_5'-gtctgctgccaaaccaggagc agcagtcctgtcagaattagtcccccggcTCAGAAGAACTCGTCAAGAAGGCGATAGAA -3'.

Sequences homologous to the BAC are shown in lower case. Recombineering was performed following the manufacturer's protocol (Red/ET recombination; Gene Bridges GmbH, Heidelberg, Germany) with minor modifications. BAC DNA isolation was carried out using a Midiprep kit (Life Technologies BV, Bleiswijk, The Netherlands). BAC DNA was injected at a concentration of 300 ng/μl in the presence of 25ng Tol2 mRNA. At 3 dpf, healthy embryos displaying robust nppa-specific fluorescence in the heart were selected and grown to adulthood. Subsequently, founder fish were identified by outcrossing and their progeny grown to adulthood to establish the transgenic line.

Zebrafish of ~ 4 to 18 months of age were used for regeneration experiments. Cryoinjuries were performed as previously described [34], except that a liquid nitrogen-cooled copper filament of 0.3 mm diameter was used instead of dry ice.

Immunofluorescence

ADULT: For immunofluorescence, hearts were extracted, fixed in 4% PFA at room temperature for 1 h and cryosectioned into 10 μm sections. Heart sections were equally distributed onto seven serial slides so each slide contained sections representing all areas of the ventricle.

Primary antibodies used were anti-PCNA (Dako #M0879), anti-GFP (aves #GFP-1010), and anti-Mef2c (Santa Cruz #SC313). Antigen retrieval was performed by heating slides containing heart sections at 85°C in 10 mM sodium citrate buffer (pH 6) for 10 minutes. Secondary antibodies conjugated to Alexa 488 (ThermoFisher Scientific), Cy3 or Cy5 (Jackson Laboratories) were used at a dilution of 1:1000. Nuclei were shown by DAPI (4',6-diamidino-2-phenylindole) staining. All images of immunofluorescence stainings are single optical planes acquired with a Leica Sp8 confocal microscope. For quantifications, 3 sections displaying the biggest wounds were analyzed per heart. Quantifications of PCNA,

Mef2, and mCitrine expression were performed in cardiomyocytes situated within 150 μm from the wound border on 3 sections of >4 hearts.
EMBRYONIC: live embryos were immobilized using ms222 and embedded in nitrocellulose + E3 to be mounted on a Leica SPE confocal microscope, followed by a Z-stack maximum projection (step size 2 μm).

In situ hybridization
ADULT: After o/n fixation in 4% PFA, hearts were washed in PBS twice, dehydrated in EtOH, and embedded in paraffin. Serial sections were made at 10 μm. *In situ* hybridization was performed on paraffin-sections as previously described [8].
EMBRYO: Embryos were fixed overnight in 4% paraformaldehyde (PFA) and stored in MeOH at -20˚C. Embryos, after rehydration to PBST(tween 0.1%), were treated with proteinase K 1mg/ml for 15 to 45 minutes depending on stage. Then, embryos were treated according to the protocol described in Noel et al [35].

Isolation of single cells from cryoinjured hearts
Cryoinjured hearts were extracted at 7 dpi. Cells were dissociated according to Tessadori et al. [33]. For cell sorting, viable cells were gated by negative DAPI staining and positive YFP-fluorescence. In brief, the FACS gating was adjusted to sort cells for nppa:mCitrine^{high} (to enrich for proliferating cardiomyocytes) and nppa:mCitrine^{low} (remote cardiomyocytes and other cell types) cells (Extended Data Fig. 3).

Isolation of single cells from embryonic zebrafish
Transgenic *tg(myl7:GFP)* 2-day-old embryos [36] were dechorionated and digested in HBSS Ca^{2+}/Mg^{2+} free media containing 0.1% collagenase type II (Gibco) at 32^{o}C for 30-40 minutes followed by 1X TrypLE Express (Gibco) for 15-30 minutes at 32^{o}C with agitation. Dissociated cells were then FACSorted and subjected to single-cell mRNA-seq.

Single-cell mRNA sequencing
Single-cell sequencing libraries were prepared using SORT-seq [9]. Live cells (n=579 mCitrine^{high} and n=192 mCitrine^{low}) were sorted into 384-well plates with Vapor-Lock oil containing a droplet with barcoded primers, spike-in RNA and dNTPs, followed by heat-induced cell lysis and cDNA syntheses using a robotic liquid handler. Primers consisted of a 24 bp polyT stretch, a 4bp random molecular barcode (UMI), a cell-specific 8bp barcode, the 5' Illumina TruSeq small RNA kit adapter and a T7 promoter. After cell-lysis for 5 minutes at 65˚C, RT and second strand mixes were distributed with the Nanodrop II liquid handling platform (Inovadyne). After pooling all cells in one library, the aqueous phase was separated from the oil phase, followed by IVT transcription. The CEL-Seq2 protocol was used for library prep [37]. Illumina sequencing libraries were prepared with the TruSeq small RNA

primers (Illumina) and paired-end sequenced at 75 bp read length on the Illumina NextSeq platform. Mapping was performed against the zebrafish reference assembly version 9 (Zv9).

Bioinformatic analysis

We detected an average of 20,885 reads per cell. Based on the distribution of the log10 total reads plotted against the frequency, we decided to introduce a cutoff at minimally 3500 reads per cell before further analysis. Moreover, we discarded genes that were not detected at >3 transcripts in >1 cell and we downsampled reads to 3500, as means of normalization. These cutoffs ensured a high quality of input sequencing data, but reduced the number of cells used in the analysis to 352. The StemID algorithm, and its extension StemID, were used as previously published [10]. In short, StemID is an approach developed for inferring the existence of stem cell populations from single-cell transcriptomics data. StemID calculates all pairwise cell-to-cell distances (1 – Pearson correlation) and uses this to cluster similar cells into clusters that correspond to the cell types present in the tissue. The StemID algorithm calculates the number of links between clusters. This is based on the assumption that cell types with less links are more canalized while cell types with a higher number of links have a higher diversity of cell fates. Besides the number of links, the StemID algorithm also calculates the change in transcriptome entropy. Differentiated cells usually express a small number of genes at high levels in order to perform cell specific functions, which is reflected by a low entropy. Stem cells and progenitor cells display a more diverse transcriptome reflected by high entropy [10, 23]. By calculating the number of links of one cluster to other clusters and multiplying this with the change in entropy, it generates a StemID score, which is representative to "stemness" of a cell population.

Inference of co-expressed gene modules

To identify modules of co-expressed genes along a specific differentiation trajectory (defined as a succession of significant links between clusters as identified by StemID) all cells assigned to these links were assembled in pseudo-temporal order based on their projection coordinate. Next, all genes that are not present with at least two transcripts in at least a single cell are discarded from the sub-sequent analysis. Subsequently, a local regression of the z-transformed expression profile for each gene is computed along the differentiation trajectory. These pseudo-temporal gene expression profiles are topologically ordered by computing a one-dimensional self-organizing map (SOM) with 1,000 nodes. Due to the large number of nodes relative to the number of clustered profiles, similar profiles are assigned to the same node. Only nodes with more than 3 assigned profiles are retained for visualization of co-expressed gene modules. Neighboring nodes with average profiles exhibiting a Pearson's correlation coefficient >0.9 are merged to common gene expression modules. These modules are depicted in the final map.

Transmission Electron Microscopy

Hearts were excised and immediately chemically fixated at room temperature with 2,5% glutaraldehyde and 2% formaldehyde (EMS, Hainfield USA) in 0.1M phosphate buffer pH 7.4 for 2 hr. Next, hearts were post fixed with 1 % OsO_4 (EMS, Hainfield USA)/ 1.5 % $K_3Fe(CN)_6$ in 0.065 M phosphate buffer for 2 h at 4 ºC and finally 1 h with 0,5% uranyl acetate. After fixation, hearts were dehydrated in a graded series of acetone and embedded in Epon epoxy resin (Polysciences). Ultrathin sections of 60 nm were cut on a Leica Ultracut T (Leica, Vienna, Austria) and contrasted with uranyl acetate (0.4% in AD, EMS, Hainfield USA) and lead citrate (Leica Vienna, Austria) using the AC20 (Leica Vienna, Austria) and examined with a Jeol 1010 electron microscope (Jeol Europe, Nieuw Vennep, The Netherlands).

Quantification of mitochondrial parameters.

In every heart, each in the borderzone and remote myocardial region, 100 well-deliniated mitochondria with clearly visible outer and inner membranes were selected. Mitochondrial perimeter and surface were measured using the freehand tool of Image J. The perimeter to surface ratio was calculated and used as a factor that describes the pluriformity of mitochondria. The amount of cristae was estimated by counting the number of cristae intersected by a line of 0.5μm length in 40 mitochondria per region according to Puente and colleagues [38].

Histology and enzyme histochemistry

Serial cryosections of the heart were cut 7μm thick and either fixed in formalin, stained with Meyer's hematoxylin and eosin (HE), dehydrated and mounted in Entellan, or incubated for enzyme histochemistry. Chemicals for histochemistry of succinate dehydrogenase (SDH) activity or glucose-6-phosphate dehydrogenase (G6PD) activity were obtained from Sigma Aldrich. Sections for SDH activity were incubated for 20 min at 28°C in 37.5 mM sodium phosphate buffer pH 7.60, 70 mM sodium succinate, 5 mM sodium azide and 0.4 mM tetranitro blue tetrazolium (TNBT) [39]. The reaction was stopped in 10mM HCl. Sections for G6PD were incubated for 30 min at 28° in 18% polyvinyl alcohol (mol mass 40000) in 100 mM sodium phosphate buffer pH 7.45, 10mM glucose-6-phosphate, 0.8 mM $NADP^+$, 4 mM $MgCl_2$, 0.2 mM phenazine methosulfate, 5mM sodium azide and 5 mM tetranitro blue tetrazolium (40 µl TNBT stock/ml: 5 mg TNBT dissolved in 20 µl ethanol and 20 µl dimethylformamide at 70°C). The reaction was stopped in 0.1 M sodium phosphate buffer pH 5.3 at 60°C [40]. Controls without succinate or glucose-6-phosphate did not stain. The incubated sections were mounted in glycerine gelatin. The absorbances of the SDH-reaction product in the sections were determined at 660 nm using a calibrated microdensitometer [41] and ImageJ.

Acknowledgements

We would like to thank V. Christoffels for critical reading of the manuscript and Life Science Editors for editing support. J.B. acknowledges support from the Netherlands Cardiovascular Research Initiative and the Dutch Heart Foundation (grants CVON2011-12 HUSTCARE and Cobra[3]). L.G. was supported by an EMBO long-term fellowship.

Author contributions

F.K. and J.B. conceived and designed the project, performed the experiments, analyzed the data and wrote the manuscript. F.T. and J.C.P. generated the nppa-reporter line. M.J.M., D.G. and A.v.O. performed the single cell sequencing and helped with bioinformatics analyses. L.G. performed embryonic zebrafish work. D.E.M.d.B. helped with in situ hybridizations. C.d.H, G.P. and J.K. performed and analyzed the electron microscopy data. W.N., W.J.v.d.L. and R.T.J. performed and analyzed enzymatic stainings. All authors approved the manuscript.

Bibliography

1. Bergmann, O. *et al*. Evidence for cardiomyocyte renewal in humans. *Science* **324**, 98-102 (2009).
2. Senyo, S.E. *et al*. Mammalian heart renewal by pre-existing cardiomyocytes. *Nature* **493**, 433-436 (2013).
3. Kimura, W. *et al*. Hypoxia fate mapping identifies cycling cardiomyocytes in the adult heart. *Nature* **523**, 226-230 (2015).
4. Tao, G. *et al*. Pitx2 promotes heart repair by activating the antioxidant response after cardiac injury. *Nature* **534**, 119-123 (2016).
5. D'Uva, G. *et al*. ERBB2 triggers mammalian heart regeneration by promoting cardiomyocyte dedifferentiation and proliferation. *Nat Cell Biol* **17**, 627-U207 (2015).
6. Jopling, C. *et al*. Zebrafish heart regeneration occurs by cardiomyocyte dedifferentiation and proliferation. *Nature* **464**, 606-609 (2010).
7. Kikuchi, K. *et al*. Primary contribution to zebrafish heart regeneration by gata4(+) cardiomyocytes. *Nature* **464**, 601-605 (2010).
8. Wu, C.C. *et al*. Spatially Resolved Genome-wide Transcriptional Profiling Identifies BMP Signaling as Essential Regulator of Zebrafish Cardiomyocyte Regeneration. *Dev Cell* **36**, 36-49 (2016).
9. Muraro, M.J. *et al*. A Single-Cell Transcriptome Atlas of the Human Pancreas. *Cell Syst* **3**, 385-394 e383 (2016).
10. Grun, D. *et al*. De Novo Prediction of Stem Cell Identity using Single-Cell Transcriptome Data. *Cell Stem Cell* **19**, 266-277 (2016).
11. Lopaschuk, G.D., Collins-Nakai, R.L. & Itoi, T. Developmental changes in energy substrate use by the heart. *Cardiovasc Res* **26**, 1172-1180 (1992).
12. Hardie, D.G. AMP-activated protein kinase: an energy sensor that regulates all aspects of cell function. *Genes Dev* **25**, 1895-1908 (2011).
13. Gong, G. *et al*. Parkin-mediated mitophagy directs perinatal cardiac metabolic maturation in mice. *Science* **350**, aad2459 (2015).
14. Giraud, M.F. *et al*. Is there a relationship between the supramolecular organization of the mitochondrial ATP synthase and the formation of cristae? *Biochim Biophys Acta* **1555**, 174-180 (2002).
15. Paumard, P. *et al*. The ATP synthase is involved in generating mitochondrial cristae morphology. *EMBO J* **21**, 221-230 (2002).
16. Warburg, O., Wind, F. & Negelein, E. The Metabolism of Tumors in the Body. *J Gen Physiol* **8**, 519-530 (1927).
17. Vander Heiden, M.G., Cantley, L.C. & Thompson, C.B. Understanding the Warburg effect:

the metabolic requirements of cell proliferation. *Science* **324**, 1029-1033 (2009).
18. Folmes, C.D. *et al*. Somatic oxidative bioenergetics transitions into pluripotency-dependent glycolysis to facilitate nuclear reprogramming. *Cell Metab* **14**, 264-271 (2011).
19. Gu, W. *et al*. Glycolytic Metabolism Plays a Functional Role in Regulating Human Pluripotent Stem Cell State. *Cell Stem Cell* **19**, 476-490 (2016).
20. Rumyantsev, P.P. Interrelations of the proliferation and differentiation processes during cardiact myogenesis and regeneration. *Int Rev Cytol* **51**, 186-273 (1977).
21. Lepilina, A. *et al*. A dynamic epicardial injury response supports progenitor cell activity during zebrafish heart regeneration. *Cell* **127**, 607-619 (2006).
22. Sallin, P., de Preux Charles, A.S., Duruz, V., Pfefferli, C. & Jazwinska, A. A dual epimorphic and compensatory mode of heart regeneration in zebrafish. *Dev Biol* **399**, 27-40 (2015).
23. Banerji, C.R.S. *et al*. Cellular network entropy as the energy potential in Waddington's differentiation landscape. *Sci Rep-Uk* **3** (2013).
24. Trapnell, C. *et al*. The dynamics and regulators of cell fate decisions are revealed by pseudotemporal ordering of single cells. *Nat Biotechnol* **32**, 381-386 (2014).
25. Ehler, E., Rothen, B.M., Hammerle, S.P., Komiyama, M. & Perriard, J.C. Myofibrillogenesis in the developing chicken heart: assembly of Z-disk, M-line and the thick filaments. *J Cell Sci* **112 (Pt 10)**, 1529-1539 (1999).
26. Sparrow, J.C. & Schock, F. The initial steps of myofibril assembly: integrins pave the way. *Nat Rev Mol Cell Biol* **10**, 293-298 (2009).
27. Haubner, B.J. *et al*. Functional Recovery of a Human Neonatal Heart After Severe Myocardial Infarction. *Circ Res* **118**, 216-221 (2016).
28. Porrello, E.R. *et al*. Transient Regenerative Potential of the Neonatal Mouse Heart. *Science* **331**, 1078-1080 (2011).
29. Fisher, D.J., Heymann, M.A. & Rudolph, A.M. Myocardial oxygen and carbohydrate consumption in fetal lambs in utero and in adult sheep. *Am J Physiol* **238**, H399-405 (1980).
30. Lopaschuk, G.D., Spafford, M.A. & Marsh, D.R. Glycolysis is predominant source of myocardial ATP production immediately after birth. *Am J Physiol* **261**, H1698-1705 (1991).
31. Nakada, Y. *et al*. Hypoxia induces heart regeneration in adult mice. *Nature* **541**, 222-227 (2017).
32. Bussmann, J. & Schulte-Merker, S. Rapid BAC selection for tol2-mediated transgenesis in zebrafish.

Development **138**, 4327-4332 (2011).

33. Tessadori, F. *et al*. Identification and functional characterization of cardiac pacemaker cells in zebrafish. *PloS one* **7**, e47644 (2012).
34. Schnabel, K., Wu, C.C., Kurth, T. & Weidinger, G. Regeneration of cryoinjury induced necrotic heart lesions in zebrafish is associated with epicardial activation and cardiomyocyte proliferation. *PloS one* **6**, e18503 (2011).
35. Noel, E.S. *et al*. A Nodal-independent and tissue-intrinsic mechanism controls heart-looping chirality. *Nat Commun* **4**, 2754 (2013).
36. Huang, C.J., Tu, C.T., Hsiao, C.D., Hsieh, F.J. & Tsai, H.J. Germ-line transmission of a myocardium-specific GFP transgene reveals critical regulatory elements in the cardiac myosin light chain 2 promoter of zebrafish. *Dev Dyn* **228**, 30-40 (2003).
37. Hashimshony, T. *et al*. CEL-Seq2: sensitive highly-multiplexed single-cell RNA-Seq. *Genome Biol* **17** (2016).
38. Puente, B.N. *et al*. The oxygen-rich postnatal environment induces cardiomyocyte cell-cycle arrest through DNA damage response. *Cell* **157**, 565-579 (2014).
39. Pool, C.W., Diegenbach, P.C. & Scholten, G. Quantitative succinate-dehydrogenase histochemistry. I. A Methodological study on mammalian and fish muscle. *Histochemistry* **64**, 251-262 (1979).
40. van Noorden, C.F., WM *Enzyme histochemistry. A laboratory manual of current methods*. (Oxford University Press, 1992).
41. Lee-de Groot, M.B., Tombe, A.L. & van der Laarse, W.J. Calibrated histochemistry of myoglobin concentration in cardiomyocytes. *J Histochem Cytochem* **46**, 1077-1084 (1998).

Extended Data Figures

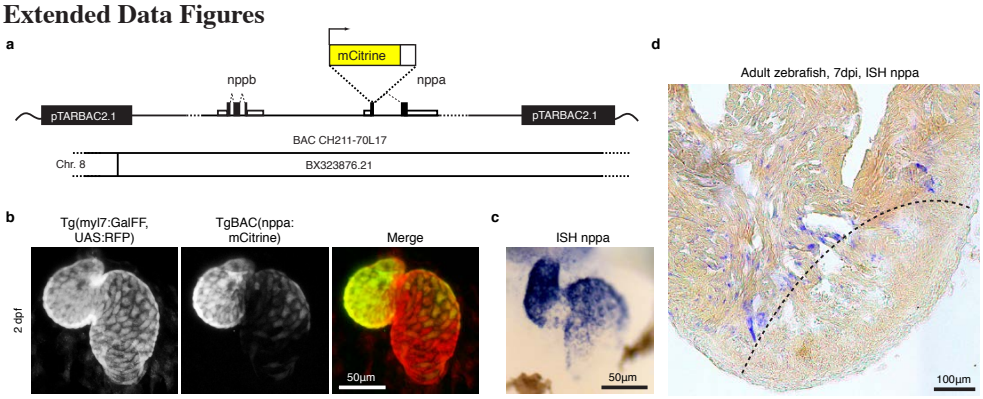

Extended Data Figure 1: Generation and validation of a novel nppa-reporter fish line.
(a) Design of the bacterial artificial chromosome (BAC) used for generation of the transgenic line TgBAC(nppa:mCitrine). (b) Transgenic mCitrine expression in the heart in relation to RFP expression in the whole myocardium of Tg(myl7:GFF, UAS:RFP, nppa:mCitrine) in embryos at 2-days post-fertilization (dpf). (c) Endogenous nppa expression as shown by whole mount in situ hybridization in embryos at 2 dpf. (d) Endogenous nppa expression at 7 days post-injury (dpi) in the adult heart. Dotted line indicates the border zone.

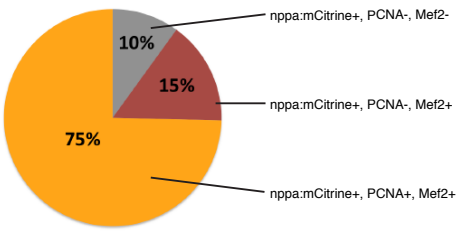

Extended Data Figure 2: *Related to Figure 1b. Immunostaining of injured TgBAC(nppa:mCitrine) hearts at 5 days-post-injury. Quantification of nppa:mCitrine, PCNA (marking proliferation), Mef2 (marking cardiomyocytes) cells in three immuno-stained sections of >5 injured hearts.*

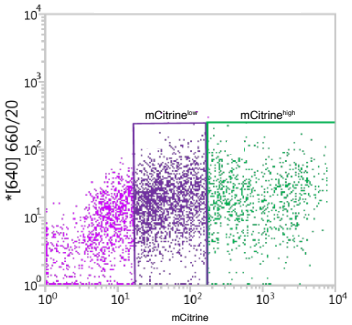

Extended Data Figure 3: *Related to Figure 1. FACS-gating for sorting mCitrine-high (green) and mCitrine-low (purple) populations, which were used for single cell mRNA sequencing.*

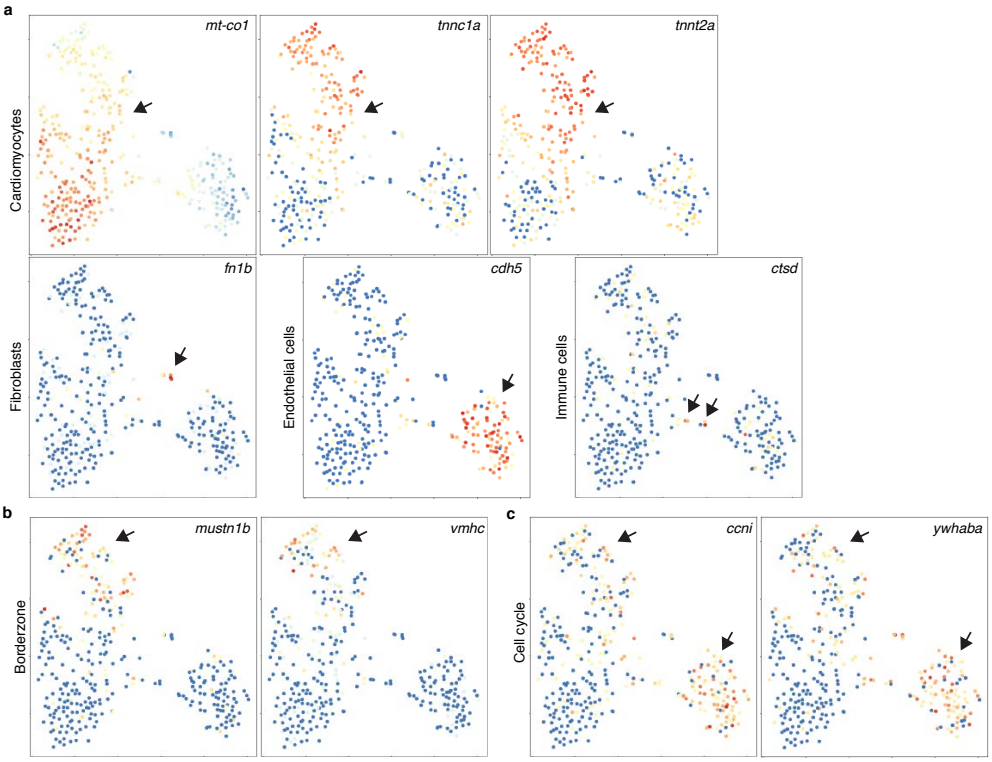

Extended Data Figure 4: Single-cell mRNA sequencing identifies different cell-populations in the injured zebrafish heart. *Related to Figure 1. (a) tSNE maps visualizing log2-transformed read-counts of mt-co1, tnnc1a, tnnt2a, fn1b, cdh5 and ctsd, and the cell type their expression identifies. Arrow indicates positive cell populations. (b) tSNE maps visualizing log2-transformed read-counts of mustn1b and vmhc, two known border zone genes. Arrow indicates positive cell populations. (c) tSNE maps visualizing log2-transformed read-counts of ccni and ywhaba, two known cell cycle genes. Arrow indicates positive cell populations.*

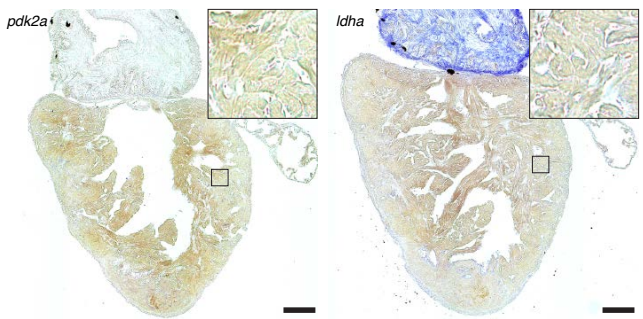

Extended Data Figure 5: *Related to Figure 3a. In situ hybridization on sham-injured hearts with pdk2a and ldha antisense probes. Magnifications of boxed areas in upper right corner. Note the absence of staining in myocardial cells. Scale bar = 100 micrometers*

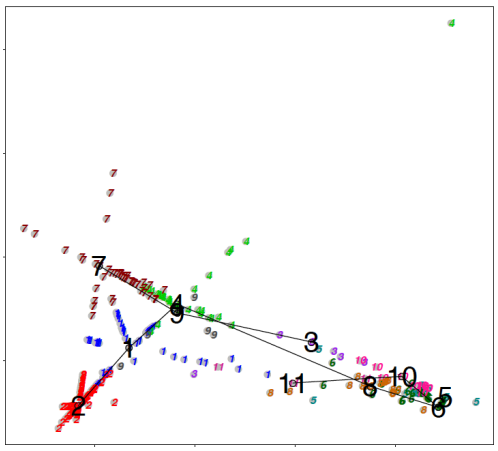

Extended Data Figure 6: *Related to Figure 4a and 4b. Minimum spanning tree connecting the clusters for StemID analysis. The position of each cell on the link connecting two cluster centres is based on how much a cell is biased towards either one of these clusters. Cells from the remote, uninjured myocardium (cluster 2) connect to the nppa-positive proliferating cardiomyoctes (cluster 7) via clusters 1, 9 and 4. Only cells on the direct links connecting the cardiomyocyte-clusters (black line) have been used for the pseudo time-line analysis in Figure 4b.*

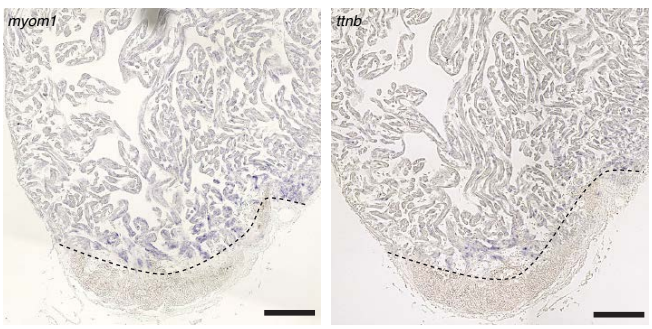

Extended Data Figure 7: *Related to Figure 4b. In situ hybridization on sections of injured hearts 7 dpi with myomesin (myom1) and titin-b (ttnb) antisense probes. Note specific blue staining in cardiomyocytes located in the border zone region. Injury area is marked by dotted line. Scale bar = 100 micrometers*

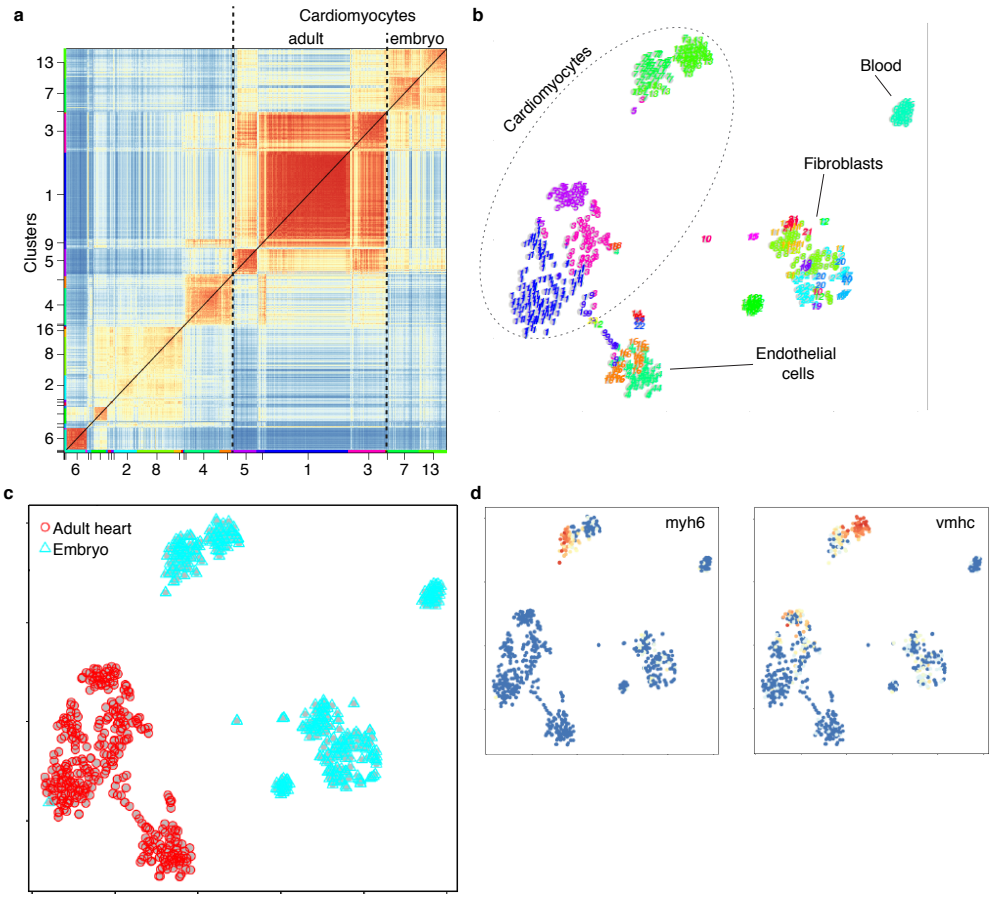

Extended Data Figure 8: Combined bioinformatics analysis of cells from injured adult hearts and embryonic hearts. *Related to Figure 4c and 4d. (a) Pairwise correlation between individual cells across all genes of the FACS sorted and single cell mRNA sequenced cells. Colour-code indicates cell-to-cell distances measured by [1 – Pearson's correlation coefficient]. StemID clusters are indicated on the x- and y-axis. (b) tSNE map representation of transcriptome similarities between individual cells. The clusters identified in (a) are number- and colour-coded and the corresponding cell types identified based on known marker genes are indicated. 2-dimensional arrangement of the clusters identified by StemID and the suggested cell-type associated with each cluster are shown. (c) tSNE map showing the origin (adult or embryonic) of the clustered cells in (b): injured adult heart in red and 2 dpf embryonic heart in cyan. (d) tSNE maps visualizing log2-transformed read-counts of myh6 (atrial marker) and vmhc (ventricle and border zone marker).*

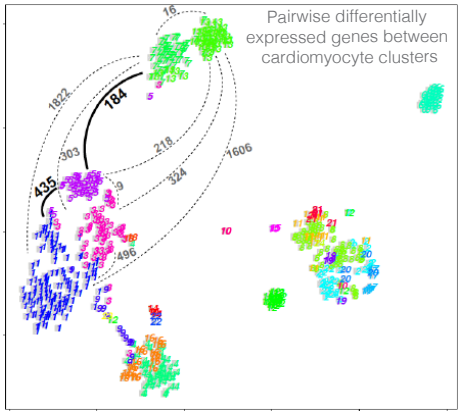

Extended Data Figure 9: *Related to Figure 4d. tSNE map of the clustered cells of the combined analysis (embryonic and adult injured cardiomyoctes), with number of pairwise differentially expressed genes (p-value<0.01) indicated between cardiomyocyte clusters.*

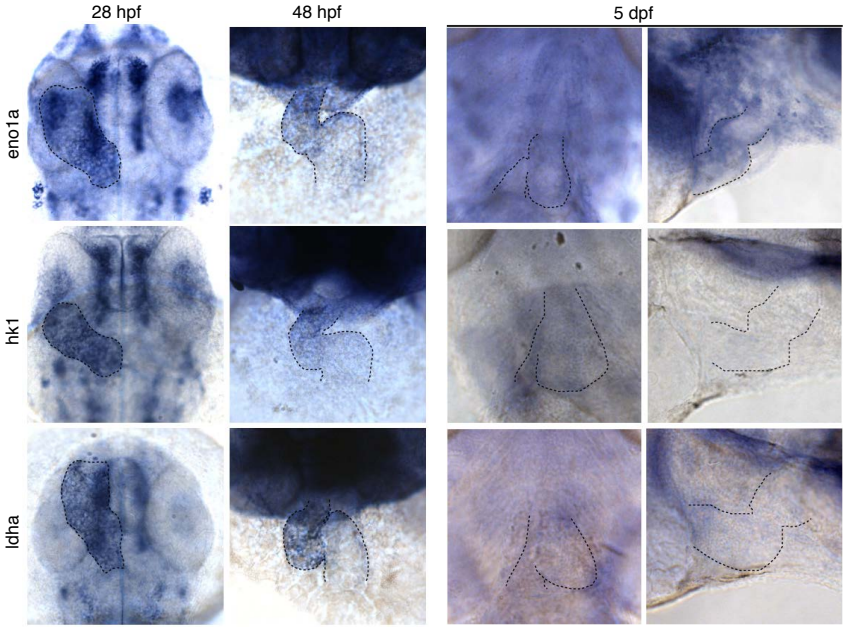

Extended Data Figure 10: *Related to Figure 4. Metabolic gene expression in zebrafish embryos. Whole mount in situ hybridization of eno1a, hk1 and ldha on zebrafish embryos 28 hours post fertilization (hpf), 48 hpf or 5 days post fertilization (dpf). Dotted line outlines the heart. Note clear expression in 28 hpf and 48 hpf hearts and absence of expression in hearts of 5 dpf embryos.*

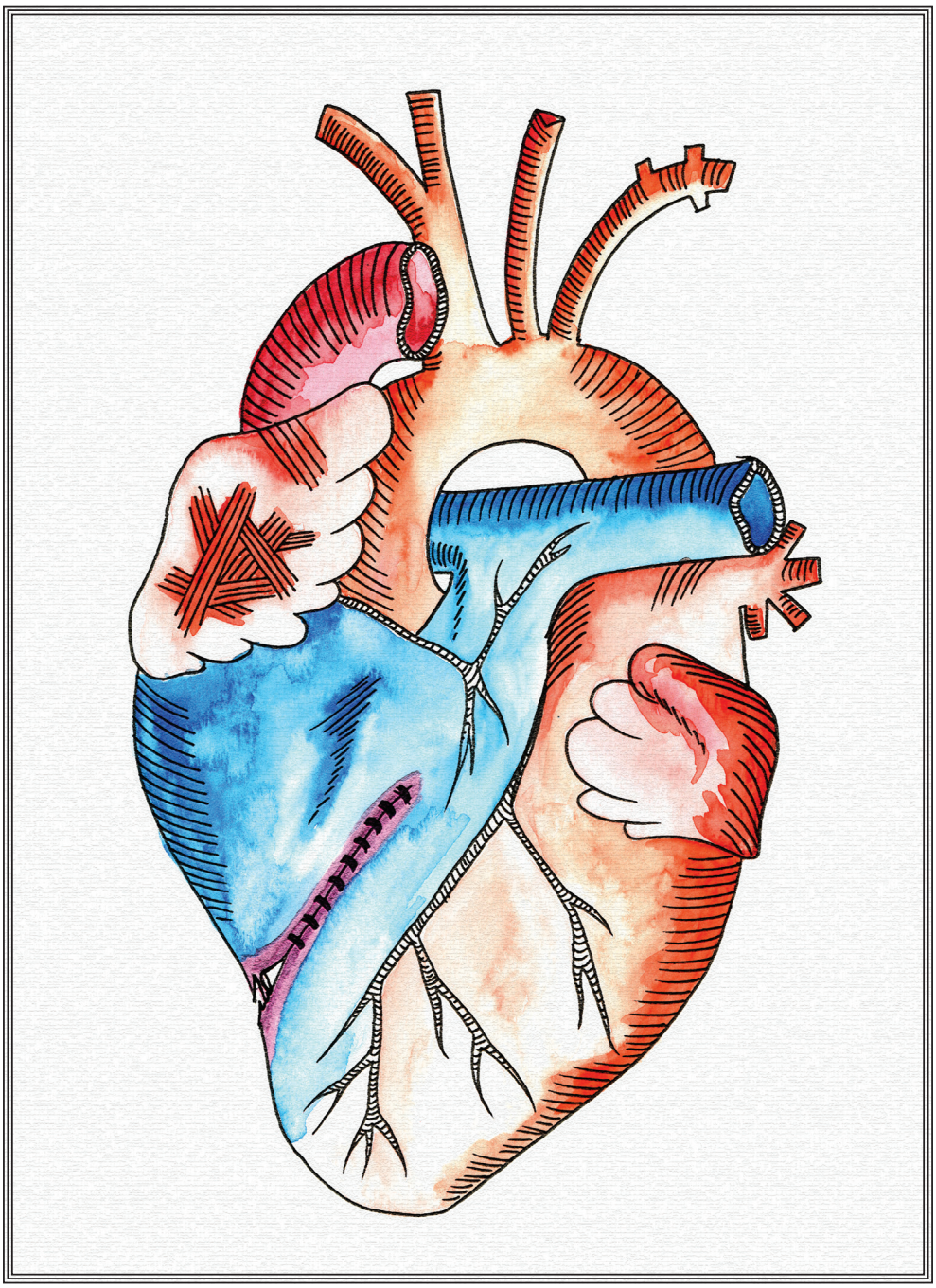

5

Dynamics of the early immune response during zebrafish heart regeneration

Fabian Kruse[1], Annemarie H. Meijer[2] & Jeroen Bakkers[1]

[1] *Hubrecht Institute and University Medical Center Utrecht, Utrecht, The Netherlands*
[2] *Institute of Biology, Leiden University, Leiden, The Netherlands*

Abstract

Unlike mammals, zebrafish have the natural ability to regenerate their heart upon injury. Despite intensive research into the molecular mechanisms triggering cardiomyocyte proliferation in the last decade, our understanding of the complex framework allowing cardiac regeneration is still rudimental. Thus far, many studies have looked at cardiomyocyte-intrinsic mechanisms promoting cell cycle re-entry. However, we hypothesize that many other cell types are at least equally, if not more, important in triggering myocardial proliferation, and regeneration in general. The innate immune response is a natural, yet underappreciated, part of the injury response. Here, we investigate the dynamics of the two main cell types of the innate immune system: neutrophils and macrophages. Besides depicting their spatio-temporal recruitment to the heart in the first 3 weeks after injury, we identify the time point of conversion from a pro-inflammatory response to a pro-repair response between 3-7 days after injury through changes in macrophage functions. This data provides the basis for future studies investigating the precise requirement of the various cell types of the innate immune system for successful heart regeneration.

Introduction

Cardiovascular disease is the leading cause of death worldwide. Opposed to humans, which form permanent scar tissue after a myocardial infarction, zebrafish have the natural ability to regenerate their heart [1]. While it is obvious that proliferation of spared cardiomyocytes is an important step towards full regeneration [2-4], it has become clear that other cell types, like endocardial and epicardial cells, are equally important in directing a successful regenerative response [5, 6]. Until recently, the role of the immune response during regeneration has been largely ignored.

A major part of the innate immune response are the phagocytic cells, mainly neutrophils and macrophages. Among other functions, they remove dead tissue through phagocytosis, thereby making space for newly formed tissue after an insult. Neutrophils are among the first-responders of inflammatory cells. Macrophages, larger phagocytes, usually enter the scene later [7]. Several studies have investigated the requirement for and contribution of neutrophils and macrophages to the regenerative process. While not rigorously addressed, there seems to be a pro-regenerative contribution of neutrophils. Immunodepletion studies have demonstrated that neutrophils have a neuroprotective role after spinal cord injury [8] and also promote axon regeneration in the optic nerve [9].

The role macrophages play during regeneration and repair in mammals and salamanders has been comprehensively studied and reviewed [10]. Macrophage depletion in mice, for instance, has established that macrophages are essential for optimal wound repair and angiogenesis [11, 12]. Similarly, limb regeneration in salamanders also requires macrophages [13]. It has been hypothesized that the pro-regenerative activity of macrophages can be attributed to (1) released growth factors that promote new blood vessel formation, but also (2) a direct effect on stem cells and their niche [14, 15].

The role of the immune response during zebrafish heart regeneration has recently been addressed. Two groups have independently shown that the early immune response is crucial for proper cardiac regeneration in zebrafish. Inhibition of the inflammatory response with glucocorticoids was shown to lead to excessive collagen deposition, and, as a consequence of reduced phagocyte recruitment, diminished angiogenesis and cell proliferation [16]. De Preux and colleagues addressed the dynamics of white blood cells during zebrafish heart regeneration in more detail using a leukocyte-specific antibody. They found that leukocyte numbers peak at 4 dpi. Moreover, inhibition of the innate immune response using clodrosomes or PLX3397 strongly suppressed mitotic activity in cardiomyocytes and heart regeneration in general [17]. While these studies shed light on the importance of the early immune response for cardiac regeneration, they did not provide information on the importance of specific immune cell types.

Next to the distinction between macrophages and neutrophils, macrophages can also be classified into different subtypes based on their function. Traditionally, there are two types of macrophages. The proinflammatory subtype of M1 “killer” macrophages is activated

by IFNgamma. M2 "repair" macrophages on the other hand encourage wound healing and repair, counteracting damage by prolonged immune system activation. How undifferentiated macrophages emerging from the blood stream are induced to differentiate into one of the subtypes is not fully understood. The M1 type seems to be induced by interferon-gamma (IFN-g) signaling and lipopolysaccharides, while the M2 type is promoted through the interleukins IL-4 and IL-13 [18]. Once macrophages have matured into a certain type, they can be distinguished based on their Arginine metabolism [19, 20]. M1 macrophages preferentially produce Nitric Oxide (NO), which inhibits cell proliferation [21]. M2 macrophages, on the contrary, produce Ornithine, thereby promoting proliferation and repair through polyamines and collagen [19, 22-24]. Ornithine and NO are the products of different enzymatic cleavages of Arginine. Importantly, intermediates in each enzyme pathway inhibit the opposing pathway, thereby creating a feedback loop [25]. Other changes in macrophages occur in concert with the different Arginine metabolisms. NO production leads to expression of IL-12/23, while Ornithine increases TGF-beta, IL-10, IFNa/g, chitinases, matrix metalloproteases and scavenger receptors [26-29]. Moreover, M1 and M2 macrophages also affect the adaptive immune system in different ways [20]. The tyrosine protein phosphatase non-receptor 6 (Ptpn6/SHP-1) has been shown to play a key role in blocking pro-inflammatory processes: Mouse mutants suffer from severe immune disorders and are lethal by 3-9 weeks of age [30-32]. SHP-1 negatively regulates Toll-like receptor mediated production of pro-inflammatory cytokines by suppressing the transcription factor NFkB and MAPK activation [33].

The innate immune response is comprised of an intricate network of different cell types with different functions. Previous studies failed to differentiate even between the two most common immune cell types: macrophages and neutrophils. Here, we aim to establish detailed dynamics of neutrophils and macrophages in the first three weeks after cryoinjury to the heart. The recruitment of these two cell types was quantified per time point, with a special focus on localization within the injured heart. Moreover, we specifically investigate alternative macrophage activation to the M2 "pro-repair"-state. Our results indicate that the peak in macrophage-numbers between 3-7 days after injury (dpi) coincides with their localization towards the borderzone. Also, at this time point we observe an alternative activation to anti-inflammatory macrophages, marking the end of inflammation and the start of tissue repair.

Results

Previously, we have conducted *tomo*-seq, a technique to perform RNA-sequencing with spatial information (Fig. 1a), on regenerating zebrafish hearts at 3 dpi [4]. This technique allowed us to identify, based on transcriptome data, different regions in the regenerating heart: the injury area, a borderzone where proliferating cardiomyocytes are located and a remote zone of uninjured heart muscle cells [4]. We identified 408 genes that are upregulated in the injury area and gene ontology (GO) analysis revealed enrichment in genes linked

to *translation*, *embryo development* and *immune response* [4]. One of the top upregulated genes was *grn1* (Fig. 1b), which has been shown to attract neutrophils and amplify acute inflammation [34]. The enrichment in the GO-term *immune response* was based on 16 genes, which can be further categorized into *actin cytoskeleton/migration/chemotaxis*, *complement activation*, *non-receptor tyrosine kinase signaling* and other *miscellaneous* functions (Fig. 1c). *Tomo*-seq expression plots confirm injury area-specific upregulation of the representative genes *coro1a*, *ptpn6* & *c1qb* (Fig. 1d-f). Together, these data suggest an involvement of the immune system in the regenerative response.

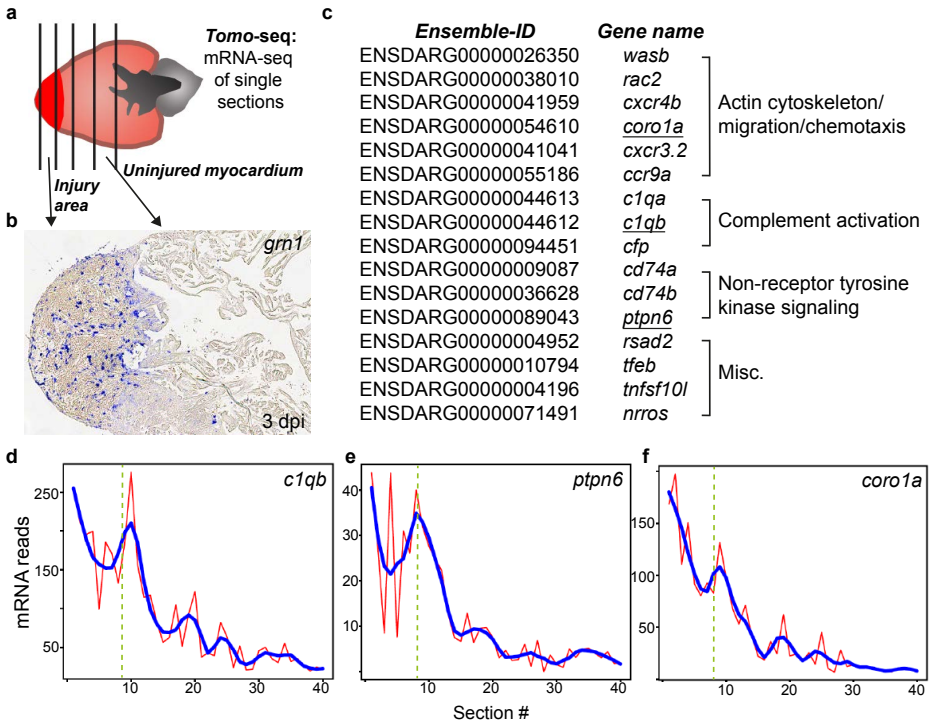

Figure 1: Tomo-seq identifies genes related to the immune response in the injury area of the regenerating zebrafish heart. *(a) Schematic of a cryoinured heart, sectioned along the injury area – uninjured myocardium axis. Arrows indicate the areas in an actual heart. (b) Cryoinjured zebrafish heart at 3 days-post-injury, in situ hybridization for grn1. (c) Genes detected by tomo-seq in the injury area under the GO-term "immune response", manually categorized into Actin cytoskeleton/migration/chemotaxis, complement activation, non-receptor tyrosine kinase signaling and miscellaneous functions. (d, e, f) Tomo-seq expression profiles for the representative genes c1qb, ptpn6 and coro1a.*

Other investigators have shown that the innate immune response plays a role in the regenerative process [16, 17]. However, their analyses concerning the different cell types was

very superficial, which is why we decided to visualize the two main components of the early immune response: neutrophils and macrophages. To do so we used transgenic zebrafish lines with macrophage-specific *mCherry* expression, Tg(*mpeg*:mCherry), and neutrophil-specific *GFP* expression, Tg(*mpx*:GFP) and analyzed their recruitment at various time points after cryoinjury.

In uninjured, sham-operated fish, no neutrophils were detectable in the heart (Fig. 2d), while there was a baseline number of 25 resident macrophages in a 250x250 mm area (Fig. 2g). These resident macrophages were on the one hand found in the trabeculated myocardium, where small macrophages were located in between the myocardial cells and large macrophages were observed at the luminal side of the trabeculae (Fig. 2k). Moreover, an accumulation of resident macrophages was seen outlining vessels in the epicardium (Fig. 2l).

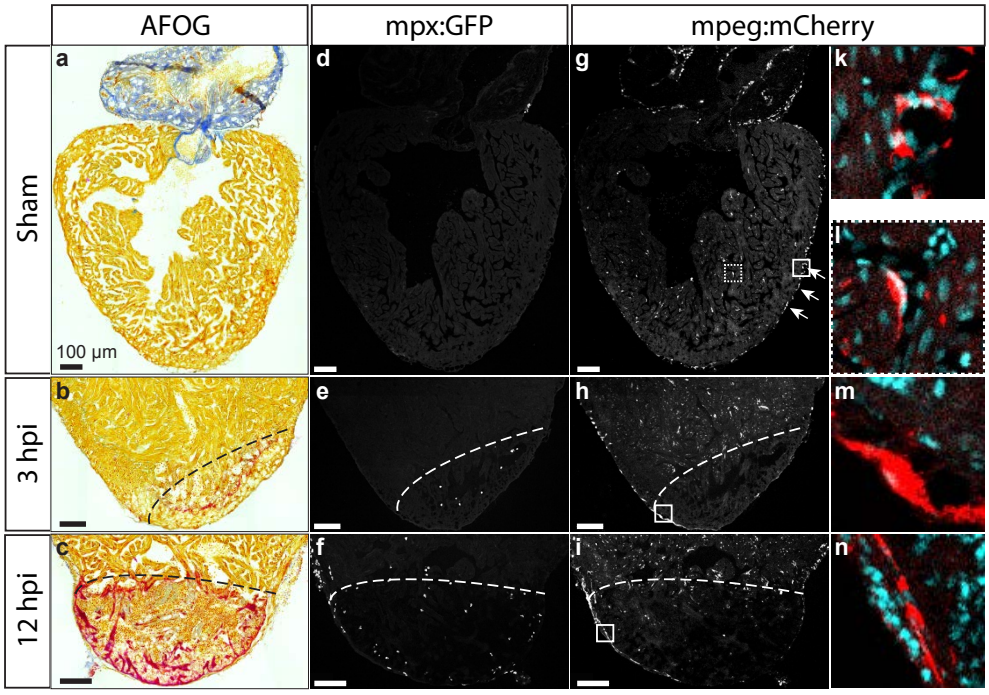

Figure 2: Early leukocyte dynamics in the regenerating zebrafish heart. *Immunostaining of neutrophil-reporter fish, Tg(mpx:GFP), and macrophage-reporter fish, Tg(mpeg:mCherry), at early time points after cryoinjury: sham-operated, 3 hrs, 12 hrs post injury (hpi). Left column: Acid Fuchsin Orange-G (AFOG) staining visualizing scar tissue. Middle column: mpx:GFP marking neutrophils. Right column: mpeg:mCherry marking macrophages. (k, l, m, n) magnifications of the boxed area of the respective time point. Dotted line demarcates injury area. Arrows highlight epicardial localization. Scalebar=100 µm.*

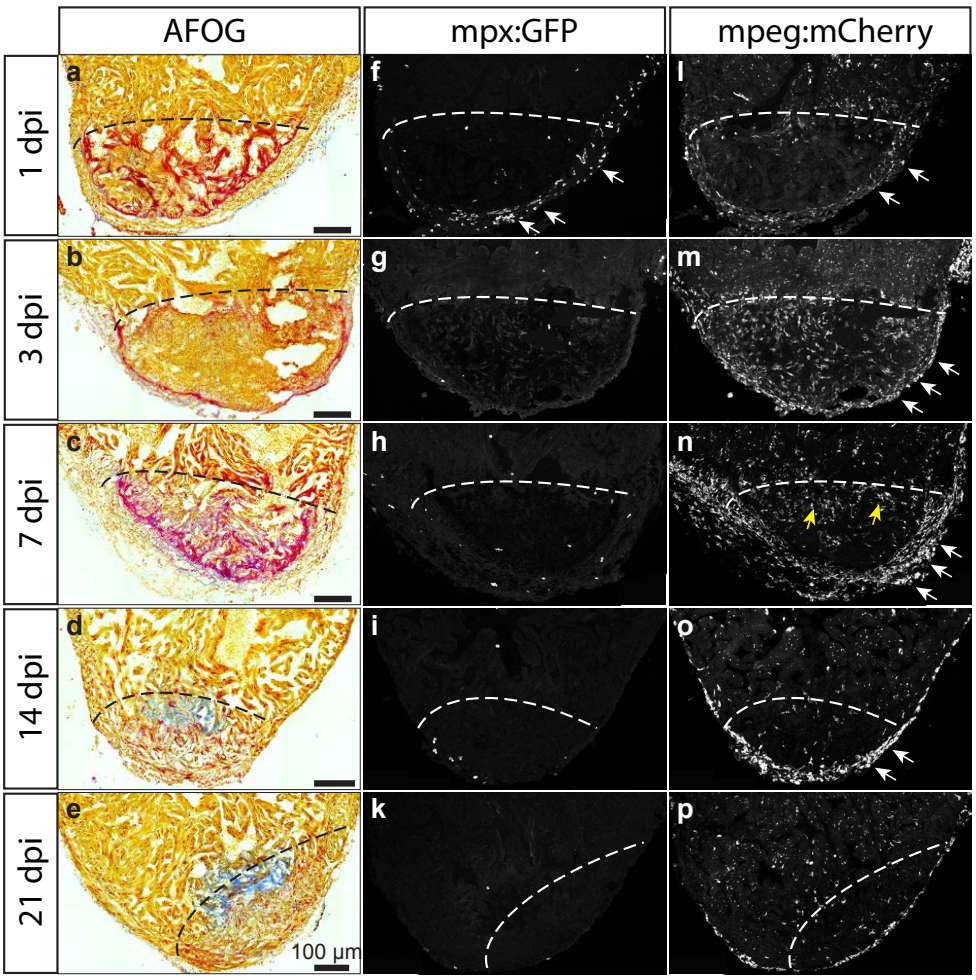

***Figure 3:* Late leukocyte dynamics in the regenerating zebrafish heart.** *Immunostaining of neutrophil-reporter fish, Tg(mpx:GFP), and macrophage-reporter fish, Tg(mpeg:mCherry), at later time points after cryoinjury: 1 day, 3 days, 7 days, 14 days and 21 days post injury (dpi). Left column: Acid Fuchsin Orange-G (AFOG) staining visualizing scar tissue. Middle column: mpx:GFP marking neutrophils. Right column: mpeg:mCherry marking macrophages. Dotted line demarcates injury area. White arrows highlight epicardial localization. Yellow arrows highlight borderzone localization. Scalebar=100 µm. .*

While *mpx*:GFP labeled neutrophils were absent from the sham hearts, already at 3 hours post injury (hpi) the first neutrophils appeared in the injury area (Fig. 2e). At 12 hpi, neutrophil numbers rose from 8 (±0.7) to 67 (±8) throughout the injury area, independent of injury size (Fig. 2f). Over 55% of neutrophils were found in the periphery of the wound area, which was slightly less evident (40%) at 1 dpi (Fig. 3f). Both at 12 and 24 hpf, Neutrophils

were also found in the epicardium covering the uninjured myocardium, while their numbers dropped with the distance to the injury site. Neutrophil numbers reached a maximum at 1 dpi, accumulating to 138 (±22), after which their numbers dropped quickly: 25±6 (3 dpi), 11±0.8 (7 dpi), 15±3 (14 dpi) and 3±0.6 (21 dpi) (Fig. 3f-k). Generally, neutrophils were only visible in the injury area and the periphery of the injury area (Fig. 4b), but did not locate near or in the myocardium.

Macrophages, on the other hand, were much slower to respond. Within the initial 12 hours, their quantity increased only marginally to 38 (±1) at 3 hpi and 67 (±2) at 12 hpi (Fig. 2h-i), while their elongated shapes suggest migration along the periphery of the wound (Fig. 2m-n). In contrast, recruitment of macrophages progressed to reach maximum numbers of 245 (±17) at 3 dpi (Fig. 3m), a time point when neutrophils had already drastically declined. At 7 and 14 dpi, macrophage numbers dropped slowly to 167 (±6) and 74 (±4), respectively, and their localization changed towards the epicardium covering the wound: while 27% of macrophages were located in the epicardium at 3 dpi, this percentage increased to 49% (7 dpi) and 46% (14 dpi) (Fig. 4c). Total macrophages reached baseline levels (42±1) at 21 dpi (Fig. 3n-p & 4c).

Together, these data unveil an early, short burst in neutrophils, followed by a longer engagement of macrophages. Interestingly, we detected a change in localization of macrophages within the injury area at 7 dpi: macrophages disappeared from the inner part of the injury area and instead were clustered in the borderzone to the myocardium and even more in the epicardium covering the injury area (Fig. 3n).

Macrophages are known to exist in different states, traditionally separated into M1 "killer" and M2 "repair" macrophages [reviewed in35]. We next sought to determine if and at which time point macrophages are alternatively activated to the M2 state. Interestingly, the tyrosine protein phosphatase non-receptor 6 (Ptpn6/SHP-1), which has been shown to play a key role in down-regulating the inflammatory response [36], was one of the injury specific genes that we identified in the *tomo*-seq dataset (Fig. 1e). We confirmed the expression of *ptpn6* in the injury area at 3 dpi by *in situ* hybridization (ISH) (Fig. 5g-h). Strikingly, *ptpn6* expression was not detectable at 1 dpi, while macrophages are present at this stage (Fig. 3l). We confirmed that macrophages can be detected by ISH at that stage by using the general macrophage marker gene *cathepsin D* (*ctsd*) (Fig. 5a). While the *ctsd* expression was detected in injury border area as well as in the rest of the injury area, *ptpn6* expression was restricted to the injury border region (Fig. 5g-k). Next, we wanted to confirm that the restricted expression of *ptpn6* is related to the M1/M2 alternative activation. Therefore, we analyzed the expression of *arginase* (*arg2*), which is an established marker for M2 macrophages [19] Corroborating an induction of the M2 activation around 3 dpi we observed a delayed expression pattern for *arg2*. While *arg2* expression was not detectable at 1 and 3 dpi, *arg2* expression was very clear at 7 dpi. As observed for *ptpn6*, *arg2* expression was confined to the injury border zone. Together, these results indicate that the anti-inflammatory markers *ptpn6* and *arg2* are

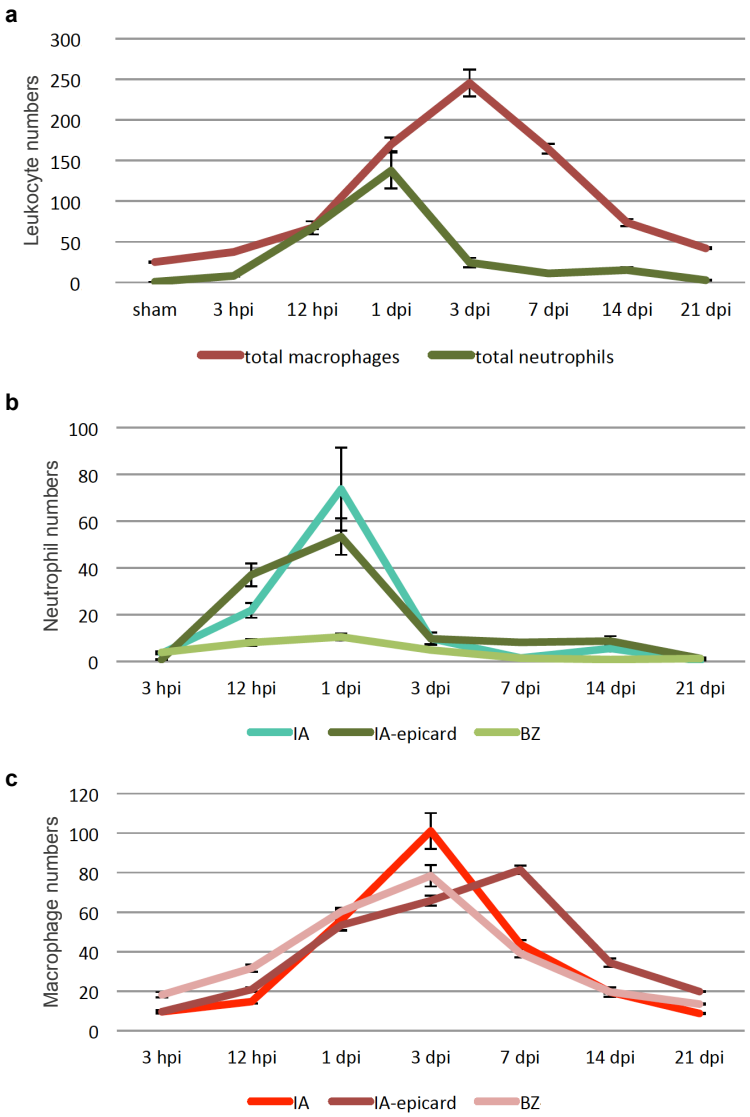

Figure 4: Quantification of leukocyte dynamics following cryoinjury. *(a) Average of total macrophages and neutrophils quantified in a radius of 150 µm around the injury area in 3 sections/ heart, in 4-6 zebrafish hearts/regenerative stage. (b) Average of neutrophil numbers segmented by zone: within the injury area (IA), in the epicardium covering the injury area (epi-IA), myocardium in the borderzone = within 150 um from the injury area (BZ). (c) Average of macrophage numbers segmented by zone: within the injury area (IA), in the epicardium covering the injury area (epi-IA), myocardium in the borderzone = within 150 µm from the injury area (BZ). Error bars show standard error of the mean.*

induced between 3-7 dpi in macrophages located around the wound border zone, suggesting that M2 activation occurs specifically in the wound border zone.

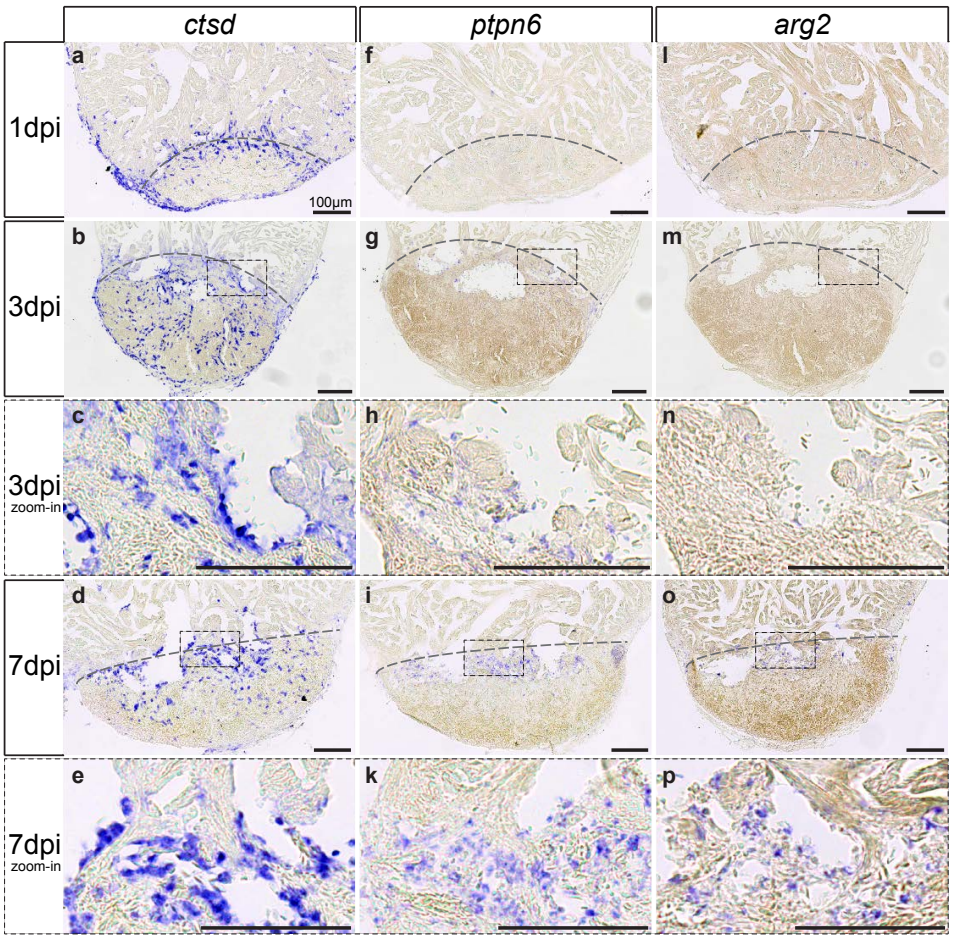

Figure 5: Change of macrophage identity to anti-inflammatory functions. *In situ hybridization for ctsd (left column), ptpn6 (middle column) and arg2 (right column) at 1, 3 and 7 days post injury. ctsd is expressed by leukocytes, while ptpn6 induces alternative activation of pro-repair/ anti-inflammatory (M2) macrophages. arg2 marks the mature M2-macrophages. Dotted lines mark the injury area. Boxes show location of higher magnification. Scalebar=100 µm.*

Discussion

Here, we show the detailed dynamics of the early immune response following heart injury in the zebrafish. An early peak in neutrophil recruitment at 1 dpi is followed by a peak of macrophages at 3 dpi. Interestingly, we identify an upregulation of anti-inflammatory genes at 3 and 7 dpi. This alternative activation of macrophages is zone-specific: confined to the area adjacent to the proliferating cardiomyocytes.

Previous experiments have shown that cardiomyocyte proliferation is highest at 7 dpi, localized to the borderzone to the injury area [4]. Remarkably, this puts anti-inflammatory macrophages in close proximity to the proliferating cardiomyocytes, suggesting a possible role in the process of cardiomyocyte renewal. The pro-regenerative activity of macrophages in other model systems of regeneration has been attributed to the release of growth factors and a direct effect on stem cells and their niche [14, 15]. Whether macrophages provide a permissive environment or if they influence cardiomyocyte proliferation directly needs to be addressed in the future. We imagine that novel transgenic lines could be used to address this issue by triggering lethal nitroreductase expression cell type-specifically, in a time-dependent manner.

At the very least, our study provides first clues advocating the importance of macrophages during myocardial regeneration. Because the alternative activation to a pro-repair state only occurs adjacent to the zone of proliferating cardiomyocytes, this suggests that these cells are communicating. Macrophages regulate a variety of processes during development, homeostasis and disease, often through secretion of a wide range of signaling molecules [reviewed in 37]. M2 macrophages are known to express high levels of transforming growth factor beta, interleukin (IL) 13, IL-10 and other chemokines including CCL22 and CCL17. One of these secreted molecules, IL-10, is a main activator of the Janus Kinase (JAK) 1 and Signal Transducer and Activator of Transcription (Stat) 3 signaling pathway [reviewed in 38]. It has been previously shown by Fang and colleagues that the Jak1/Stat3 injury response is required for heart regeneration [39]. Jak1/Stat3 pathway members were shown to be restricted to the borderzone at 7 days after amputation. When the signaling cascade was blocked, cardiomyocyte proliferation, and heart regeneration in general, was hampered. While there is no direct evidence for a link between macrophage-released factors and the induction of cardiomyocyte proliferation, the example above suggests that there may be more pathways of regeneration that are affected by the immune response.

Interestingly, the induction of the anti-inflammatory response in Macrophages coincides with the disappearance of the Neutrophils. This might suggest an organ-wide shift towards repair – away from inflammation. However, the differential macrophage activation is zone-specific, raising the question if the signal is also locally restricted. It is known that the differential activation of Macrophages is dependent on the cytokines present in the extracellular environment. Especially IL-4 and IL-10 are known for their anti-inflammatory roles [40, 41]. Arginase-expression, for instance, is induced by IL-4 [41]. Moreover, it has been shown that tumor cell-secreted Ccl2 and Csf1 induce M2 macrophage specification, which in

turn provide a pro-tumorigenic environment and protect the cancer from immune clearance [42]. However, in the majority of cases it is not clear where, and in response to which signal, these cytokines are produced. It is commonly believed that some these cytokines are mainly produced by other monocytes, for example basophils [43]. Further research will have to address these questions.

Methods

Transgenic fish lines and cryoinjury

All procedures involving animals were approved by the local animal experiments committees and performed in compliance with animal welfare laws, guidelines and policies, according to national and European law.

Transgenic zebrafish Tg(*mpeg1*:mChreey-F, *mpx*:eGFP)[44, 45] of ~ 4 to 18 months of age were used for regeneration experiments. Cryoinjuries were performed as previously described [4].

Immunofluorescence

For immunofluorescence, hearts were extracted, fixed in 4% PFA at room temperature for 1 h and cryosectioned into 10 μm sections. Heart sections were equally distributed onto seven serial slides so each slide contained sections representing all areas of the ventricle.

Primary antibodies used were anti-GFP (aves #GFP-1010), and anti-dsRed (Clontech #632496). Antigen retrieval was performed by heating slides containing heart sections at 85°C in 10 mM sodium citrate buffer (pH 6) for 10 minutes. Secondary antibodies conjugated to Alexa 488 (ThermoFisher Scientific) and Cy3 (Jackson Laboratories) were used at a dilution of 1:500. Nuclei were shown by DAPI (4',6-diamidino-2-phenylindole) staining. All images of immunofluorescence stainings are single optical planes acquired with a Leica Sp8 confocal microscope. For quantifications, 3 sections displaying the biggest wounds were analyzed per heart for >5 hearts per condition.

In situ hybridization

After o/n fixation in 4% PFA, hearts were washed in PBS twice, dehydrated in EtOH, and embedded in paraffin. Serial sections were made at 10 μm. *In situ* hybridization was performed on paraffin-sections as previously described [4].

Bibliography

1. Poss, K.D., Wilson, L.G. & Keating, M.T. Heart regeneration in zebrafish. *Science* **298**, 2188-2190 (2002).
2. Gemberling, M., Bailey, T.J., Hyde, D.R. & Poss, K.D. The zebrafish as a model for complex tissue regeneration. *Trends Genet* **29**, 611-620 (2013).
3. Gemberling, M., Karra, R., Dickson, A.L. & Poss, K.D. Nrg1 is an injury-induced cardiomyocyte mitogen for the endogenous heart regeneration program in zebrafish. *Elife* **4** (2015).
4. Wu, C.C. *et al*. Spatially Resolved Genome-wide Transcriptional Profiling Identifies BMP Signaling as Essential Regulator of Zebrafish Cardiomyocyte Regeneration. *Developmental Cell* **36**, 36-49 (2016).
5. Kikuchi, K. *et al*. Retinoic acid production by endocardium and epicardium is an injury response essential for zebrafish heart regeneration. *Dev Cell* **20**, 397-404 (2011).
6. Lepilina, A. *et al*. A dynamic epicardial injury response supports progenitor cell activity during zebrafish heart regeneration. *Cell* **127**, 607-619 (2006).
7. Mescher, A.L., Neff, A.W. & King, M.W. Inflammation and immunity in organ regeneration. *Dev Comp Immunol* **66**, 98-110 (2017).
8. Stirling, D.P., Liu, S., Kubes, P. & Yong, V.W. Depletion of Ly6G/Gr-1 leukocytes after spinal cord injury in mice alters wound healing and worsens neurological outcome. *J Neurosci* **29**, 753-764 (2009).
9. Kurimoto, T. *et al*. Neutrophils express oncomodulin and promote optic nerve regeneration. *J Neurosci* **33**, 14816-14824 (2013).
10. Chazaud, B. Macrophages: supportive cells for tissue repair and regeneration. *Immunobiology* **219**, 172-178 (2014).
11. Goren, I. *et al*. A transgenic mouse model of inducible macrophage depletion: effects of diphtheria toxin-driven lysozyme M-specific cell lineage ablation on wound inflammatory, angiogenic, and contractive processes. *Am J Pathol* **175**, 132-147 (2009).
12. Sindrilaru, A. *et al*. Wound healing defect of Vav3-/- mice due to impaired {beta}2-integrin-dependent macrophage phagocytosis of apoptotic neutrophils. *Blood* **113**, 5266-5276 (2009).
13. Godwin, J.W., Pinto, A.R. & Rosenthal, N.A. Macrophages are required for adult salamander limb regeneration. *Proc Natl Acad Sci U S A* **110**, 9415-9420 (2013).
14. Koh, T.J. & DiPietro, L.A. Inflammation and wound healing: the role of the macrophage. *Expert Rev Mol Med* **13**, e23 (2011).
15. Santini, M.P. & Rosenthal, N.

Myocardial regenerative properties of macrophage populations and stem cells. *J Cardiovasc Transl Res* **5**, 700-712 (2012).
16. Huang, W.C. *et al*. Treatment of Glucocorticoids Inhibited Early Immune Responses and Impaired Cardiac Repair in Adult Zebrafish. *PLoS One* **8**, e66613 (2013).
17. de Preux Charles, A.S., Bise, T., Baier, F., Marro, J. & Jazwinska, A. Distinct effects of inflammation on preconditioning and regeneration of the adult zebrafish heart. *Open Biol* **6** (2016).
18. Martinez, F.O. & Gordon, S. The M1 and M2 paradigm of macrophage activation: time for reassessment. *F1000Prime Rep* **6**, 13 (2014).
19. Mills, C.D. Macrophage arginine metabolism to ornithine/urea or nitric oxide/citrulline: a life or death issue. *Crit Rev Immunol* **21**, 399-425 (2001).
20. Mills, C.D., Kincaid, K., Alt, J.M., Heilman, M.J. & Hill, A.M. M-1/M-2 macrophages and the Th1/Th2 paradigm. *J Immunol* **164**, 6166-6173 (2000).
21. Hibbs, J.B., Jr., Vavrin, Z. & Taintor, R.R. L-arginine is required for expression of the activated macrophage effector mechanism causing selective metabolic inhibition in target cells. *J Immunol* **138**, 550-565 (1987).
22. Williams-Ashman, H.G. & Canellakis, Z.N. Polyamines in mammalian biology and medicine. *Perspect Biol Med* **22**, 421-453 (1979).
23. Wu, G. & Morris, S.M., Jr. Arginine metabolism: nitric oxide and beyond. *Biochem J* **336 (Pt 1)**, 1-17 (1998).
24. Morris, S.M., Jr. Arginine metabolism: boundaries of our knowledge. *J Nutr* **137**, 1602S-1609S (2007).
25. Morris, S.M., Jr. Recent advances in arginine metabolism: roles and regulation of the arginases. *Br J Pharmacol* **157**, 922-930 (2009).
26. Cassetta, L., Cassol, E. & Poli, G. Macrophage polarization in health and disease. *ScientificWorldJournal* **11**, 2391-2402 (2011).
27. Gabrilovich, D.I., Ostrand-Rosenberg, S. & Bronte, V. Coordinated regulation of myeloid cells by tumours. *Nat Rev Immunol* **12**, 253-268 (2012).
28. Lawrence, T. & Natoli, G. Transcriptional regulation of macrophage polarization: enabling diversity with identity. *Nat Rev Immunol* **11**, 750-761 (2011).
29. Murray, P.J. & Wynn, T.A. Protective and pathogenic functions of macrophage subsets. *Nat Rev Immunol* **11**, 723-737 (2011).
30. Kozlowski, M. *et al*. Expression and catalytic activity of the tyrosine phosphatase PTP1C is severely impaired in motheaten and viable motheaten mice. *J Exp*

Med **178**, 2157-2163 (1993).
31. Shultz, L.D. *et al*. Mutations at the murine motheaten locus are within the hematopoietic cell protein-tyrosine phosphatase (Hcph) gene. *Cell* **73**, 1445-1454 (1993).
32. Tsui, H.W., Siminovitch, K.A., de Souza, L. & Tsui, F.W. Motheaten and viable motheaten mice have mutations in the haematopoietic cell phosphatase gene. *Nat Genet* **4**, 124-129 (1993).
33. An, H. *et al*. Phosphatase SHP-1 promotes TLR- and RIG-I-activated production of type I interferon by inhibiting the kinase IRAK1. *Nat Immunol* **9**, 542-550 (2008).
34. Zhu, J. *et al*. Conversion of proepithelin to epithelins: roles of SLPI and elastase in host defense and wound repair. *Cell* **111**, 867-878 (2002).
35. Mills, C.D. M1 and M2 Macrophages: Oracles of Health and Disease. *Crit Rev Immunol* **32**, 463-488 (2012).
36. Kanwal, Z. *et al*. Deficiency in hematopoietic phosphatase ptpn6/Shp1 hyperactivates the innate immune system and impairs control of bacterial infections in zebrafish embryos. *J Immunol* **190**, 1631-1645 (2013).
37. Stefater, J.A., 3rd, Ren, S., Lang, R.A. & Duffield, J.S. Metchnikoff's policemen: macrophages in development, homeostasis and regeneration. *Trends Mol Med* **17**, 743-752 (2011).
38. Schindler, C., Levy, D.E. & Decker, T. JAK-STAT signaling: from interferons to cytokines. *J Biol Chem* **282**, 20059-20063 (2007).
39. Fang, Y. *et al*. Translational profiling of cardiomyocytes identifies an early Jak1/Stat3 injury response required for zebrafish heart regeneration. *Proc Natl Acad Sci U S A* **110**, 13416-13421 (2013).
40. Mosser, D.M. & Zhang, X. Interleukin-10: new perspectives on an old cytokine. *Immunol Rev* **226**, 205-218 (2008).
41. Whyte, C.S. *et al*. Suppressor of cytokine signaling (SOCS)1 is a key determinant of differential macrophage activation and function. *J Leukoc Biol* **90**, 845-854 (2011).
42. Guo, X. *et al*. Single tumor-initiating cells evade immune clearance by recruiting type II macrophages. *Genes Dev* **31**, 247-259 (2017).
43. Sokol, C.L., Barton, G.M., Farr, A.G. & Medzhitov, R. A mechanism for the initiation of allergen-induced T helper type 2 responses. *Nat Immunol* **9**, 310-318 (2008).
44. Bernut, A. *et al*. Mycobacterium abscessus cording prevents phagocytosis and promotes abscess formation. *Proc Natl Acad Sci U S*

A **111**, E943-952 (2014).
45. Renshaw, S.A. *et al*. A transgenic zebrafish model of neutrophilic inflammation. *Blood* **108**, 3976-3978 (2006).

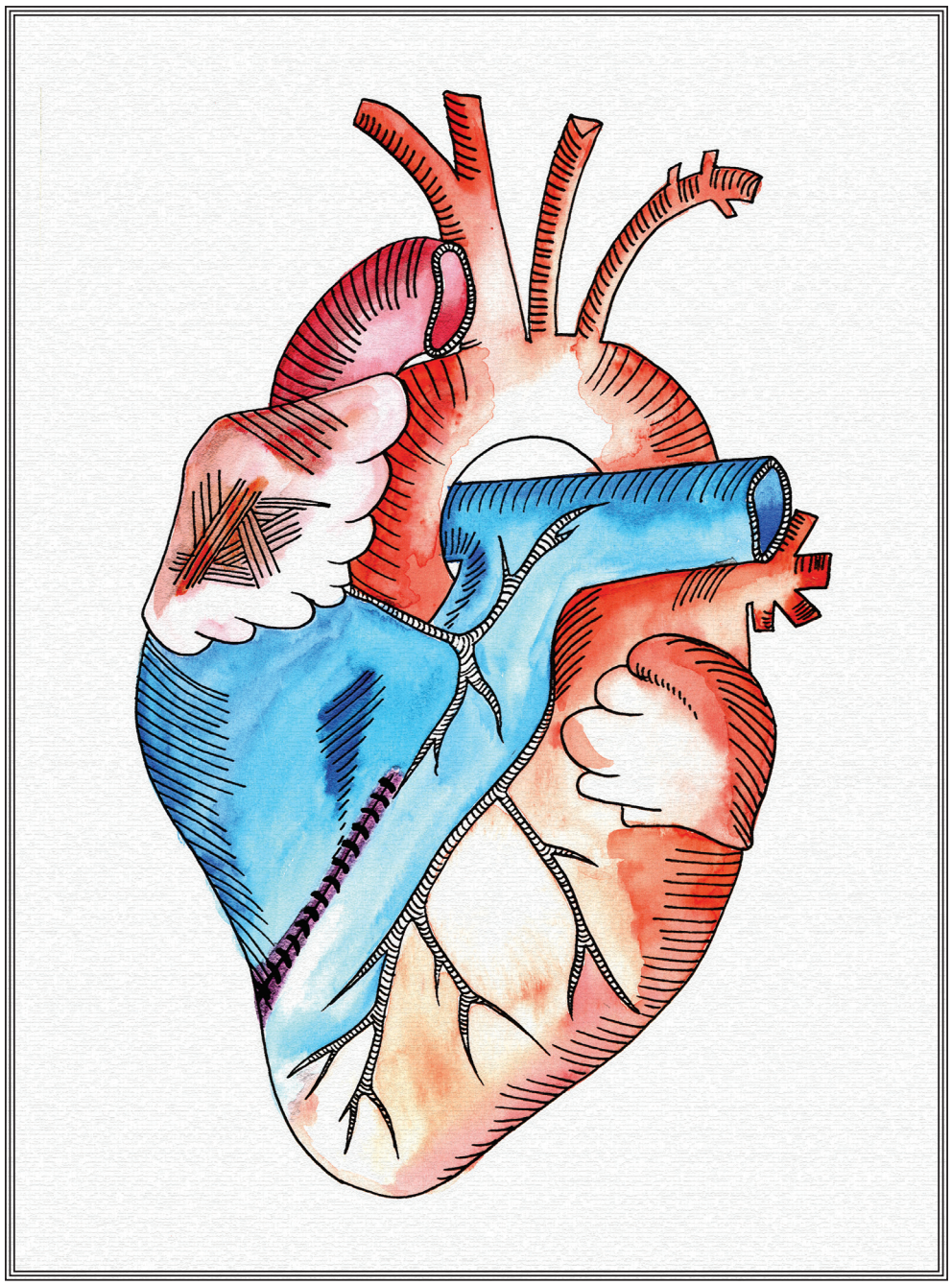

6

Summarizing discussion

Fabian Kruse & Jeroen Bakkers

Hubrecht Institute and University Medical Centre Utrecht, Utrecht, The Netherlands

Through the work described in this thesis, I attempted to advance our understanding of regeneration in the injured zebrafish heart.

The field of cardiac regeneration has evolved rapidly over the past decade, especially in the last few years. A lot of the earlier work described single genes and pathways that seem to play a role during the regeneration of the heart. However, these isolated findings have never been put in perspective and integrated with each other. Our aim in studying heart regeneration was to provide a more holistic approach, by developing and applying new technologies that allow us to study whole gene networks. Empowered by increased sensitivity of mRNA sequencing techniques, but also the decreasing costs of such sequencing efforts, we were able to generate large amounts of exciting data.

Tomo-~~seq~~ seek *(Merriam-Webster dictionary: "to seek" = "to try to discover")*

In **Chapter 2**, the development and application of a novel method to generate whole transcriptomics data with spatial resolution has been described: *tomo*-seq. **Chapter 3** then uses *tomo*-seq in a proof-of-concept study. We show how incredibly sensitive *tomo*-seq is in detecting gene expression changes in between the different zones of the regenerating zebrafish heart. *Tomo*-seq has the power to identify the different zones in the regenerating heart in an unbiased manner: not only did we detect the borderzone, which we had already expected based on other experiments, but using *tomo*-seq we were able to separate the borderzone into two sub-zones. This exciting result shows the specificity with which *tomo*-seq can help in identifying transcriptionally and functionally distinct regions. After characterizing the borderzone on a transcriptional level, we investigated one of the identified pathways, BMP signaling. We show that cardiomyocytes require BMP signaling in order to properly regenerate after injury and that experimentally increased BMP signaling enhances regeneration. These results again demonstrate the power and value of the *tomo*-seq method in studying heart regeneration.

It would be very interesting to study the different zones in more detail to understand what their actual function during the regenerative process is. To follow up on the *tomo*-seq results that showed two distinct borderzones, novel transgenic lines would be of much value. Lineage tracing of the borderzone cardiomyocytes needs to answer the question to what extend the newly regenerated tissue originates from these cells. Moreover, ablation of only these borderzone cardiomyocytes can further address how important they are for myocardial regeneration. Moreover, the non-myocardial borderzone cells need more attention. They presumably play a role in signaling processes that guide cardiomyocyte-proliferation. First, we need to describe these in more detail: what cells are specifically in this zone? When do they appear and what function do they have? Transgenic labeling will be a first step in providing answers, as will time-dependent ablation. Apart from these experiments, it would

also be interesting to study the transcriptional changes of the borderzone(s) during the course of time. By now, we have generated more *tomo*-seq datasets for other time points of zebrafish heart regeneration. A careful bioinformatic comparison will yield additional insights into gene programs that are required for certain phases of heart regeneration. An initial attempt at such a comparison exposed challenges in terms of data normalization: a direct comparison of read counts is not easily possible, due to technical differences during the sequencing process. However, a comparison between the processes that are most prominent at a certain time point would be a first step in understanding the dynamics of myocardial regeneration.

Energy to regenerate

Moreover, *tomo*-seq data can easily be used to validate results obtained through other means or to complement methods with different properties (as outlined in **Chapter 1**, Figure 3). One possibility is to combine *tomo*-seq with single cell mRNA-sequencing results. While single cell mRNA-sequencing has the power to identify expression programs in defined cell populations, *tomo*-seq will be able to put these results in the spatial context of the tissue that is under investigation. Vice versa, *tomo*-seq can identify genetic markers, which subsequently can be used to genetically label these cells for more detailed analysis by FACS sorting and single cell mRNA-sequencing.

We made use of the latter approach in **Chapter 4**. Trading off spatial information for single cell-specificity, we applied single-cell sequencing to the injured zebrafish heart. To enrich for the regenerating heart muscle cells, we used information from *tomo*-seq data to make a transgenic *nppa*-reporter zebrafish line. Our sequencing data unraveled metabolic reprogramming to glycolysis, which is indicative of dedifferentiation of this sub-population of cardiomyocytes.

Interestingly, hypoxia can stimulate proliferation of mammalian cardiomyocytes by reducing mitochondrial Reactive Oxygen Species production. In turn, these hearts are able to regenerate following myocardial infarction [1]. A reverse metabolic switch from glycolysis towards mitochondrial oxidative phosphorylation occurs after birth, when oxygen concentrations rise in the mammalian neonate [2-5]. Coincidentally, mammals lose the ability to regenerate their heart at 7 days after birth [6]. It has been suggested that this increased oxygen concentration negatively affects cardiomyocyte proliferation in the neonate [7]. The same authors claim that aforementioned oxygen availability is the reason why zebrafish are still able to regenerate as adults, since oxygen concentrations in the water are 30 times lower than in the air. What has been disregarded in these studies is the fact that the adult zebrafish heart also relies on oxidative phosphorylation, as we show in **Chapter 4**. Furthermore, the zebrafish embryo, without being subjected to any changes in oxygen levels, restricts and turns off glycolysis in the heart between 1-5 days after fertilization. These results indicate that hypoxia and metabolism can function in an uncoupled manner. Inducing a metabolism switch in a heart

attack patient without the need to place the patient in a hypoxic environment would greatly increase the chances to realize such a therapeutic approach. But I am getting ahead of myself. First, we need to show experimentally that the metabolic switch alone can drive cardiomyocyte proliferation and lead to functional regeneration of the heart. This should be addressed by pharmacologically inhibiting glycolysis and assessing the regenerative capacity. Moreover, it needs to be shown in the mammalian system that induced glycolysis improves recovery of the heart. Combined, these experiments should bring us closer to a novel therapeutic strategy to help patients suffering from myocardial infarction.

A new side-kick

Once again using *tomo*-seq as a starting point, **Chapter 5** describes the dynamics of the immune system. We identify the time point when the inflammatory response ceases and the repair-phase of regeneration commences, through macrophage M1-M2 alternative activation between 3-7 dpi. These pro-repair M2 macrophages are located in close proximity to the dedifferentiating and proliferating cardiomyocytes described in the earlier chapters. Interestingly, macrophages are known to secrete a plethora of signaling molecules. M2 macrophages, for instance, were shown to express Bmp-5 and-7 ligands in cell culture [8]. Moreover, expression of Bmp-4 and -7 by tumor associated macrophages enhanced the aggressiveness and invasion of gastric cancer cells [9]. Together, these results suggest expression and secretion of BMP ligands by macrophages. In **Chapter 3** we were unable to identify the source of BMP signaling, but it should be tested if macrophages might be responsible for the proliferation-inductive BMP signal in cardiomyocytes.

"Big data" – a double-edged sword

The results described in the previous chapters heavily relied on RNA sequencing approaches. These experiments yielded millions of reads of thousands of genes in hundreds of cells, generating immense amounts of data. The advantages appear obvious: more data equals more results equals more knowledge. However, this statement is treacherous. While it has gotten much easier to obtain such sets of "big data", analysis and mining of the data is lagging behind.

Big data is a term for data sets that are so large/complex that it cannot be handled by traditional data processing software. Challenges generally associated with big data include analysis, data curation, sharing, visualization and querying. It has been recognized that big data analysis is often shallow compared to analysis of smaller data sets [10].

We as scientists should invest more time to retrieve a larger amount of meaningful information from the datasets we generate. There is a tendency to move on to new sequencing experiments after publication of the current data. Of course this problem is also imposed by the publishing

industry: it is difficult to publish new data that originates from already published datasets. Another issue is that oftentimes scientists not trained for bioinformatic data-retrieval start using available tools to analyze their data, which might not always be the correct way to proceed. Having trained personal devoted to data analysis will certainly help the quality of output, but also the efficiency of data-retrieval. More and more large datasets are being published and the coming years will show how the way we handle them can become more efficient to tackle the big questions in biology.

Are we only "re-inventing the wheel" with fancy new techniques?

The previous two decades of heart regenerative medicine have been under the heavy influence of stem cell research. Research into stem cells gained momentum during the 1960s and '70s, leading to the first human bone marrow transplant by E. Donnall Thomas in 1968 and other great achievements. Recognizing the great potential of stem cells to aid heart regeneration, many cardiologists and researchers started looking for stem cells in the heart, pushing forward a dogma where the heart can be repaired by mesenchymal stem cells or cardiac progenitor/stem cells, as explained in **Chapter 1**. While this research certainly led to important results and advanced our understanding of cell biology and cardiology, this "hype" was followed without further hesitation. Research that did not support this new direction has been forgotten, like the findings of Pavel P. Rumyantsev. In 1977, he summarized original literature [11-14] by stating that "*myocardial cells posses an intrinsic capacity to dedifferentiate and multiply at the borders of necrosis which, however, is not manifested overtly because of the lack of permissive conditions and appropriate stimuli*" [15]. Interestingly, this is exactly what we see in mouse and human heart MI tissue (D.E.M. de Bakker, unpublished), while the zebrafish obviously provides a "permissive" environment for cardiomyocyte proliferation to occur. Moreover, Rumyantsev describes dedifferentiation of borderzone cardiomyocytes in the injured frog heart, evidenced by the "*striking resemblance of most transformed myocytes to cells of early embryonic myocardium*". He also disregards the hypothesis of cardiac stem cells involved in the regenerative process, finding "*no evidence […] of free myoblast formation*". All of these findings have been regarded major breakthroughs at the time they were reported for zebrafish heart regeneration [16, 17], while Rumyantsev's results – if taken into consideration – should not have led us to expect anything else. So why did these findings fall into oblivion? Are we not taking "older" literature into consideration or was it overshadowed by the emerging, possibly hyped, stem cell field? Or are we so overwhelmed by the large amounts of new literature that is published every day, making it impossible to keep up with the field? Which ever the answer is, what is clear is that we should not disregard older literature as obsolete. As seen in this example, there is still much we can learn from publications that are over 40 years old.

This is not to say that recent research, including the results described in this thesis, did not

further our understanding of heart regeneration. State-of-the-art techniques of the 21st century validate, but also massively improve upon the results obtained in previous decades. While the "old" studies were excellent in describing processes in detail, we now have the means to functionally interfere with biological processes. Rumyantsev put forth many hypotheses based on his observations, which we and others have unknowingly addressed in the recent years. However, we could have reached these conclusions faster and more efficiently, would we have been aware of Rumyantsev's results and ideas. In conclusion, we are not re-inventing the wheel, instead we are "pimping the ride".

Final remarks

In this thesis, I have compiled five years' worth of data, generated in endless hours in the laboratory and in front of a computer screen. I sincerely hope to have pushed the boundaries of what we know about heart regeneration and that some of my results – either published or still hidden in the data – will someday benefit a patient in the clinic.

Bibliography

1. Nakada, Y. *et al*. Hypoxia induces heart regeneration in adult mice. *Nature* **541**, 222-227 (2017).
2. Fisher, D.J., Heymann, M.A. & Rudolph, A.M. Myocardial oxygen and carbohydrate consumption in fetal lambs in utero and in adult sheep. *Am J Physiol* **238**, H399-405 (1980).
3. Lopaschuk, G.D., Collins-Nakai, R.L. & Itoi, T. Developmental changes in energy substrate use by the heart. *Cardiovasc Res* **26**, 1172-1180 (1992).
4. Gertz, E.W., Wisneski, J.A., Stanley, W.C. & Neese, R.A. Myocardial substrate utilization during exercise in humans. Dual carbon-labeled carbohydrate isotope experiments. *J Clin Invest* **82**, 2017-2025 (1988).
5. Wisneski, J.A. *et al*. Metabolic fate of extracted glucose in normal human myocardium. *J Clin Invest* **76**, 1819-1827 (1985).
6. Porrello, E.R. *et al*. Transient regenerative potential of the neonatal mouse heart. *Science* **331**, 1078-1080 (2011).
7. Puente, B.N. *et al*. The oxygen-rich postnatal environment induces cardiomyocyte cell-cycle arrest through DNA damage response. *Cell* **157**, 565-579 (2014).
8. Maciel, J. *et al*. Adsorbed fibrinogen enhances production of bone- and angiogenic-related factors by monocytes/ macrophages. *Tissue Eng Part A* **20**, 250-263 (2014).
9. Shen, Z. *et al*. Macrophage coculture enhanced invasion of gastric cancer cells via TGF-beta and BMP pathways. *Scand J Gastroenterol* **48**, 466-472 (2013).
10. Berthold, M. in KDnuggets. (ed. G. Piatetsky) (2014).
11. Polezhaev, L.V. *Loss and Restoration of the Regenerative Capacity in Tissues and Organs of Animals*. (Havard Univ. Press, Cambridge, Massaschusetts, 1972).
12. Polezhaev, L.V. *Organ Regeneration in Animals*. (Thomas, Springfield, Illinois, 1972).
13. Polezhaev, L.V.A., L.V.; Muzlaeva, N.A.; Yavitsh, M.P. *Stimulation of the Heart Muscle Regeneration*. (Nauka, Moscow (in Russian), 1965).
14. Hay, E.D. *Regeneration*. (Holt, New York, 1966).
15. Rumyantsev, P.P. Interrelations of the proliferation and differentiation processes during cardiact myogenesis and regeneration. *Int Rev Cytol* **51**, 186-273 (1977).
16. Jopling, C. *et al*. Zebrafish heart regeneration occurs by cardiomyocyte dedifferentiation and proliferation. *Nature* **464**, 606-609 (2010).
17. Kikuchi, K. *et al*. Primary contribution to zebrafish heart regeneration by gata4(+) cardiomyocytes. *Nature* **464**, 601-605 (2010).

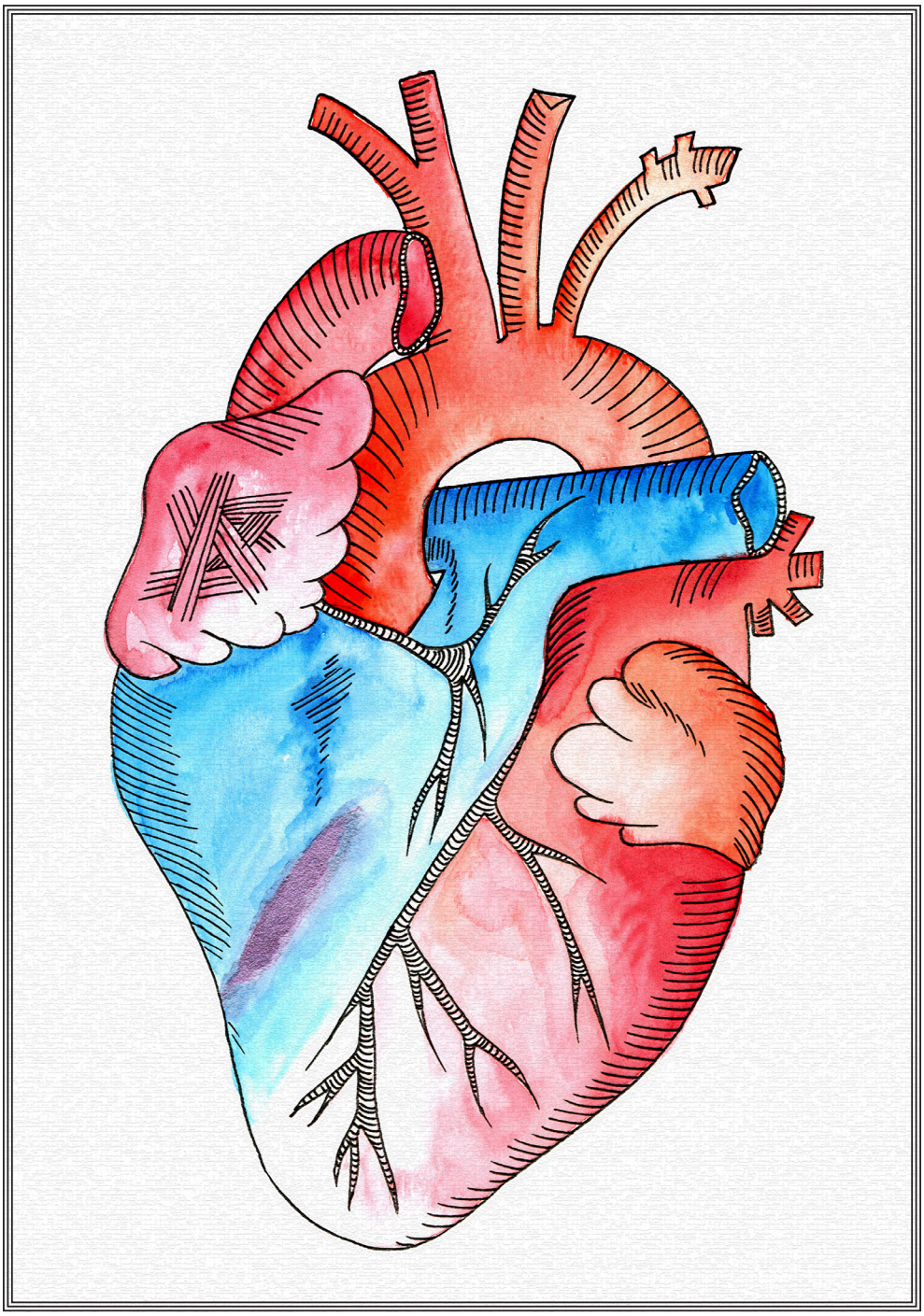

&

Nederlandse samenvatting

Deutsche Zusammenfassung

Acknowledgements

Curriculum vitae

Nederlandse samenvatting

Hart- en vaatziekten zijn ‘s werelds grootste doodsoorzaak, goed voor meer dan 30% van alle sterfgevallen. Het eist meer levens dan alle vormen van kanker bij elkaar. De noodzaak is dus hoog, onderzoek in dit veld is hard nodig. Een hartaanval, ook bekend als *hartinfarct* ontstaat als een van de kransslagaders wordt afgesloten en er geen bloed meer door heen kan stromen. Het resultaat is dat de hartspiercellen onvoldoende toevoer krijgen van zuurstof en voedingstoffen, hierdoor gaan minstens één miljard cellen dood. Ons lichaam maakt geen vernieuwing aan, maar in plaats daarvan wordt er littekenweefsel gevormd. Littekens zijn essentieel om het orgaan intact te houden, maar niet kloppend littekenweefsel kan de hartfunctie niet herstellen - bijvoorbeeld het pompen van voldoende bloed door het lichaam - en kan hartritme stoornissen veroorzaken, wat kan lijden tot hartstilstand. Als we regeneratieve therapie kunnen gebruiken om het hartspierweefsel te herstellen na de hartaanval, kunnen we duizenden patiënten helpen.

Een van de mogelijkheden is om het hart te stimuleren om zichzelf te helen. Hoe? Als we begrijpen hoe een hart regenereert onder natuurlijk omstandigheden, kunnen we strategieën bedenken om het menselijk hart aan te zetten tot herstel. Een diersoort die van nature zijn hart regenereert na schade is de zebravis. Zebravissen zijn kleine dieren, 2-3 cm lang. Ze worden overal ter wereld gebruikt in laboratoria om allerlei verschillende mechanismes en processen te bestuderen, variërend van de ontwikkeling van een bevruchte eicel naar een volwassen dier tot gedragsstudies, maar ook regeneratie wordt hierin veelvuldig onderzocht.

In dit proefschrift heb ik de zebravis gebruikt om het regenererende hart in zijn natuurlijke omstandigheden beter te begrijpen. In **hoofdstuk 2** beschrijf ik de ontwikkeling van een nieuwe techniek: *tomo*-seq. Hierbij wordt een orgaan, bijvoorbeeld het hart, over de gehele doorsnede in hele kleine plakjes gesneden. In ons geval van het beschadigde gebied naar het gezonde/onbeschadigde deel van het hart. Daarna sporen we op welke genen er actief zijn in elke plakje. Door te analyseren welke genen er actief zijn in welk plakje krijgen we een beter beeld van welke processen en signaalroutes er actief zijn en in welk gebied deze plaats vindt. Om dit beter te begrijpen stellen we ons een hypothetisch *gen A* voor, die in alle hartspiercellen actief is, *gen B* wordt echter in plakjes aangetroffen waar *gen A* niet actief is. Verder is van *gen B* bekend dat deze een rol speelt in de immuunafweer, terwijl *gen A* hartspiercellen markeert. Nu kun je exact bepalen waar de grens is tussen het beschadigde gebied en de intacte hartspier. Stel je nu een derde *gen C* voor, die actief is in een smalle strook tussen het beschadigde gebied en de intacte spiercellen: van dit gen is bekend dat het actief is als cellen delen, met andere woorden als nieuwe hartspiercellen worden gevormd. Dit is dan dus de plek waar regeneratie plaatsvindt! Vervolgens vinden we nog de *genen D, E, F, G & H* in dezelfde strook als *gen C*, maar de functie van deze genen is nog onbekend.

Wat je wel weet is dat deze genen hoogstwaarschijnlijk op een of andere manier betrokken zijn bij het herstelproces.

In **hoofdstuk 3** beschrijf ik de resultaten van de *tomo*-seq techniek voor het regenererende hart van de zebravis, vergelijkbaar met het bovenstaand beschreven hypothetische voorbeeld. Ik analyseerde al deze data en valideerde dit met andere bestaande methodes. Als laatste heb ik me gericht op een specifiek proces, betrokken bij de signaalafgifte van een bot morfogenetisch eiwit (BMP) en heb ik aangetoond dat actieve BMP signaalafgifte noodzakelijk is voor een succesvol herstel van het hart.
Het nadeel van de *tomo*-seq techniek is dat je alleen maar de genactiviteit per plakje in kaart brengt, maar een plakje kan bestaan uit veel verschillende cellen en celtypes. In **hoofdstuk 4** heb ik de genen onderzocht die tot expressie komen in afzonderlijke regenererende hartspiercellen. Ik beschrijf hoe ze de wijze waarop ze energie opwekken veranderen in vergelijking tot onbeschadigde hartspiercellen. Opmerkelijk is dat de manier van energie opwekken hetzelfde is als in het embryo. Vervolgens is gebleken, door de afzonderlijke cellen verder te vergelijken, dat de nieuwe hartspiercellen die worden gevormd "verjongd" zijn. Ze zijn hetzelfde als embryonale cellen en ze worden beschouwd als een soort stamcellen, die over de mogelijkheid beschikken om meer cellen te maken.

In **hoofdstuk 3** hebben we veel genen gevonden, die in relatie kunnen worden gebracht met de immuunreactie en die eruit sprongen vanwege hun betrokkenheid met het immuunsysteem in het herstellend proces. De dynamica van de twee belangrijkste celtypes van de aangeboren immuniteit, macrofagen en neutrofielen, wordt beschreven in **hoofdstuk 5.** Wanneer, waar en in welke hoeveelheid deze twee celtypes worden aangetrokken tot het beschadigde hart wordt hier gedetailleerd omschreven. Als laatste ontrafel ik op welk tijdstip de ontsteking uit wordt gezet en hoeveel dagen de macrofagen nodig hebben om na de schade herstellende signaalstoffen te gaan afgeven.

Deutsche Zusammenfassung

Herz-Kreislauf-Erkrankungen sind mit über 30% aller Todesfälle weltweit die führende Todesursache. Neue Therapien sind daher dringend nötig, um das Leiden sowie das Sterberisiko der jährlich wachsenden Anzahl von Patienten zu verringern. Hierbei spielt die Grundlagenforschung eine wichtige Rolle in der Identifikation neuer Therapieansätze.
Ein Herzinfarkt entsteht, wenn die Blutzufuhr in einer der großen Kranzarterien im Herzen blockiert ist. Daraus resultiert ein Sauerstoff- und Nährstoffmangel in einem Teil des Herzmuskels, wodurch bis zu eine Milliarde Zellen absterben. Die toten Herzmuskelzellen werden nicht durch neue ersetzt und es bildet sich Narbengewebe. Narbengewebe ist anfänglich durchaus nützlich, um die Wunde zu verschließen und dadurch eine grundlegende Funktion des Herzens zu gewährleisten. Narbengewebe kann sich allerdings, im Gegensatz zu gesundem Herzgewebe, nicht ausdehnen und zusammenziehen und somit nicht effizient Blut pumpen. Dadurch entstehen Folgeerkrankungen, wie etwa Herzrhythmusstörungen, mit schwerwiegenden Folgen. Tausenden Patienten könnte mit neuen Therapien geholfen werden, die die Herzfunktion nach einem Herzinfarkt wiederherstellen.
Eine Möglichkeit der Verbesserung der Herzfunktion, besteht in dessen Stimulation zur Selbstheilung. Dazu müssen wir verstehen, wie die Regeneration des Herzens unter natürlichen Umständen abläuft. Zebrafische besitzen diese natürliche Kapazität ihr Herz zu regenerieren. Zebrafische sind klein (ca. 2-3 cm groß) und werden weltweit in Laboratorien benutzt, um verschiedenste Mechanismen und Prozesse zu studieren, z.B. die Entwicklung einer befruchteten Eizelle zu einem ausgewachsenen Organismus entwickelt oder Verhaltensstudien.

In dieser Doktorarbeit verwende ich den Zebrafisch, um die Regeneration des Herzens besser zu verstehen. In **Kapitel 2** beschreibe ich die Anwendung einer neuartigen Methode, genannt *tomo*-seq. Mit dieser Methode schneidet man ein Organ in sehr dünne „Scheiben". Dies geschieht entlang einer festgelegten Axe, im Beispiel des Herzens von der Wunde in Richtung des unbeschädigten Teils des Herzens. Danach wird detektiert, welche Gene in jeder einzelnen „Scheibe" aktiviert wurden. Durch das Aktivitätsmuster verschiedener Gene in den unterschiedlichen Scheiben können Schlüsse darüber gezogen werden, welche Signalwege und Prozesse in welchen Regionen des regenerierenden Herzens aktiv sind. Die einzelnen Schritte in einer solchen Analyse möchte ich im Folgenden anhand eines Beispiels illustrieren.
Gen A ist in allen Herzmuskelzellen aktiv. *Gen B* dagegen ist nur in Scheiben aktiv, in denen *Gen A* nicht aktiv ist. Nun wissen wir schon einmal, wie weit sich die Wunde erstreckt und wo der intakte Herzmuskel beginnt. Eine nähere Untersuchung zeigt, dass *Gen B* in der Immunabwehr eine Rolle spielt. Nehmen wir nun an, *Gen C* ist nur an der Grenze zwischen Wunde und Herzmuskelzellen aktiv, nirgendwo sonst. *Gen C* spielt eine Rolle in der

Zellteilung. Das bedeutet, dass hier neue Herzmuskelzellen entstehen. Es findet Regeneration statt. Außerdem sind noch die *Gene D, E, F, G & H* in derselben Region wie *Gen C* aktiv, allerdings ist die genaue Funktion dieser Gene nicht bekannt. Die sehr spezifische Aktivität dieser Gene erlaubt jedoch die Annahme, dass sie eine Rolle in der Regeneration spielen. Folglich können diese unbekannten Gene genauer untersucht werden und uns einen genauen Einblick in die Prozesse während der Herzregeneration erlauben.

In **Kapitel 3** beschreibe ich die *tomo*-seq Resultate, angewendet an dem sich regenerierenden Herzen. Ähnlich dem oben aufgeführten Beispiel analysiere ich die Daten und validiere sie anhand alternativer Methoden. Darüber hinaus wende ich mich einem spezifischen Prozess zu, dem Bone Morphogenetic Protein (BMP) Signalweg, und zeige, dass aktives BMP für erfolgreiche Herzregeneration nötig ist.

Der Nachteil der *tomo*-seq Methode ist, dass man nur die Gen-Aktivität pro „Scheibe" erhält. Allerdings sind in jeder Scheibe viele verschiedene Zellen und Zelltypen, die mit dieser Methode nicht unterschieden werden können. In **Kapitel 4** benutze ich deswegen eine andere Methode mit der die aktivierten Gene in einzelnen regenerierenden Herzmuskelzellen analysiert werden können. Die Ergebnisse zeigen, dass Subpopulationen von Zellen ihren Metabolismus im Vergleich zu unbeschädigtem Herzgewebe ändern. Interessanterweise ist dieser veränderte Metabolismus vergleichbar mit dem des embryonalen Herzens. Mithilfe von weiteren Analysen zeige ich, dass die regenerierenden, sich teilenden Herzmuskelzellen im ausgewachsenen Fisch „jünger" werden. Diese Zellen sind den embryonalen Herzzellen sehr ähnlich und können als eine Art Stammzelle oder Vorläuferzelle bezeichnet werden.

In den *tomo*-seq Resultaten von **Kapitel 3** habe ich unter anderem viele Gene detektiert, die in der Immunabwehr involviert sind. Dies hat mein Interesse geweckt, die Rolle des Immunsystems während der Herzregeneration genauer zu untersuchen. In **Kapitel 5** beschreibe ich die Dynamik der zwei wichtigsten Immunzellen: Macrophagen und Neutrophilen. Hier ist beschrieben, wann, wo und in welcher Anzahl diese Zellen in den ersten drei Wochen der Regeneration auftreten. Schließlich wird der Zeitpunkt identifiziert, an dem das Immunsystem den Entzündungsprozess beendet und die Regeneration einleitet.

Die hier dargelegte Doktorarbeit ist das Ergebnis von fünf Jahren Laborarbeit, aber auch unzähligen Stunden der Datenanalyse. Ist unser Wissen über Herzregeneration deutlich besser als es im Jahr 2012 war? Ich glaube nicht. Jedoch bieten die Technologie-Ansätze, welche die Basis dieser Thesis bilden, einen wichtigen Ausgangspunkt für zukünftige Forschung. Die Herausforderung der nächsten Jahre wird sein, einzelne Ereignisse zu verknüpfen und Netzwerke von Prozessen zusammenzufügen, um Herzregeneration fundamental zu verstehen.

Acknowledgements

My time at the Hubrecht is coming to an end, but before I move on to the next stage of my career I want to take the time to thank all the people that made these last five years such an amazing, fun, exciting and educational experience. I truly feel that I have progressed tremendously as a person and as a professional, and this is also thanks to YOU!

Where else to start than with **Jeroen**?! You gave me the opportunity to work on this exciting project. Although it was a completely new line of research among all the "embryonic heart development"-stuff, I never felt that I did not receive enough guidance and help – from you and the rest of the group. I sincerely thank you for all the discussions we had, the advice you offered and the (constructive) criticism you gave. And also for the money you spent on my various sequencing ventures ;)

Next in line: **Sven** and **Alex**, thanks for being my paranymphs, you guys are awesome! Alex, we had amazing times during our PhD time at the Hubrecht: 5th of November bonfires, BBQs and not to mention that you made me jump out of a fully functional airplane…Sven, your enthusiasm for cars and technology always makes for a welcome contrast to the cat-talk from the girls office ;)

Of course I would not have nearly enjoyed my time at the Hubrecht as much as I have without the great people that "breathe" science around here…first and foremost, the Bakkers' group. Every afternoon beer, every lab retreat, every dinner in the city, countless coffees and cakes and cookies shared – I could not have wished for a better atmosphere! You guys are the best! **Sonja**, there is not enough space here to emphasize how big of a part you are in the lab: with only the highest honors are you called the *lab-queen*! Your advice is always valued, be it scientifically or baby-related. I will never forget the 10-km-race we ran in March '17 where we ended up chatting and laughing throughout the whole run (to the annoyance of the people suffering around us)! **Sven** & **Dennis**, our gym-sessions in Olympos have more than once been the highlight of my working day! Thanks for enduring my dictatorship as your drill instructor. Keep up the good work without me! :P **Laurence**, you have been a fantastic addition to the lab! You brought us French cheese and wine and you were always a great person to have a chat with. Your passion for art is obvious (as can be seen in the thesis cover) and I truly hope you find a career that fits your hobby. **Fede**, you have supervised me already during my internship, but you did not stop to offer great advice inside and outside the lab once I started my PhD. I only regret that I was not able to talk more about football with you ;) **Melanie**, we embarked on this PhD-journey together, going through all the different phases. It has been a pleasure sharing an office with you for a few years. **Silja**, the German-connection in the lab. Although we hardly ever spoke German to each other, we shared the frustration

about Dutch bread (if it even deserves that name, having less texture than toast). Becoming beerpong champion with you at the PV weekend has been a major accomplishment. **Lotte**, I admire your skilled photography, thanks for all the pictures you took for me over the years. **Phong**, your excitement for castles and Pokémon is as big as your enthusiasm for science. **Sarah**, you started of as a student of mine, but by now you have returned to the group and you are well into your own PhD studies. It's great to see you grow as a scientist (although you will always stay short – physically :P). **Emily**, your British humor and personality certainly made the lab-life more enjoyable, I hope you found satisfaction becoming a PI. **Hanil**, you welcomed me to the Dutch culture and whenever we meet it's always great fun.

What would the Hubrecht be without the famous Personeelsvereniging (PV)? Together with **Alex**, **Geert**, **Kay** and **Axel**, we organized some legendary parties and events! We always forgot to get the soft drinks for the borrels/parties, but what else do you expect of 5 guys?! The PV weekends with all former and present members have been a blast!

Jacco's angels: **Laila**, **Anoek**, **Evelyne**, **Arianna**, **Colinda**, **Nienke**, **Saskia**, **Carrie**, **Danielle**, **Maria**, **Anko** and **Sander** (YES you are angels, too!) and whoever I forgot (you guys have become a huge group). It was a great pleasure sharing office- and lab-space with you on the first floor, before we all moved on to different parts of the Hubrecht Institute to accommodate the growing number of people. Best of luck to all of you at the NKI, I hope the move goes smoothly!

Many thanks also go to the AvO boys (and girls): **Mauro**, **Lennart**, **Dylan**, **Philipp**, **Bastiaan**, **Chloé**, **Maria**, **Anna**, **Susanne** and **Judith**. Whenever I needed to borrow reagents or help with R, you came to the rescue! **Rainier**, thanks for all the FACS sorts that only worked half of the time.

I also want to thank **Catherine Rabouille**: always a little rough around the edges, but inside a truly wonderful person. You and **Alexander v. O.** supported my idea to inform PhDs about alternative career opportunities without hesitation. It was great working with you and the **Career Development Committee**, I believe we made a difference with our seminars, workshops, etc.

Without the relentless efforts of our Animal Care Takers, no fish work would have been possible. Thanks **Mark**, **Erma**, **Rob**, **Luuk** and **Bert**! And while I'm at it, all the other service departments at the Hubrecht should also not go unmentioned: **IT**, **finances**, **personal**, **technical, civil** dpts and our lovely **receptionists**! Your work behind the scenes is greatly appreciated, thanks for keeping everything running. Also thanks to **Litha** for all the thesis-related help!

Also, thanks to the countless people who I had chats with at the coffee machine, scientific discussions at borrels, etc: **Bas M.**, **Hesther**, **Charlotte**, **Joep**, **Bas C.**, **Spiro**, **Suzanne**, **Roel**, **Angelica**, **Petra**, **Jelmer**, **Sasja**, **Lorenzo**, **Annabel**, **Christian**, **Valerio**, **Erica**, **Carien**, **Ismael**, **Anna**, and **Laurent**.

Moving away from the work-life at the Hubrecht, I also want to thank **Ola**, **Selwyn**, **Emma** and **Max** for the countless play-dates, BBQs and Parties. While we got to know you during dancing classes, we are so happy that a real friendship developed out of it. You guys are such a great contrast to our "science friends", haha!

Ina, **Allard**, **Robin** & **Emilie**, thanks for all the baby-related things we could borrow from you, but more than that we enjoyed the various tee/coffee/cookie/cake-afternoons we shared!

I'd also like to thank everyone from **Crossfit Newstyle**, **Crossfit U1** and **Crossfit 1412**, and especially my workout-buddy **Damian**: a challenging workout at the end of a day in the lab is always enjoyable and relaxing.

Ich möchte mich auch bei meinen Freunden aus Deutschland bedanken: **Christian** (Nadine und Sami), **Björn** (& Sandra), **Daniel** (& Paula), **Rene** (& Patricia), **Sebastian** und **Jakob** (& Kathi). Auch wenn wir uns in den letzten Jahren nicht oft gesehen haben, habt ihr immer Verständnis gezeigt, wenn ich es mal nicht zu einer Feier oder Ähnlichem geschafft habe.

Selbstverständlich darf ich auch nicht meine Freunde aus dem Bachelor Studium vergessen: **Nadine** (& Matthias), **Michael** und **Yannick**! Ich bin sehr froh, euch kennen gelernt zu haben und dass wir immer noch Kontakt haben, obwohl unsere Wege in verschiedene Richtungen gegangen sind. Trotz OC und Physik muss ich ehrlich zugeben, dass ich den Bachelor (dank euch) sehr genossen habe!

Natürlich gilt auch meiner Familie viel Dank: mein kleiner Brudi **Maxi**, **Henriette**, **Klaus** & **Uschi**, **Claudia**, **Ronja**, meine beiden **Omis** sowie **Karin** & **Bernd**. Ich erinnere mich noch an das erste Jahr als ich angefangen habe: ihr habt mich gefragt ob ich denn schon „was geschrieben" habe, wordaufdessen ich erstmal erklären musste, dass die eigentliche Doktorarbeit erst zum Schluss geschrieben wird und ich erstmal Ergebnisse im Labor bekommen muss bevor ich was zum Schreiben habe. Auch meiner angeheiratete Familie, **Kiriakos**, **Athina** und **Dimi**, bin ich dankbar: ihr seid immer eine erfrischende Abwechslung! Und selbstverständlich meine **Eltern**: eure uneingeschränkte Unterstützung hat es mir erlaubt meinen eigenen Weg zu gehen, Grenzen zu überschreiten, erwachsen zu werden. Ich bin euch unendlich dankbar für alles was ihr für mich getan habt (womit ich problemlos mehrere Bücher füllen könnte).

Und letztendlich: meine beiden Frauen. **Antonia**, mein Engelchen, dein (zahnloses) Lächeln lässt mich alles um mich herum vergessen. Missglückte Experimente – wen interessiert‘s?! Und **Elisabeth**, Worte können nicht beschreiben wie viel du mir bedeutest. Du bist meine Liebe, mein Leben, mein support system. Ohne dich wäre ich nie so weit gekommen. Wie unsere Tochter hast auch du die Gabe, mit deinem Lachen alles Andere in den Schatten zu stellen. Zum Glück ist dein Lächeln aber nicht zahnlos ;)

Curriculum vitae

Fabian Kruse, born on the 18th of January 1987, grew up in the town of Meinerzhagen in Germany. His interest in biology has been sparked by his grandfather, with whom he has watched countless animal documentaries during his childhood. After finishing High School, he completed the obligatory military service from 2006-2007, before starting his studies. Fabian studied Biology at the University of Cologne, where he received his B.Sc. degree in 2010. Owing to his interest in Genetics and Developmental Biology, he wrote his thesis in the lab of Prof Hammerschmidt, who also introduced him to the zebrafish model system. Inspired by this experience, Fabian moved to Utrecht, The Netherlands, to follow the "Cancer Genomics & Developmental Biology" Master's program. He performed his internships in the groups of Prof Jeroen Bakkers (Hubrecht Institute, Utrecht) and Prof Emile Voest (UMCU, Utrecht). After obtaining his M.Sc. degree in 2012, he returned to the Bakkers group for his doctoral studies. Intrigued by regeneration research, which he reviewed in his Master thesis with Zhenya Berezikov (Hubrecht Institute), he started to work on adult zebrafish to study heart regeneration. The results of his research are described in this doctoral dissertation. In the future, Fabian will apply his analytical skills in a more practical manner as life science consultant at Charles River Associates International.